



# **IV Lithuanian- Ukrainian-Polish meeting on physics of ferroelectrics**

Programme & abstracts



5th-9th of September 2016

Palanga, Lithuania

## TABLE OF CONTENTS

<b>Conference Committees</b>	<b>1</b>
<b>Welcome</b>	<b>2</b>
<b>General Information</b>	<b>3</b>
<b>Scientific Programme</b>	<b>5</b>
<b>Detailed Programme</b>	<b>6</b>
<b>Oral Abstracts</b>	<b>9</b>
<b>List of Poster Presentations</b>	<b>49</b>
<b>Poster Abstracts</b>	<b>51</b>
<b>Index of Authors</b>	<b>95</b>

## CONFERENCE COMMITTEES

### Scientific Programme Committee

Jūras Banys ( <b>Chairman</b> )	Vilnius University	Lithuania
Ryszard Cach	University of Wrocław	Poland
Zbigniew Czapla	Opole University of Technology	Poland
Ryszard Poprawski	Wrocław University of Technology	Poland
Jan Dec	University of Silesia	Poland
Maya D. Glinchuk	Institute for Problems in Materials Science	Ukraine
Adam Pietraszko	Institute of Low Temperatures and Structure Research	Poland
Krystian Roleder	University of Silesia	Poland
Ihor V. Stasyuk	Institute for Condensed Matter Physics	Ukraine
Jan Suchanicz	Pedagogical University of Kraków	Poland
Rostyslav O. Vlokh	Institute of Physical Optics	Ukraine
Yulian M. Vysochanskii	Uzhgorod National University	Ukraine

### Local organising committee

Jūras Banys (**Chairman**)  
Robertas Grigalaitis  
Vytautas Samulionis  
Evaldas Tornau  
Vidmantas Kalendra  
Maksim Ivanov  
Rūta Mackevičiūtė  
Edita Palaimienė  
Šarūnas Svirskas  
Džiugas Jablonskas  
Ieva Kranauskaitė  
Mantas Šimėnas  
Ilonas Zamaraitė  
Sergejus Balčiūnas  
Andrius Džiaugys  
Saulius Rudys  
Martynas Kinka

## WELCOME WORD



**Dear Colleagues,**

On behalf of the Local Organising and Programme Committees we are delighted to welcome you to the fourth Lithuanian-Ukrainian-Polish Meeting on Physics of Ferroelectrics (LUP IV) in Palanga.

The ferroelectric communities of Lithuania, Ukraine and Poland developed fruitful collaborations over the years. This led to a joint decision to establish a meeting which is held every two years. The first meeting was organized in Taujėnai, Lithuania in 2010.

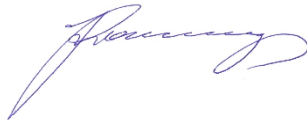
Afterwards, it was in Lviv, Ukraine in 2012 and Wrocław, Poland in 2014.

The general topic of the conference is devoted to the contemporary fundamental studies and applications in the field of ferroelectricity and related materials. The important purpose of this symposium is to continue collaborations and extend them further by involving young scientists and students who are encouraged to participate. It is an important task to pass the knowledge to the younger generation and involve them in the current activities.

This year the meeting takes place in Palanga – a small town near the Baltic seaside which is a popular holiday resort well renowned for fascinating dunes.

Conference Chair

**Prof. Jūras Banys**





## **GENERAL INFORMATION**

### **Conference Venue**

IV Lithuanian-Ukrainian-Polish Meeting on Physics of Ferroelectrics (LUP IV) takes place in the recreation house of Vilnius University called “Romuva” in resort Palanga.

Palanga is located in the western part of Lithuania on the shore of the Baltic Sea. It is the most popular resort in Lithuania which attracts not only local people but also many foreigners. Palanga is known since 12th century when it was mentioned in the historical documents.

### **Address**

Birutės av. 35, 37, 37a, Palanga, Lithuania.

### **Accommodation**

The accommodation will be provided for the participants in “Romuva” as well.

### **Official Language**

The official Conference language is English. No translation will be provided

### **Name Badges**

All participants have been issued name tags, which must be worn to gain admission to the Conference facilities and social program.

### **Technical Instructions for Presenters**

Oral presentations and poster presentation will take place in “Romuva”. Meeting hall will be equipped with PC, LCD projector and microphones. The date/hour/room of your presentation(s) is available in the Conference Program. If you are using a slide presentation make sure that you bring it on the USB stick. Supported file types: ppt, pptx, pdf, avi.

Note! If you are planning to use your own computer for presentation, please inform secretariat about that in advance.

## Coffee Breaks

Coffee, tea and other refreshments will be served next to the conference rooms.

September 6	10:00 – 10:30 and 15:20 – 15:40
September 7	10:00 – 10:30 and 15:20 – 15:40
September 8	10:00 – 10:30
September 9	10:00 – 10:30

**Breakfast, Lunch, Dinner and Gala Dinner** will be available in restaurant “Pajūrio Alka”, S. Daukanto str. 21, Palanga.

## Breakfast

September 6	08:00 – 09:00
September 7	08:00 – 09:00
September 8	08:00 – 09:00
September 9	08:00 – 09:00

## Lunch

September 6	12:30 – 14:00
September 7	12:30 – 14:00
September 8	12:30 – 14:00

## Dinner

September 6	19:00 – 20:00
September 7	19:00 – 20:00

## Gala Dinner

September 8, 19:00 – 22:00

## Social Event

Excursion to Klaipėda – the third largest city in Lithuania.

September 8, 14:00 – 19:00

Excursion is free of charge for Conference participants.

## Internet Area

Wireless Internet access is available throughout the Conference venue.

## SCIENTIFIC PROGRAMME

Time	Monday (5 <sup>th</sup> September)	Tuesday (6 <sup>th</sup> September)	Wednesday (7 <sup>th</sup> September)	Thursday (8 <sup>th</sup> September)	Friday (9 <sup>th</sup> September)	
08:00 - 08:50		Registration	Registration	Registration	Registration	
08:50 - 09:00		Opening				
09:00 - 10:00		Seiji Kojima	Maya Glinchuk	Zbigniew Czapla	Andrius Džiaugys	
10:00 - 10:30		Coffee	Coffee	Coffee	Coffee	
10:30 - 11:10		Oksana Mys	Renata Bujakiewicz-Koronska	Valentyn Laguta	Mikhail Trubitsyn	
11:10 - 11:30		Michal Piasecki	Maxim Silibin	Ryszard Poprawski	Jan Macutkevic	
11:30 - 11:50		Xusheng Wang	Elena Fertman		Galyna Dovbeshko	
11:50 - 12:10		Olga Malyshkina	Bogdan Dabrowski	Aneta Ciupa	Artyom Plyushch	
12:10 - 12:30		Antoni Kania	Ryszard Skulski	Dorota Komornicka	Closing	
12:30 - 14:00		Lunch	Lunch	Lunch	Refreshments	
14:00 - 14:40		Registration	Vytautas Samulionis	Alexander Grabar	Excursion	
14:40 - 15:00			Piotr Czaja	Bohdan Andriyevskyy		
15:00 - 15:20	Evaldas Tornau		Robertas Grigalaitis			
15:20 - 15:40	Coffee		Coffee			
15:40 - 16:20	Jan Dec		Gunnar Suchanek			
16:20 - 16:40	Šarūnas Svirskas		Tongqing Yang			
16:40 - 17:00	Roman Kuzian		Yuri Genenko			
17:00 - 17:20	Poster session I		Poster session II			
17:20 - 17:40						
17:40 - 18:00	Welcome Reception				Gala Dinner	
18:00 - 18:20						
18:20 - 18:40						
18:40 - 19:00						
19:00 - 19:20						
19:20 - 19:40						
19:40 - 20:00						
20:00 - 20:20						
20:20 - 20:40						
20:40 - 21:00						
21:20 - 22:00						

## Tuesday (6<sup>th</sup> September)

8:00	Breakfast	
9:00	<i>Seiji Kojima</i> (chair Zbigniew Czapla) Broadband Brillouin Scattering Spectroscopy on Crossover from Strong to Weak Relaxor Nature of Uniaxial Tungsten Bronze Ferroelectrics	PL-1
10:00	Coffee break	
Oral session 1 (chair Gunnar Suchanek)		
10:30	<i>Oksana Mys</i> Acoustooptic anisotropy of ferroic crystals	O1-1
11:10	<i>Michal Piasecki</i> Photoinduced nonlinear properties of Rare Earth doped Bi <sub>2</sub> Fe <sub>4</sub> O <sub>9</sub> multiferroics near phase transitions	O1-2
11:30	<i>Xusheng Wang</i> Luminescent properties in perovskite ferroelectric ceramics	O1-3
11:50	<i>Olga Malyshkina</i> Determination the specific heat by use the switching processes	O1-4
12:10	<i>Antoni Kania</i> Dielectric and Raman scattering studies of Ag <sub>1-x</sub> Li <sub>x</sub> NbO <sub>3</sub> ceramics	O1-5
12:30	Lunch	
Oral session 2 (chair Oksana Mys)		
14:00	<i>Vytautas Samulionis</i> High frequency ultrasonic waves in ferroelectrics and related materials	O2-1
14:40	<i>Piotr Czaja</i> Raman Spectroscopy, dielectric and optical properties of PbTiO <sub>3</sub> , Na <sub>0.5</sub> Bi <sub>0.5</sub> TiO <sub>3</sub> , PbTiO <sub>3</sub> -Na <sub>0.5</sub> Bi <sub>0.5</sub> TiO <sub>3</sub> single crystals	O2-2
15:00	<i>Evaldas Torna</i> Structural Potts-type Phase Transition in Perovskite Metal-Formate Frameworks: Effect of Dipolar Interactions	O2-3
15:20	Coffee break	
Oral session 3 (chair Renata Bujakiewicz-Koronska)		
15:40	<i>Jan Dec</i> Aging in a relaxor ferroelectric: what can we learn from it	O3-1
16:20	<i>Šarūnas Svirskas</i> Phase transition in 0.1Na <sub>0.5</sub> Bi <sub>0.5</sub> TiO <sub>3</sub> -0.6SrTiO <sub>3</sub> -0.3PbTiO <sub>3</sub> solid solutions	O3-2
16:40	<i>Roman Kuzian</i> Chemical disorder and 207Pb hyperfine fields in the new magnetoelectric multiferroic Pb(Fe <sub>1/2</sub> Sb <sub>1/2</sub> )O <sub>3</sub>	O3-3
17:00	Poster session 1	
19:00	Dinner	

## Wednesday (7<sup>th</sup> September)

8:00	Breakfast	
09:00	<b>Maya Glinchuk</b> (chair Seiji Kojima) Size Induced Phase Transitions without Critical Size and Reentrant Phase Appearance in Nanoferroelectrics Originated from Flexoelectric and Vegard Effects	PL-2
10:00	Coffee break	
Oral session 4 (chair Valentyn Laguta)		
10:30	<b>Renata Bujakiewicz-Koronska</b> Cobalt Doped Barium Titanate – New Multiferroic?	O4-1
11:10	<b>Maxim Silibin</b> Structural and magnetic phase transitions in Bi <sub>1-x</sub> Ca <sub>x</sub> Fe <sub>1-x</sub> Mn <sub>x</sub> O <sub>3</sub> multiferroics	O4-2
11:30	<b>Elena Fertman</b> Magnetic properties of the Bi <sub>1-x</sub> La <sub>x</sub> Fe <sub>0.5</sub> Sc <sub>0.5</sub> O <sub>3</sub> (0.00 ≤ x ≤ 0.80) perovskites	O4-3
11:50	<b>Bogdan Dabrowski</b> Multiferroelectricity of perovskite manganates	O4-4
12:10	<b>Ryszard Skulski</b> Electrophysical properties of PMN-PT-ferrite ceramic composites	O4-5
12:30	Lunch	
Oral session 5 (chair Jan Dec)		
14:00	<b>Alexander Grabar</b> Modifications of tin thiohypodiphospate ferroelectrics by doping and indiffusion	O5-1
14:40	<b>Bohdan Andriyevskyy</b> Ab initio band electronic structure and molecular dynamics of (C <sub>3</sub> N <sub>2</sub> H <sub>5</sub> ) <sub>2</sub> SbF <sub>5</sub> crystals	O5-2
15:00	<b>Robertas Grigalaitis</b> Dielectric Spectroscopy of Barium Strontium Titanate Epitaxial Thin Films	O5-3
15:20	Coffee break	
Oral session 6 (chair Mikhail Trubitsyn)		
15:40	<b>Gunnar Suchanek</b> Physical limits of electrocaloric cooling devices	O6-1
16:20	<b>Tongqing Yang</b> Hysteresis Loop of Electrocaloric Effect in Ferroelectricity	O6-2
16:40	<b>Yuri Genenko</b> Polarization switching kinetics in composite ferroelectrics: case studies on porous and fatigued ceramics	O6-3
17:00	Poster session 2	
19:00	Dinner	

## Thursday (8<sup>th</sup> September)

8:00	Breakfast	
09:00	<b>Zbigniew Czapla</b> ( <i>chair Maya Glinchuk</i> ) Phase transitions, ferroelasticity, possible ferroelectricity and antiferroelectricity in [(C <sub>2</sub> H <sub>5</sub> ) <sub>4</sub> N(CH <sub>3</sub> ) <sub>4</sub> N]MeX <sub>4</sub> crystals	PL-3
10:00	Coffee break	
Oral session 7 (chair Alexander Grabar)		
10:30	<b>Valentyn Laguta</b> Anomalous Magnetoelectric Effect in Multiferroic Pb(Fe <sub>1/2</sub> Nb <sub>1/2</sub> )O <sub>3</sub> and its Solid Solution with PbTiO <sub>3</sub>	O7-1
11:10	<b>Ryszard Poprawski</b> Ferroelectric and antiferroelectric generators of electric current	O7-2
11:50	<b>Aneta Ciupa</b> Multiferroic properties and order-disorder phase transition in the ammonium templated metal-organic frameworks	O7-3
12:10	<b>Dorota Komornicka</b> Synthesis and characterization of 2-amino-3-nitropyridinium hydrogen sulfate	O7-4
12:30	Lunch	
14:00	Excursion	
19:00	Gala Dinner	

## Friday (9<sup>th</sup> September)

8:00	Breakfast	
9:00	<i>Andrius Džiaugys</i> (chair Ryszard Poprawski) Peculiar polarization domains in the layered ferroelectric CuInP <sub>2</sub> Se <sub>6</sub>	PL-4
10:00	Coffee break	
Oral session 8 (chair Jūras Banys)		
10:30	<i>Mikhail Trubitsyn</i> Amorphous, nano- and microcrystalline phases of lithium germanate oxides	O8-1
11:10	<i>Jan Macutkevici</i> Dielectric properties and the phase diagram of (Bi <sub>x</sub> Na <sub>1-x</sub> )(Mn <sub>y</sub> Nb <sub>1-y</sub> )O <sub>3</sub> ceramics	O8-2
11:30	<i>Galyna Dovbeshko</i> CARS spectroscopy and imaging of graphene layers and nanoplatelets	O8-3
11:50	<i>Artyom Plyushch</i> Dielectric and shielding properties of Ni@C/ polydimethylsiloxane composites	O8-4
Refreshments		
12:10	Refreshments	

**ABSTRACTS OF ORAL PRESENTATIONS**  
**6<sup>th</sup> September**

# Brillouin Scattering Spectroscopy on Crossover from Strong to Weak Relaxor Ferroelectrics with Tungsten Bronze Structure

**S. Kojima<sup>1</sup>, M. Aftabuzzaman<sup>1</sup>, J. Dec<sup>2</sup>, and W. Kleemann<sup>3</sup>**

*1- Division of Materials Science, University of Tsukuba, Tsukuba, Ibaraki 305-8573, Japan*

*2- Institute of Materials Science, University of Silesia, PL 40-007 Katowice, Poland*

*3- Applied Physics, Duisburg-Essen University, D 47048 Duisburg, Germany*

[kojima@bk.tsukuba.ac.jp](mailto:kojima@bk.tsukuba.ac.jp)

Relaxor ferroelectric strontium barium niobate,  $\text{Sr}_{0.61}\text{Ba}_{0.39}\text{Nb}_2\text{O}_6$  (SBN61) with a strong charge disorder, undergoes a diffuse phase transition on cooling from a prototypic tetragonal  $4/mmm$  phase to a ferroelectric tetragonal  $4mm$  phase with a spontaneous polarization along the c-axis [1,2]. In contrast,  $\text{Ca}_{0.28}\text{Ba}_{0.72}\text{Nb}_2\text{O}_6$  (CBN28) with lower charge disorder undergoes a sharp ferroelectric phase transition [3]. In the present work, Brillouin scattering of the solid solutions of  $\text{Sr}_x\text{Ba}_{1-x}\text{Nb}_2\text{O}_6$  (SBN100x),  $\text{Ca}_x\text{Ba}_{1-x}\text{Nb}_2\text{O}_6$  (CBN100x), and mixed solid solutions of SBN61 and CBN28 was studied using a tandem Fabry-Perot interferometer [4]. The temperature dependence of the sound velocity of a longitudinal acoustic (LA) mode along the c-axis of SBN26 and SBN70 on zero field cooling (ZFC) is shown in Fig. 1(a). The LA shift of SBN26 with weak charge disorder shows the a sharp anomaly at the Curie temperature,  $T_C$ , while that of SBN70 shows the broad diffusive anomaly in the vicinity of  $T_C$  due to by the existence of polar nanoregions (PNR) caused by strong charge disorder. The temperature dependence of the LA velocity of SBN61 on field cooling and ZFC is shown in Fig. 1(b). Field cooled SBN61 without PNR shows a sharp elastic anomaly being similar to that of SBN26, while ZFC of SBN61 gives rise to a broad diffusive anomaly similar to SBN70 as shown in Fig. 1(b) [5]. Critical slowing down towards  $T_C$  was clearly observed for the central peaks in both SBN26 and CBN28 [3], while it becomes diffusive as the Sr content increases. In SBN61 and SBN70 diffusive broad slowing down was observed in the vicinity of  $T_C$ .

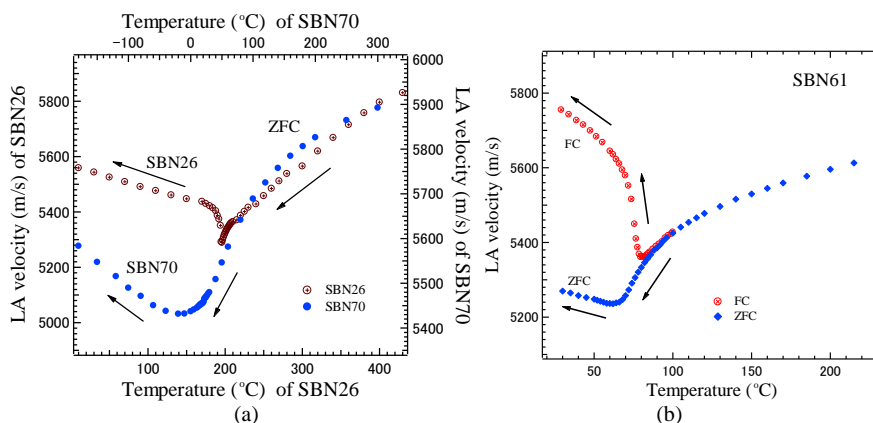


Figure 1 Temperature dependence of LA velocity, (a) ZFC of SBN26 and SBN70, (b) ZFC and FC of SBN61.

## References

- [1] V. V. Shvartsman, J. Dec, S. Miga, T. Łukasiewicz, and W. Kleemann, Ferroelectric domains in  $\text{Sr}_x\text{Ba}_{1-x}\text{Nb}_2\text{O}_6$  single crystals ( $0.4 \leq x \leq 0.75$ ), *Ferroelectrics* **376**, 1-7 (2008).
- [2] F. Jiang and S. Kojima, Central peaks and Brillouin scattering in uniaxial relaxor single crystals of  $\text{Sr}_{0.61}\text{Ba}_{0.39}\text{Nb}_2\text{O}_6$ , *Phys. Rev. B* **66**, 184301-1-7 (2002).
- [3] K. Suzuki, K. Matsumoto, J. Dec, T. Łukasiewicz, W. Kleemann, and S. Kojima, Critical slowing down and elastic anomaly of uniaxial ferroelectric  $\text{Ca}_{0.28}\text{Ba}_{0.72}\text{Nb}_2\text{O}_6$  crystals with tungsten bronze structure, *Phys. Rev. B* **90**, 064110-1-4 (2014).
- [4] S. Kojima, Gigahertz acoustic spectroscopy by micro-Brillouin scattering, *Jpn. J. Appl. Phys.* **49**, 07HA01-1-6 (2010).
- [5] K. Matsumoto and S. Kojima, Effect of electric field on uniaxial relaxor ferroelectric strontium barium niobate, *Jpn. J. Appl. Phys.* **54**, 10NC04-1-4 (2015).



# Acoustooptic anisotropy of ferroic crystals

**O. Mys, O. Krupych, B. Zapeka, R. Vlokh**

*Vlokh Institute of Physical Optics, 23 Dragomanov Str., 79005, Lviv, Ukraine, mys@ifp.lviv.ua*

We suggest a new approach for analyzing anisotropy of acoustooptic figure of merit (AOFM). The relations for the effective elastooptic coefficients and the AOFM are derived for all possible types of acoustooptic (AO) interactions in optically isotropic media, including non-solid-state and solid-state amorphous media [1], crystals belonging to the cubic [1], tetragonal [2], hexagonal and trigonal systems [3]. It has been shown that nine types of the AO interactions can be implemented in crystals, six of them for the isotropic interactions and three for the anisotropic ones. In general, the six isotropic interactions can be presented as the interactions of the two optical eigenwaves having orthogonal polarizations with the three acoustic eigenwaves (two of them being transverse and one longitudinal). The remaining three types of the anisotropic interactions are as follows: the interaction of linearly polarized incident optical wave with the longitudinal acoustic wave and the interactions of linearly polarized incident optical wave with the two transverse acoustic waves with orthogonal polarization.

Our approach allows for finding the optimal geometries of AO interactions characterized by the highest AOFM for a given material. The analysis is carried out on the examples of cubic KBr and  $\text{KAl}(\text{SO}_4)_2 \cdot 12\text{H}_2\text{O}$  crystals which represent different subgroups of the cubic symmetry class; on the examples of  $\text{LiNbO}_3$  crystals which represent the trigonal system as well as  $\text{TeO}_2$  and  $\text{NaBi}(\text{MoO}_4)_2$  crystals, which represent the tetragonal system. The peculiarities of extreme values of AOFM in proper ( $\text{TeO}_2$ ) and improper ( $\text{NaBi}(\text{MoO}_4)_2$ ) ferroelastic materials are discussed.

[1] O. Mys, M. Kostyrko, M. Smyk, O. Krupych, and R. Vlokh, Anisotropy of acousto-optic figure of merit in optically isotropic media, *Applied Optics*, vol. 53, pp. 4616-4627 (2014).

[2] O. Mys, M. Kostyrko, M. Smyk, O. Krupych and R. Vlokh, Anisotropy of acoustooptic figure of merit for  $\text{TeO}_2$  crystals. 1. Isotropic diffraction, *Ukr. J. Phys. Opt.* vol. 15, pp.132-154 (2014).

[3] O. Mys, M. Kostyrko, O. Krupych, R. Vlokh, Anisotropy of the acousto-optic figure of merit for  $\text{LiNbO}_3$  crystals: isotropic diffraction, *Applied Optics*, vol. 54, pp. 8176-8186 (2015).

# Photoinduced nonlinear properties of Rare Earth doped $\text{Bi}_2\text{Fe}_4\text{O}_9$ multiferroics near phase transitions

**M. Piasecki<sup>a</sup>, A. El-Bey<sup>b</sup>, T. El Bahraoui<sup>b</sup>, M. Taibi<sup>c</sup>, A. Belayachi<sup>b</sup>, M. Abd-Lefdil<sup>b</sup>,  
A. M. El-Naggar<sup>d,e</sup>, A. A. Albassam<sup>e</sup>, P. Bragiel<sup>a</sup>, I.V. Kityk<sup>f</sup>,**

<sup>a</sup> Institute of Physics, J. Dlugosz University Armii Krajowej 13/15, 42-200 Czeszochowa, Poland

<sup>b</sup> University of Mohammed V, Materials Physics Laboratory, P.B. 1014, Rabat, Morocco

<sup>c</sup> University of Mohammed V, LPCMIN, Ecole Normale Supérieure, Rabat, Morocco

<sup>d</sup> Research Chair of Exploitation of Renewable Energy Applications in Saudi Arabia, Physics and Astronomy Department, College of Science, King Saud University, P.O. Box 2455, Riyadh 11451, Saudi Arabia

<sup>e</sup> Physics Department, Faculty of Science, Ain Shams University, Abbasia, Cairo 11566, Egypt

<sup>f</sup> Faculty of Electrical Engineering, Czeszochowa University Technology, Armii Krajowej 17, PL-42-201 Czeszochowa, Poland

[m.piasecki@ajd.czest.pl](mailto:m.piasecki@ajd.czest.pl)

We have performed complex measurements of the thermal and photoinduced NLO effects for Nd and Er doped  $\text{Bi}_2\text{Fe}_4\text{O}_9$  multiferroic compound near phase transitions. The possible mechanisms of ferroelectricity are discussed within the phenomenological and microscopic approaches. Results are compared with undoped material [1]. We have found substantial increase of the infrared third harmonic generation (THG) for the fundamental wavelength  $9.4 \mu\text{m}$  of microsecond  $\text{CO}_2$  laser for  $\text{Bi}_2\text{Fe}_4\text{O}_9$  microcrystalline powders. Additional enhancement of the THG signal was achieved by use of Er:glass 20 ns laser generating at 1540 nm before the IR probing of the THG. At the same time the analogous effect for the photoinduced two-photon absorption (TPA) was substantially less. The observed effect is explained within a framework of phenomenological description. Principal role here is played by magneto-electric interactions due to interactions of ferroelectric polarizations and ferromagnetic states. The observed effect may be used for creation of IR laser magneto-optical materials. The external fields change are occupied near the ground state dipole moments were explored in vicinity of the phase transitions including anti-ferromagnetic. The additional superposition of the magnetic field favours an enhanced THG. The observed processes were determined by the magneto electric coupling described the fourth rank tensors. The principal role is played by voids which during the doping change effective charge density distribution. The processes completely reversible and they are very sensitive to the applied films. The angle range  $35 \dots 52$  degrees are very narrow near the angles of the phase matching. All the materials were in the form of nano crystallites with sizes varying within the  $35 \dots 80 \text{ nm}$ .

[1] A.El-Bey, T.El Bahraoui, M.Taibi, A.Belayachi, M.Abd-Lefdil, A.M.El-Naggar, A.A.Albassam, A.O.Fedorchuk, G.Lakshminarayana, P.Czaja, I.V.Kityk, Third order nonlinear optical features of  $\text{Bi}_2\text{Fe}_4\text{O}_9$  multiferroic near antiferromagnetic phase transitions, Journal of Alloys and Compounds, 2016, in press: doi:10.1016/j.jallcom.2016.05.130

# Luminescent properties in perovskite ferroelectric ceramics

**X. Wang**

*School of Materials Science and Engineering, Tongji University, 4800 Cao'an Road, Shanghai 201804, China*

*email address: xs-wang@tongji.edu.cn*

Since the first perovskite-type ferroelectric ceramic, BaTiO<sub>3</sub>, was discovered 70 years ago [1], this type of ferroelectric materials has been studied intensively and applied widely in sensors and actuators, FRAMs, etc. Ferroelectric ceramics possess multiple functions like ferroelectric, pyroelectric and dielectric properties in nature, therefore they are the best candidates for multiple functional materials to be selected. Recent years, with novel and accurate optical detections developed, various novel luminescent properties have been found in piezoelectric materials, especially in lead-free perovskite and layered perovskite piezoelectric ceramics. This report deals with our research result on the perovskite ferroelectric ceramics and their various luminescent properties.

Rare earth (Pr, Eu, Dy, Er, Yb, Ho) doped barium titanate based and bismuth layered titanate based ceramics were prepared by conventional ceramic processes. Their properties of structures, ferroelectric, photoluminescence, mechanoluminescence and upconversion luminescence were characterized. Some sensing applications based on luminescence have been given. Large electrostrain in BaTiO<sub>3</sub> based solid solution or composites, stress sensor by means of mechanoluminescence, and temperature sensor by upconversion luminescence were introduced and their sensing properties were discussed [2-4].

This work was supported by the National Science Foundation of China (Grant no. 51572195).

[1] B. Wul, Dielectric constants of some titanates, *Nature*, 156, 480, (1945); Barium titanate: a new ferroelectric, *Nature*, 157, 808, (1946).

[2] X. Wang, C. N. Xu, H. Yamada, K. Nishikubo, and X. G. Zheng, Electro-mechano-optical conversions in Pr<sup>3+</sup>-doped BaTiO<sub>3</sub>-CaTiO<sub>3</sub> ceramics, *Adv. Mater.* **17**, 1254-1258, (2005).

[3] J. Li, X. Chai, X. Wang, C. N. Xu, Y. Gu, H. Zhao, and X. Yao, Large electrostrain and high optical temperature sensitivity in BaTiO<sub>3</sub>-(Na<sub>0.5</sub>Ho<sub>0.5</sub>)TiO<sub>3</sub> multifunctional ferroelectric ceramics, *Dalton Trans.*, DOI: 10.1039/c6dt01424k, (2016).

[4] H. Zou, J. Li, X. Wang, D. Peng, Y. Li, and X. Yao, Color-tunable upconversion emission and optical temperature sensing behaviour in Er-Yb-Mo codoped Bi<sub>7</sub>Ti<sub>4</sub>NbO<sub>21</sub> multifunctional ferroelectric oxide, *Opt. Mater. Express*, **4**, 1545-1554, (2014).

## Determination the specific heat by use the switching processes.

**O. Malyshkina, A. Eliseev**

*Tver State University, Sadovij per., 35, 170002 Tver, Russia*

*Olga.Malyshkina@mail.ru*

A study is made of the polarization processes in ferroelectric lead zirconate-titanate ceramics (PZT) in AC (sine and meander) electric fields with an amplitude of 500 – 2100 V/mm in a frequency range of 50 to 1500 Hz. Dielectric hysteresis loops were measured by the Sawyer-Tower method simultaneously with distant temperature control with the aid of thermal vision camera Testo–875-1. High voltage amplifier TREK 677B was exploited as a source of high AC voltage. The experimental results given below were obtained for samples with a thickness of the size of 1 x 5 x 5 mm.

It is shown that when the sample is switched by square wave voltage, the magnitude of the reversal polarization is larger than with sine AC field (Fig. 1a curves 1, 2) other conditions being equal. In the case of decreasing square wave switching voltage the onset of the loop opening begins at higher frequencies. At the same time, the magnitude of the reversal polarization ( $P_r$ ) of the loop after its opening is independent of voltage value and decreases with frequency increases (Fig. 1a curves 2, 3, 4). This decrease obeys the exponential rule. The frequency dependence of the self-heating temperature of the sample (Fig. 1b) is similar to that observed for reversal polarization (Fig. 1a). A linear self-heating temperature increase, reviewed in [1], takes place only for minor loops observed at the start time of the AC field or at low frequencies.

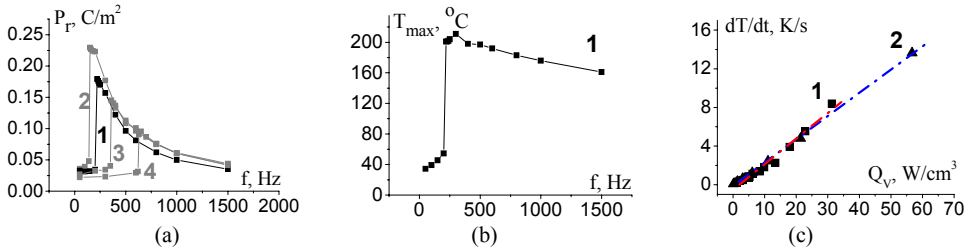


Figure 1. Frequency dependence of the reversal polarization for saturation hysteresis loop (a) and self-heating temperature of the sample (b). Curves 1 for sine AC; 2, 3, 4 – meander; 1, 2 –  $E_{amp} = 840$  V/mm, 3 –  $E_{amp} = 700$  V/mm, 4 –  $E_{amp} = 600$  V/mm. Function  $dT/dt$  ( $Q_v$ ) at start time of the sine AC (c). Curves 1 for different frequencies ( $E_{amp} = 840$  V/mm); 2 – for different amplitudes AC ( $f = 300$  Hz).

We suggested the method of estimated the volumetric heat capacity coefficient ( $c_v = \rho \cdot c$ ) by following equation

$$\frac{dT}{dt} = \frac{1}{\rho c} \cdot \frac{v}{V} \cdot Q_v [1]. \quad (1)$$

It connected the power dissipated by a unit volume of the sample ( $Q_v = EPf$ ) with the heating rate ( $dT/dt$ ) at start time of AC field. Here  $\rho$  – is the sample density;  $c$  – specific heat. Coefficient  $\frac{1}{c_v} \cdot \frac{v}{V}$  can be interpreted as

the slope for linear function  $dT/dt(Q_v) \cdot v/V$  is the ratio of the switchable sample volume ( $v$ ) to the total volume ( $V$ ). It can be expressed as the ratio of the reversal polarization ( $P_r$ ) to the maximum allowed ( $P_s$ ). The latter was determined by approximation of the experimental data (Fig. 1a, curve 1) using of exponential regression with the aid of MathCad14. For switching of PZT ceramic by sine AC, we had  $v/V = P_r/P_s = 0.64$ . Coefficient  $\frac{1}{c_v} \cdot \frac{v}{V}$  was determined from the graphs (Fig. 1c). As result, we obtain the value of the volumetric heat capacity of PZT ceramics:  $c_v = (2.6 \pm 0.2) \cdot 10^6$ .

The presented work was performed under the government assignment of Russian Ministry of Science and Education No 11.1937-2014/K

[1] J. Zheng, S. Takahashi, Sh. Yoshikawa, K. Uchino, J.W.C. de Vries Heat Generation in Multilayer Piezoelectric Actuators, Journal of the American Ceramic Society, vol. 79, pp 3193–3198, (1996).

# Dielectric and Raman scattering studies of $\text{Ag}_{1-x}\text{Li}_x\text{NbO}_3$ ceramics

**A. Kania<sup>1</sup>, A. Niewiadomski<sup>1</sup>, S. Miga<sup>2</sup>, G. E. Kugel<sup>3</sup>, M. Hafid<sup>4</sup>, J. Dec<sup>2</sup>**

*1- Institute of Physics, University of Silesia, Uniwersytecka 4, 40-007 Katowice, Poland*

*2- Institute of Materials Science, University of Silesia, 75 Pulkę Piechoty 1A, 41-500 Chorzów, Poland*

*3- LMPOS, University of Metz and Supélec Metz, 2 rue E. Belin, Metz 57070, France*

*4- LPGC Dept. of Physics BP 133, Faculty of Science, Ibn Tofail University, 14000 Kenitra, Morocco*

*antoni.kania@us.edu.pl*

Silver lithium niobate  $\text{Ag}_{1-x}\text{Li}_x\text{NbO}_3$  (ALN) solid solutions are promising lead-free piezoelectrics. For Li concentration  $x$  close to 0.1 they exhibit high values of piezoelectric constant ( $d_{33}=210$  pC/N), electro-mechanical coupling factor ( $k_{31}=0.7$ ) and Curie temperature ( $T_C=540$  K) [1,2]. X-ray and dielectric studies showed that for  $x \leq 0.05$  ALN solid solutions behave similarly to  $\text{AgNbO}_3$  and undergo the same sequence of phase transitions:  $M_1$ - $M_2$ - $M_3$ - $O_1$ - $O_2$ - $T$ - $C$ , where  $M_1$  is ferrielectric,  $M_2$  and  $M_3$  are antiferroelectric, and  $O_1$ ,  $O_2$ ,  $T$  and  $C$  are paraelectric phases [3,4] ( $M$  and  $O$  denote orthorhombic,  $T$  tetragonal and  $C$  cubic symmetries). Specific behavior of these compounds is related to structural disorder existing in the Nb-ion displacement subsystem. ALN materials with  $x \geq 0.06$  exhibit normal ferroelectric state and undergo transitions between ferroelectric rhombohedral  $R$ , antiferroelectric monoclinic  $M$ , and paraelectric tetragonal  $T$  and cubic  $C$  phases [3]. Study of lattice dynamics and its correlation with peculiarities of dielectric behavior of ALN system is a main aim of this study.

The yellow-green  $\text{Ag}_{1-x}\text{Li}_x\text{NbO}_3$  ( $0 \leq x \leq 0.1$ ) ceramics, with negligible amounts of secondary phases and density of 96% of theoretical value, have been prepared by the conventional solid state reaction method. They were examined by linear and nonlinear dielectric (100÷870 K), Raman scattering (10÷670 K) and differential scanning calorimetry DSC (200÷870 K) studies. The medium and high frequency parts (above 60  $\text{cm}^{-1}$ ) of the Raman spectra related to phonon modes were fitted using the model of independent damped oscillators. The low frequency (0÷60  $\text{cm}^{-1}$ ) of spectra, which consists of central peak CP and distinct vibrational band at 50  $\text{cm}^{-1}$  were fitted using the model of uncoupled relaxational and damped oscillator modes.

The main physical results were obtained from analysis of the low frequency part of Raman spectra. For  $x \leq 0.05$  the relaxational frequency  $\gamma_R$  significantly slows down at freezing temperature  $T_f$  and at the ferroelectric  $M_1$ - $M_2$  phase transition, while temperature dependence of total intensity of central peak corresponds to the  $M_2$ - $M_3$  maximum of dielectric permittivity. For  $x \geq 0.06$  a significant softening of two low frequency modes is observed when approaching the ferroelectric-paraelectric ( $R$ - $M$ ) phase transition. These, described above, characteristic temperatures were confirmed by nonlinear dielectric studies, which are very sensitive for instabilities of physical systems. Raman and dielectric studies showed that Nb-ion dynamics plays a crucial role in appearance of specific properties of silver niobate based materials.

Basing on results of dielectric and DSC studies the modified phase diagram of  $\text{Ag}_{1-x}\text{Li}_x\text{NbO}_3$  solid solutions was also proposed.

- [1] A. Saito, S. Uraki, H. Kakemoto, T. Tsurumi, S. Wada, Growth of lithium doped silver niobate single crystals and their piezoelectric properties, *Mat. Sci. Eng. B*, 120, 166-169, (2005).
- [2] D. Fu, M. Endo, H. Taniguchi, T. Taniyama, S. Koshihara, M. Itoh, Piezoelectric properties of lithium modified silver niobate perovskite single crystals, *Appl. Phys. Lett.* 92, 172905(3p.), (2008).
- [3] D. Fu, M. Endo, T. Taniguchi, M. Taniyama, S. Koshihara, Ferroelectricity of Li doped silver niobate ( $\text{Ag,Li}$ ) $\text{NbO}_3$ , *J. Phys.: Condens. Mater* 23, 75901(7p.), (2011).
- [4] A. Kania, S. Miga, Preparation and dielectric properties of  $\text{Ag}_{1-x}\text{Li}_x\text{NbO}_3$  (ALN) solid solutions ceramics, *Mat. Sci. Eng. B* 86, 128-133, (2001).

## **High frequency ultrasonic waves in ferroelectrics and related materials**

V. Samulionis<sup>1</sup>, J. Banys<sup>1</sup>, Yu. Vysochanskii<sup>2</sup>

<sup>1</sup> Physics Faculty, Vilnius University, Vilnius, Lithuania

<sup>2</sup> Institute of Solid State Physics, Uzhgorod University, Uzhgorod, Ukraine  
vytautas.samulionis@ff.vu.lt

High frequency ultrasonic spectroscopy is very useful to study ferroelectric materials since ultrasound directly probe elastic vibrations of a lattice. The investigation of linear and nonlinear ultrasonic properties of ferroelectrics and piezoelectrics is presented in this review contribution. The interaction of ultrasonic wave with various excitations such as polarization, free electrons, fast ions, ferroelectric domains and domain boundaries is discussed. Ultrasonic investigation of relaxation processes that govern nanocomposite elastic behaviour in various elastomers with inorganic and piezoelectric nanofillers also is presented.

# Raman Spectroscopy, Dielectric and Optical Properties of $\text{PbTiO}_3$ , $\text{Na}_{0.5}\text{Bi}_{0.5}\text{TiO}_3$ , $\text{PbTiO}_3\text{-Na}_{0.5}\text{Bi}_{0.5}\text{TiO}_3$ single crystals

P. Czaja<sup>1</sup>, J. Suchanicz<sup>1</sup>, K. Konieczny<sup>1</sup>, G. Stachowski<sup>2</sup>, D. Sitko<sup>2</sup>

*Institute of Technics, Pedagogical University, ul. Podchorążych 2, 30-084 Kraków, Poland*

*Institute of Physics, Pedagogical University, ul. Podchorążych 2, 30-084 Kraków, Poland*

e-mail of the presenting author: pczaja@up.krakow.pl

Ferroelectric crystals with perovskite structure, such as  $\text{PbTiO}_3$ ,  $\text{Na}_{0.5}\text{Bi}_{0.5}\text{TiO}_3$  and their solid solutions  $\text{PbTiO}_3\text{-Na}_{0.5}\text{Bi}_{0.5}\text{TiO}_3$  are very interesting materials. They exhibit strong anomalies in their physical properties (dielectric, optical, pyroelectric and piezoelectric). Lead titanate has a tetragonally distorted lattice and a Curie temperature of 763K [1]. Sodium bismuth titanate is a lead-free material with a Curie temperature of 593K [2-4]. Single crystals of  $\text{PbTiO}_3$  and  $\text{PbTiO}_3\text{-Na}_{0.5}\text{Bi}_{0.5}\text{TiO}_3$  were obtained by the flux growth method whereas crystals of  $\text{Na}_{0.5}\text{Bi}_{0.5}\text{TiO}_3$  were made by the Czochralski method. Raman spectroscopy and polarized light microscopy were performed at room temperature. The Raman patterns showed changes of the spectra of  $\text{PbTiO}_3\text{-Na}_{0.5}\text{Bi}_{0.5}\text{TiO}_3$  as compared to the spectra of the base materials  $\text{PbTiO}_3$  and  $\text{Na}_{0.5}\text{Bi}_{0.5}\text{TiO}_3$ . Using polarized light microscopy a domain structure was detected in examined samples. Dielectric permittivity measurements were carried out over a temperature range from 293K to 873K and a frequency range from 0.1 kHz to 2 MHz. These studies showed an increase of the dielectric permittivity from the solid solutions  $\text{PbTiO}_3\text{-Na}_{0.5}\text{Bi}_{0.5}\text{TiO}_3$  to the pristine materials  $\text{PbTiO}_3$  and  $\text{Na}_{0.5}\text{Bi}_{0.5}\text{TiO}_3$ . These crystals show interesting properties from the point of view of potential applications.

[1] B. Jaffe, W. Cook, H. Jaffe, Piezoelectric ceramics, London and New York: Academic Press, (1971).

[2] G. A. Smolenskii, V. A. Isupov, A. I. Agranovskaya, N. N. Krainik, New ferroelectrics of complex composition, Sov. Phys. Solid state, 2 (196) (1961), pp. 2651.

[3] C. F. Buhrer, Some properties of bismuth perovskites, J. Chem. Phys., 36(3) (1962), pp. 798-803.

[4] I.P. Pronin, P.P. Syrnikov, V. A. Isupov, V. M. Egorov, N. V. Zaitseva, Peculiarities of phase transitions in sodium bismuth titanate, Ferroelectrics, 25(1) (1980), pp. 395-397.

# Structural Potts-type Phase Transition in Perovskite Metal-Formate Frameworks: Effect of Dipolar Interactions

M. Šimėnas<sup>1</sup>, S. Balčiūnas<sup>1</sup>, M. Maczka<sup>2</sup>, J. Banys<sup>1</sup> and E. E. Tornau<sup>3</sup>

*1- Faculty of Physics, Vilnius University, Saulėtekio 9, LT-10222 Vilnius, Lithuania*

*2- Institute of Low Temperature and Structure Research, Polish Academy of Sciences, P. O. Box-1410, PL-50-950 Wrocław 2, Poland*

*3- Semiconductor Physics Institute, Center for Physical Sciences and Technology, Saulėtekio 3, LT-10257 Vilnius, Lithuania*

*Email address: mantas.simenas@ff.vu.lt*

Recently, the so called metal-organic frameworks (MOFs) emerged as a new type of crystalline compounds. They consist of metal centers, called nodes, and organic linkers, which connect the nodes together into functional frameworks. Some of the MOFs exhibit ferroelectric properties. In particular, the perovskite-based  $[(\text{CH}_3)_2\text{NH}_2][\text{M}(\text{HCOO})_3]$  ( $\text{M} = \text{Zn}^{2+}$ ,  $\text{Mn}^{2+}$ ,  $\text{Fe}^{2+}$ ,  $\text{Co}^{2+}$  and  $\text{Ni}^{2+}$ ) family demonstrates the inherent ferroelectric-type phase transition in 160–180 K temperature range [1, 2]. A proper microscopic description of the observed phase transition in this family requires a detailed study of the experimentally determined MOF structures. As a representative of this family we have chosen the compound with  $\text{M} = \text{Mn}^{2+}$ , since the structure of this MOF is known [3] in both high- and low-temperature phases.

We proposed and numerically studied the model which describes the order-disorder structural phase transition in  $[(\text{CH}_3)_2\text{NH}_2][\text{Mn}(\text{HCOO})_3]$ . In this MOF the three-fold degeneracy of the molecular cation in the HT phase implies that each  $\text{DMA}^+$  ion might be described by the three states. Therefore, in our model the bonding between the  $\text{DMA}^+$  cations and  $\text{M}(\text{HCOO})_3^-$  cages is effectively mimicked by the three-state nearest-neighbour Potts-type interaction supplemented by the dipolar interactions between the cations. The model is constructed on a simple cubic lattice where each lattice point can be occupied by a  $\text{DMA}^+$  cation in one of the available states. In our model the main interaction is the nearest-neighbor Potts-type interaction, which effectively accounts for the H-bonding between the  $\text{DMA}^+$  and the  $\text{M}(\text{HCOO})_3^-$ . The established bonding significantly deforms the  $\text{MnO}_6$  octahedra which in turn influence the whole  $\text{Mn}(\text{HCOO})_3^-$  cage causing a certain state of the neighboring cation.

The model also accounts for the dipolar interactions which are evaluated for the real monoclinic lattice based on a thorough analysis of the structural information and density functional theory calculations. The magnitude of the dipolar interaction was estimated to be approximately 50 K, which is much smaller than the observed phase transition temperature, indicating that this interaction is important, but not the main ordering mechanism. We employ the Monte Carlo method to numerically solve the model. The calculations are supplemented with the experimental measurements of the temperature dependent electric polarization. The obtained results indicate that the three-state Potts model correctly describes the phase transition order in these MOFs, while the dipolar interactions are necessary to obtain a better agreement with the experimental polarization. We show that substantial dipolar interactions can modify the ground state of our model: instead of uniform layers with the same polarization direction we can obtain the layers with alternating polarization direction.

[1] P. Jain, N. S. Dalal, B. H. Toby, H. W. Kroto and A. K. Cheetham, *Journal of the American Chemical Society*, 130, 10450–10451 (2008).

[2] P. Jain, V. Ramachandran, R. J. Clark, H. D. Zhou, B. H. Toby, N. S. Dalal, H. W. Kroto and A. K. Cheetham, *JACS*, 131, 13625–13627 (2009).

[3] M. Sánchez-Andújar, S. Presedo, S. Yáñez-Vilar, S. Castro-García, J. Shamir and M. A. Senaris-Rodríguez, *Inorganic Chemistry*, 49, 1510–1516 (2010).



# Aging in a Relaxor Ferroelectric: what can we learn from it

**J. Dec<sup>1</sup>, W. Kleemann<sup>2</sup>**

*1- Institute of materials Sciences, University of Silesia, PL-40-007 Katowice Poland*

*2- Angewandte Physik, Universität Duisburg-Essen, D-47048 Duisburg, Germany*

*jan.dec@us.edu.pl*

Relaxor ferroelectrics (REFs) have attracted much attention owing to their significant piezoelectric response and their wide variety of applications to numerous piezoelectric devices [1]. However, despite long-standing intensive studies the microscopic origin of relaxoriness still remains a subject of hot debates. As a result a number of conflicting models explaining the physical nature of this very unique, among solids, phenomenon. While one group of researchers believes in the relevance of so called polar nanoregions (PNRs) [2 - 6], others promote an alternative model, which attributes the unusual properties of REFs to the development of a state formed by nanoscale multidomains [7 - 9].

The polar correlations are usually considered as being promoted by quenched random electric fields (RFs) [10]. Within this approach the local polarization of individual PNR is controlled by the fluctuations of the RFs and thus precludes macroscopic ferroelectric symmetry breaking, even if uniformly charged chemically ordered regions counteract as observed in the heterogeneous relaxor-like lead magnesium niobate,  $\text{PbMg}_{1/3}\text{Nb}_{2/3}\text{O}_3$  (PMN), [11]. These PNR interact dipolarly and consequently, on cooling, a cluster-glassy ground state sets in as proposed in [12]

Within the other model the unusual dielectric response of REFs comes from the side-wall motion of the nanoscale domains [7]. Actually the glassy state concept versus nanodomain model is intensely debated

One of the experimental possibilities for distinguishing between these two models is to study effects of aging. While the domain-like growth typically displays cumulative aging, the aging in glassy systems includes characteristic rejuvenation and memory effects [13].

The goal of this contribution is to report results of our systematic studies of the aging processes in the canonical PMN relaxor system in the vicinity of its glass temperature. The experimental results confirm the superdipolar glassy scenario of relaxors.

- [1] K. Uchino, *Piezoelectric Actuators and Ultrasonic Motors* (Kluwer, Deventer, 1996).
- [2] D. Viehland, S. J. Jang, L. E Cross, and M. Wuttig, *J. Appl. Phys.* **68**, pp. 2916-2921 (1990).
- [3] B. Dkhil, J. M. Kiat, G. Calvarin, G. Baldinozzi, S. B. Vakhrushev, and E. Suard, *Phys. Rev. B* **65**, pp. 024104/1-8 (2001).
- [4] P. M. Gehring, S. Wakimoto, Z.-G. Ye, and G. Shirane, *Phys. Rev. Lett.* **87**, 277601 (2001).
- [5] R. Blinc, V. V. Laguta, and B. Zalar, *Phys. Rev. Lett.* **91**, pp. 247601/1-4 (2003).
- [6] V. V. Shvartsman, W. Kleemann, T. Łukasiewicz, and J. Dec, *Phys. Rev. B* **77**, pp. 054105/1-7 (2008).
- [7] A. K. Tagantsev and A. E. Glazounov, *Phys. Rev. B* **57**, 18 (1998).
- [8] D. Fu, H. Taniguchi, M. Itoh, S.-ya Koshihara, N. Yamamoto, and S. Mori, *Phys. Rev. Lett.* **103**, pp. 207601/1-4 (2009).
- [9] J. Hlinka, *J. Adv. Dielectr.* **2**, pp. 124006/1-6 (2009).
- [10] V. Westphal, W. Kleemann, and M. Glinchuk, *Phys. Rev. Lett.* **68**, pp. 847-950 (1992).
- [11] B. P. Burton, E. Cockayne, and U. V. Waghmare, *Phys. Rev. B* **72**, 063113 (2005).
- [12] W. Kleemann, *J. Mater. Sci.* **41**, 106 (2006); *J. Adv. Dielectr.* **2**, pp. 1241001/1-13 (2012).
- [13] E. V. Colla K. Sullivan, and M. B. Weissman, *J. Appl. Phys.* **119**, 014109 (2016).

# Phase transition in $0.1\text{Na}_{0.5}\text{Bi}_{0.5}\text{TiO}_3$ - $0.6\text{SrTiO}_3$ - $0.3\text{PbTiO}_3$ solid solutions

Š. Svirskas<sup>1</sup> J. Banys<sup>1</sup> V. V. Shvartsman<sup>2</sup> D. Lupascu<sup>2</sup> M. Duncce<sup>3</sup> E. Birks<sup>3</sup> R. Ignatans<sup>3</sup>

<sup>1</sup>Faculty of Physics, Vilnius University, Sauletekio av. 9/3b., Vilnius, Lithuania

<sup>2</sup>Institute for Materials Science and Center for Nanointegration Duisburg-Essen (CENIDE), University of Duisburg-Essen, Universitätsstrasse 15, Essen, Germany

<sup>3</sup>Institute of Solid State Physics, University of Latvia, Kengaraga 8, Riga, Latvia

Main author email address: sarunas.svirskas@ff.vu.lt

Sodium bismuth titanate ( $\text{Na}_{0.5}\text{Bi}_{0.5}\text{TiO}_3$ ) is one of the most promising lead-free piezoelectric materials. Recently, multi-component solid solutions based on  $\text{Na}_{0.5}\text{Bi}_{0.5}\text{TiO}_3$  have attracted significant attention [1, 2]. Such solid solutions may drastically enhance piezoelectric properties of the parent material. Moreover, sometimes it is possible to increase the depolarization temperature, as well as to reduce the dielectric losses and conductivity.

This report deals with  $0.4\text{Na}_{0.5}\text{Bi}_{0.5}\text{TiO}_3$ - $0.6\text{SrTiO}_3$  solid solutions with addition of lead titanate ( $\text{PbTiO}_3$ ). Particular compositions of this family have a spontaneous 1st order phase transition from relaxor to ferroelectric state. The aim of this report is to discuss the origin and peculiar behavior of this phase transition in the  $0.1\text{Na}_{0.5}\text{Bi}_{0.5}\text{TiO}_3$ - $0.6\text{SrTiO}_3$ - $0.3\text{PbTiO}_3$  (0.1NBT-0.6ST-0.3PT) solid solution.

The report concentrates on the results of several experimental techniques. The X-ray diffraction, broadband dielectric spectroscopy experiments were carried out. In addition, the measurements of polarization, displacement and pyroelectric current measurements were performed. The temperature dependence of remnant polarization extracted from measurements of pyroelectric current shows an unusual critical exponent  $\beta$  ( $P \sim (T - T_c)^\beta$ ). The critical exponents which do not coincide with Landau-Ginzburg-Devonshire (LGD) theory were already reported for several relaxor-like systems [3]. There are several interpretations of such behavior: 1) the deviation from the LGD theory is related to the rich defective states in the material [4], 2) according to Kleemann some relaxor systems have critical exponents which are consistent with random-field Ising model [5, 6].

The broadband dielectric spectroscopy data show large dispersion above the phase transition temperature in microwave region. Such behavior resembles the order-disorder type ferroelectrics although obvious critical slowing down is not observed. It is important to stress that at temperatures above the phase transition the ferroelectric state can be induced by external electric field in a significant temperature interval. This allows us to attribute the high temperature phase as a relaxor phase.

Finally, the nanoscale measurements by piezoresponse force microscopy (PFM) revealed unusual behavior of local polarization. There exist several types of grains which have very different domain structure and show different temperature dependences of the local piezoresponse. This may explain the peculiar macroscopic response of the material under investigation. It seems that some kind of frustration exists between the different grains which complicate the formation of long range order, thus giving rise to a relaxor-like properties at elevated temperatures. The relation between the microscopic and macroscopic properties will be revealed in the report and discussed in more detailed manner.

## References

- [1] J. Roedel, W. Jo et al. J. Amer. Ceram. Soc., vol. 92(6) 1153-1177 (2009)
- [2] D. Damjanovic, N. Klein et al. Funct. Mater. Lett., 03, 5 (2010)
- [3] P. Lehnen, W. Kleemann et al., The European Physical Journal B, vol. 14, 633-637 (2000)
- [4] J. F. Scott, J. Phys.: Cond. Matt., vol. 18, 7123-7134 (2006)
- [5] W. Kleemann, J. Dec et al. Europhys. Lett., vol. 57, 14 (2002)
- [6] W. Kleemann, J. Mat. Sci., vol. 41, 129-136 (2006)

# Chemical disorder and $^{207}\text{Pb}$ hyperfine fields in the new magnetoelectric multiferroic $\text{Pb}(\text{Fe}_{1/2}\text{Sb}_{1/2})\text{O}_3$

R. O. Kuzian<sup>1</sup>, **I. V. Kondakova**<sup>1</sup>, Yu. Zagorodny<sup>1</sup>, V. V. Laguta<sup>1,2</sup>, V. Chlan<sup>3</sup>, H. Štěpánková<sup>3</sup>

1- Institute for Problems of Materials Science NAS Ukraine, Krjijanovsky 3, 03142 Kyiv, Ukraine

2- Institute of Physics AS CR, Cukrovarnicka 10, 162 00 Prague 6, Czech Republic

3 - Charles University in Prague, Faculty of Mathematics and Physics, V Holešovičkách 2, 180 00 Prague 8, Czech Republic

[ikondakova@gmail.com](mailto:ikondakova@gmail.com)

Multiferroics are materials having two or more order parameters (for instance, magnetic, electric or elastic) coexisting in the same phase. Among them, magnetoelectric materials that exhibit coupling of electric polarization and magnetization are very promising for spintronic and magnetic random access memory applications.

In the present study we report a detailed NMR experiments on recently synthesized samples of the double perovskite  $\text{Pb}(\text{Fe}_{1/2}\text{Sb}_{1/2})\text{O}_3$  (PFS) [1] which have revealed strong correlation of hyperfine field on  $^{207}\text{Pb}$  nucleus with the disorder in Fe/Sb sublattice (Figure 1).

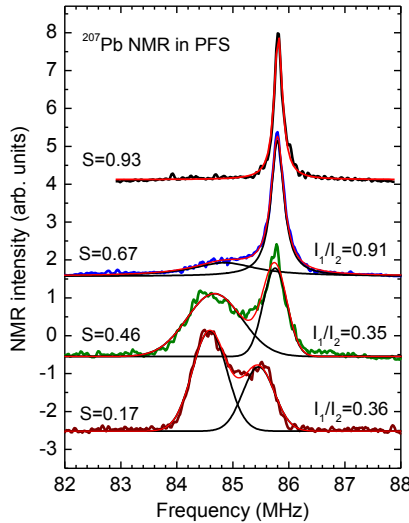


Figure 1  $^{207}\text{Pb}$  NMR spectra measured in PFS with different degree of the chemical ordering between  $\text{Fe}^{3+}$  and  $\text{Sb}^{5+}$  ions, from  $S=0.93$  (the most ordered sample) to  $S=0.17$  (almost disordered sample). The ratio of integral intensities of two components in the spectra corresponding to chemically ordered and disordered regions is indicated as well.

We have studied this phenomenon by considering the electronic structure of PFS within the framework of LSDA+U scheme implemented in the full- potential local-orbital (FPLO) code. We have assumed that stoichiometry of PFN is preserved on a short-range scale. In order to model the disorder in PFS, we consider a periodic lattice with a supercell containing several perovskite cells and study such periodic system with different configurations of chemical order (ion distributions) [2]. When the supercell contains 40 atom ( $2 \times 2 \times 2$ ,  $\text{Pb}_8\text{Fe}_4\text{Sb}_4\text{O}_{24}$ ), six configurations of chemical ordering are possible in the double perovskites. For every configuration, nearest Fe ions occupy four vertexes of the cube formed by B ions around the Pb. Thus, each Pb ion is surrounded by four equidistant nearest Fe ions (the calculations were performed for the ideal cubic structure). Surprisingly, the calculations show that the value of electron density on Pb nucleus drastically depends on the arrangement of Fe ions. We discuss the physical reasons of such dependence for PFS and other Pb-based double perovskite compounds.

The support of the GA CR under project No. 13-11473S is gratefully acknowledged.

[1] V. V. Laguta, V. A. Stephanovich, M. Savinov, M. Marysko, R. O. Kuzian, I. V. Kondakova, N. M. Olekhovich, A. V. Pushkarev, Yu. V. Radyush, I. P. Raevski, S. I. Raevskaya and S. A. Prosandeev, Superspin glass phase and hierarchy of interactions in multiferroic  $\text{PbFe}_{1/2}\text{Sb}_{1/2}\text{O}_3$ : an analog of ferroelectric relaxors? *New J. Phys.* **16**, 113041(1) - 113041(19), (2014).

[2] R. O. Kuzian, I. V. Kondakova, A. M. Dar'c, and V. V. Laguta, Magnetic interactions in disordered perovskite  $\text{PbFe}_{1/2}\text{Nb}_{1/2}\text{O}_3$  and related compounds: Dominance of nearest-neighbor interaction. *Phys. Rev. B* **89**, 024402(1) - 024402(9), (2014).



**ABSTRACTS OF ORAL PRESENTATIONS**  
**7<sup>th</sup> September**

# Size Induced Phase Transitions without Critical Size and Reentrant Phase Appearance in Nanoferroelectrics Originated from Flexoelectric and Vegard Effects

**M. Glinchuk<sup>1</sup>, A. Morozovska<sup>2</sup>**

*1- Institute for Problems of Materials Science, National Academy of Sciences of Ukraine, Krjijanovskogo 3, 03680 Kyiv-142, Ukraine*

*2- Institute of Physics, National Academy of Sciences of Ukraine, pr. Nauky 46, 03028 Kyiv, Ukraine*

*Main author email address: glin@materials.kiev.ua*

Based on Landau-Ginzburg-Devonshire approach, we explore the critical size disappearance at size induced phase transitions and reentrant phase occurrence in nanoferroics. Our calculations have shown that the physical mechanism of the exciting phenomenon can be the flexo-chemo effect, being the synergy of the spontaneous flexoelectric stresses and the chemical pressure induced by ion vacancies via Vegard effect. The flexo-chemo effect can lead to the remarkable changes of the nanoferroics phase diagrams, such as non-monotonic increase of the transition temperature and long-range order enhancement appearing under the size decrease and fulfilment of definite conditions. Namely, these phenomena take place when contribution to transition temperature of flexoelectric and Vegard effects is larger than sum of depolarization field, surface tension and correlation effect contributions. The conditions of coexistence of critical size and conventional size induced phase transition from ferroelectric to paraelectric phase at the size smaller than critical one are also considered. Since the flexo-chemo effect should exist in any nanostructured ferroics, obtained analytical results can be predictive for many of them. As a concrete example of the primary ferroics, we consider ferroelectric nanoparticles and have shown that a commonly expected transition from the ferroelectric to paraelectric phase at some small critical size is absent, so that the critical size loses its sense. Contrarily, the stabilization of the ferroelectric phase manifests itself by the enhancement of the transition temperature and polarization with the particle size decrease (ferroelectric phase reentrance), which was observed earlier in the tetragonal BaTiO<sub>3</sub> nanospheres of radii 5–50 nm [1] and stayed unexplained up to now. The main results are published recently in the paper [2].

[1] J. Zhu, W. Han, H. Zhang, Z. Yuan, X. Wang, L. Li, C. Jin, Phase coexistence evolution of nano BaTiO<sub>3</sub> as function of particle sizes and temperatures, *J. Appl. Phys.*, **112**, 064110 (2012).

[2] A. N. Morozovska and M. D. Glinchuk, Flexo-chemo effect in nanoferroics as a source of critical size disappearance at size-induced phase transitions, *J. Appl. Phys.*, **119**, 094109 (2016).

# Cobalt Doped Barium Titanate - New Multiferroic?

R. Bujakiewicz-Koronska<sup>1</sup>

1- Institute of Physics, Pedagogical University, Podchorążych Str.2, 30-084 Krakow, Poland  
Email address: sfbujaki@cyf-kr.edu.pl

In the aim of searching new multiferroics, the effects of  $\text{Co}^{3+}$  dopant on structural, magnetic, mechanical, dielectric and piezoelectric properties of  $(1-x)\text{Ba}_{0.95}\text{Pb}_{0.05}\text{TiO}_3+x\text{Co}_2\text{O}_3$ ,  $x \leq 0.10$  (BPTC) ceramics were studied [1-3]. New ceramics were prepared by the conventional hot-sintering method.

The Co-doping induces a small decrease of the  $(c/a)$  tetragonality of the perovskite lattice and leads to the gradual shift of the ferroelectric transition temperature from 398K for  $x=0$  down to 357K for  $x \leq 0.02$ . The conductivity activation energies are about 0.8–0.9 eV in agreement with the results of ab initio calculations. The high temperature region of the conductivity can be described by the migration of oxygen vacancies added to compensate for the charge deficiency due to  $\text{Co}^{3+}$  valence at the B-site of the perovskite lattice. The doping of barium titanate with  $\text{Co}^{3+}$  ions reduced high dielectric losses in the ferroelectric-paraelectric phase transition in BPTC. The BPTC shows relaxor-like behaviour in the temperature range from 125 to 225 K. (dielectric data) - Fig. 1a,b. the polar nanoregions, which exist in the material, are caused by the presence of acceptor-oxygen vacancy dipoles  $\text{Co}^{3+}\text{-V}_{\text{O}}^{1-}$  in highly polarizable lattice. Substitution  $\text{Pb}^{2+}$  ions in A-site caused reduction of the Curie temperature and smoothed of Young modulus in wide range of temperatures (DMA data).

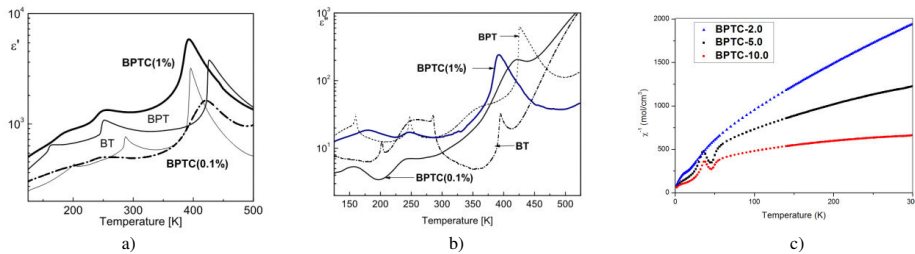


Figure 1. Results of measurements: a) real part of dielectric permittivity for BT, BPT, BPTC samples, b) imaginary part of dielectric permittivity for BT, BPT, BPTC samples, c) reciprocal susceptibility as a function of temperature for samples BPTC at 2 K and  $H=50$  Oe .

The X-ray diffraction revealed that all specimens show tetragonal perovskite structure with Co ions in Ti positions. For the different  $x$  values, the lattice parameters remain very similar to unsubstituted BPT. The Young modulus  $E$  was measured by an ultrasound method. An increase of  $\text{Co}^{3+}$  in BPTC led to an increase of  $E$  values from 106 GPa for pure BPT to 133 GPa for BPTC with  $x=0.10$ . Moreover, the Poisson number changed from 0.25 to 0.3 while a stiffness moduli changed from 42 to 52 GPa. The doping by  $\text{Co}^{3+}$  modifies the electromechanical properties significantly. We observed the existence of a boundary of a solubility  $\text{Co}_2\text{O}_3$  in BPT around  $x=0.02$  value. The mechanical quality factor  $Q_{\text{mt}}$  increases, whereas the other parameters we mentioned, exhibit more complex changes with increasing  $x$  in the studied systems. Positron annihilation studies of defects in BPTC showed that besides the acceptor-like vacancies  $\text{V}_{\text{Ba}}$  and  $\text{V}_{\text{Ti}}$  donor-like oxygen vacancies  $\text{V}_{\text{O}}$  are present abundantly. Additionally, grain boundaries may contain open volume, e.g. vacancy complexes.

Based on our analysis, we can conclude that BPTC is the type I, new multiferroic material (Khomskii classification [4]) with a weak coupling between magnetic and ferroelectric properties.

**Acknowledgements.** The author acknowledges the CPU time allocation at Academic Computer Centre CYFRONET AGH in Cracow and the PL-Grid Infrastructure.

- [1] R. Bujakiewicz-Koronska, A. Kalvane, Y. Zhydachevskii, B. Garbarz-Głos, W. Śmiga, L. Vasylechko, J. Czerwicz, A. Suchocki, A. Kamińska, W. Piekarczyk, Structural and dielectric properties of  $\text{Ba}_{0.95}\text{Pb}_{0.05}\text{TiO}_3+0.1\%\text{Co}_2\text{O}_3$ , *Ferroelectrics*, 436:1, pp. 62–71, (2012).
- [2] E. Markiewicz, R. Bujakiewicz – Koronska, D. Majda, L. Vasylechko, A. Kalvane, M. Matczak, Effect of cobalt doping on the dielectric response of  $\text{Ba}_{0.95}\text{Pb}_{0.05}\text{TiO}_3$  ceramics, *J Electroceram*, 32, pp. 92–101, (2014).
- [3] R. Bujakiewicz-Koronska, E. Markiewicz, D. M. Nalecz, L. Vasylechko, M. Balanda, M. Fitta, E. Juszyńska-Galazka, A. Kalvane Physical properties of  $(1-x)\text{Ba}_{0.95}\text{Pb}_{0.05}\text{TiO}_3+x\text{Co}_2\text{O}_3$  ( $x=0, 0.1, 0.3, 0.5, 1.0, 2.0\text{wt}\%$ ) ceramics, *Ceram Int*, 41:3, pp. 3983–3991, (2015).
- [4] D. Khomskii, Classifying multiferroics: Mechanisms and effects, *Physics*, 2:20, pp. 1–8, (2009).

# Structural and magnetic phase transitions in $\text{Bi}_{1-x}\text{Ca}_x\text{Fe}_{1-x}\text{Mn}_x\text{O}_3$ multiferroics

M. V. Silibin<sup>1\*</sup>, D.V. Karpinsky<sup>2</sup>, I.O. Troyanchuk<sup>1</sup>

<sup>1</sup>National Research University of Electronic Technology "MIET", 124498 Zelenograd, Moscow, Russia

<sup>2</sup>Scientific-Practical Materials Research Centre of NAS of Belarus, 220072 Minsk, Belarus

sil\_m@mail.ru

$\text{BiFeO}_3$ -based perovskite-like materials have attracted a great attention of the researchers in the field of condensed matter physics [1]. Magnetic and electric dipole ordering coexist in these materials well above room temperature and corresponding cross-coupling effects are interesting for basic and applied physics [2]. To be appropriate for technological applications these materials should have a remnant magnetization which is cancelled due to cycloidal modulation while it can be managed via chemical substitution [3].

Crystal and magnetic structure of  $\text{Bi}_{1-x}\text{Ca}_x\text{Fe}_{1-x}\text{Mn}_x\text{O}_3$  ( $x \leq 0.3$ ) multiferroics have been studied by X-ray diffraction and magnetometry techniques. It is shown that dopant concentration increase leads to the phase transition from the polar rhombohedral phase into the nonpolar orthorhombic one. The polar phase is characterized by antiferromagnetic structure, wherein the lightly-doped compounds show metamagnetic behavior. Remnant magnetization grows up with dopant concentration increase.

X-ray diffraction data obtained for the  $\text{Bi}_{1-x}\text{Ca}_x\text{Fe}_{1-x}\text{Mn}_x\text{O}_3$  ceramics at room temperature have testified that the compounds with  $x \leq 0.18$  are single-phase with rhombohedral structure characteristic of pure  $\text{BiFeO}_3$  [4]. Chemical doping leads to a decrease of the rhombohedral distortions and modifies structural parameters (Fig. 1) of the compounds thus affecting their magnetic properties. Calculated structural data have indicated an increase of the chemical bond angle  $\text{Fe}(\text{Mn}) - \text{O} - \text{Mn}(\text{Fe})$  and related bond length with doping concentration which strongly affect the exchange interactions between  $\text{Fe}^{3+}$  and  $\text{Mn}^{4+}$  ions.

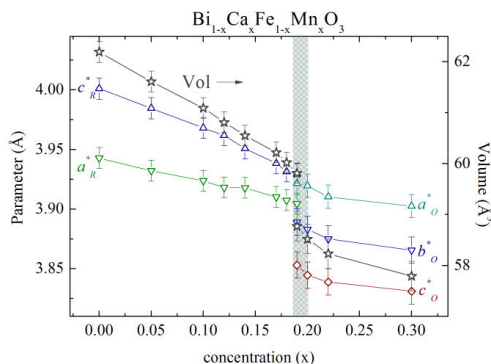


Fig. 1. The unit cell parameters calculated for  $\text{Bi}_{1-x}\text{Ca}_x\text{Fe}_{1-x}\text{Mn}_x\text{O}_3$  ceramics based on X-ray and neutron diffraction data

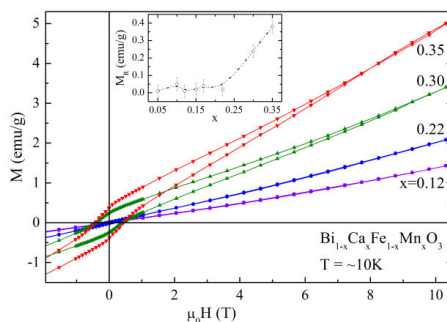


Fig. 2. Field dependencies of magnetization obtained at  $T \approx 10$  K. The inset shows the evolution of remnant magnetization of the compounds.

Structural transition into the nonpolar orthorhombic phase does not change significantly the magnetic structure of the compounds. Increase of the dopant concentration modifies the magnetic structure from spatially modulated antiferromagnetic one into antiferromagnetic with weak ferromagnetic component. The remnant magnetization gradually increases with dopant concentration (up to  $\sim 0.07$  emu/g at room temperature for  $x=0.17$  compound). Temperature decrease down to 10 K leads to notable change in magnetic anisotropy and spontaneous magnetization. Magnetization dependencies observed for heavily doped compounds have testified their complex magnetic behavior which can be explained in the model assuming a coexistence of long-range antiferromagnetic order along with the short-range clusters having dominant ferromagnetic interactions.

This work was supported by the BRFFR (project #F16R-066, F15RM-012) and RFBR (project #16-58-0082 bel\_a, 15-58-04009 bel\_mol\_a).

[1] G. Catalan, J.F. Scott, Physics and Applications of Bismuth Ferrite, Adv. Mater., 21, 2463 (2009)

[2] M. Fiebig, Revival of the magnetoelectric effect, J. Phys. D: Appl. Phys., 38, R123 (2005)

[3] D. V. Karpinsky et al., Enhanced ferroelectric, magnetic and magnetoelectric properties of  $\text{Bi}_{1-x}\text{Ca}_x\text{Fe}_{1-x}\text{Ti}_x\text{O}_3$  solid solutions, Solid State Commun., 151, 536 (2011).

[4] A. Palewicz et al., Atomic displacements in  $\text{BiFeO}_3$  as a function of temperature: neutron diffraction study, Acta Cryst. B63, 537 (2007).



# Magnetic properties of the $\text{Bi}_{1-x}\text{La}_x\text{Fe}_{0.5}\text{Sc}_{0.5}\text{O}_3$ ( $0.00 \leq x \leq 0.80$ ) perovskites

**E.L. Fertman<sup>1</sup>, A.V. Fedorchenko<sup>1,2</sup>, V.A. Desnenko<sup>1</sup>, O.V. Kotlyar<sup>1</sup>, A.N. Salak<sup>3</sup>, D.D. Khalyavin<sup>4</sup>, N.M. Olekhovich<sup>5</sup>, A.V. Pushkarev<sup>5</sup>, Yu.V. Radyush<sup>5</sup>, A. Feher<sup>2</sup>**

<sup>1</sup>B.Verkin Institute for Low Temperature Physics and Engineering of NAS of Ukraine, Prospekt Nauky, 47, 61103 Kharkiv, Ukraine

<sup>2</sup>Institute of Physics, Faculty of Science, P.J. Šafárik University in Košice, 9 Park Angelinum, 04154 Košice, Slovakia

<sup>3</sup>DEMaC/CICECO, University of Aveiro, 3810-193 Aveiro, Portugal

<sup>4</sup>STFC, Rutherford Appleton Laboratory, Chilton, Didcot, Oxfordshire, OX11 0QX, United Kingdom

<sup>5</sup>Scientific-Practical Materials Research Centre of NASB, P. Brovka Str., 19, 220072 Minsk, Belarus

fertman@ilt.kharkov.ua

Magnetic properties of multiferroic metastable  $\text{Bi}_{1-x}\text{La}_x\text{Fe}_{0.5}\text{Sc}_{0.5}\text{O}_3$  ( $0.00 \leq x \leq 0.80$ ) ceramics synthesized under high-pressure (6 GPa, 1500 K) were studied using a SQUID magnetometer technique between 5 K and 300 K in an applied fields up to 6 kOe under both zero-field-cooled (ZFC) and field-cooled (FC) conditions. Isothermal magnetization measurements were performed between  $-50$  kOe and  $50$  kOe between  $5$  K and  $230$  K.

$\text{Bi}_{1-x}\text{La}_x\text{Fe}_{0.5}\text{Sc}_{0.5}\text{O}_3$  is a multiferroic perovskite system with a rich phase diagram. Three consecutive phases with different crystal structures appear as the lanthanum content is increased: the as-prepared phase at  $x \leq 0.05$  is an antipolar  $Pnma$  [1] while an incommensurately modulated phase with the  $Imma(00\gamma)s00$  superspace group [2] is observed for  $0.10 \leq x \leq 0.30$  and a non-polar  $Pnma$  phase [3] is stable at  $x \geq 0.35$ . Temperature-dependent magnetic measurements revealed a long-range magnetic ordering of the antiferromagnetic type with a weak ferromagnetic contribution below  $T_N \sim 206$ – $260$  K for all the compositions studied (Fig. 1a). The ferromagnetic contribution increases with decreasing temperature down to  $5$  K. Both the Neel temperature  $T_N$  and the paramagnetic Curie temperature  $\Theta$  increase in a non-monotonous way with increase of the lanthanum content. It indicates both the enhancement of ferromagnetic correlations in paramagnetic state on the approaching  $T_N$  and the enlargement of the ferromagnetic contribution in the magnetically-ordered state.

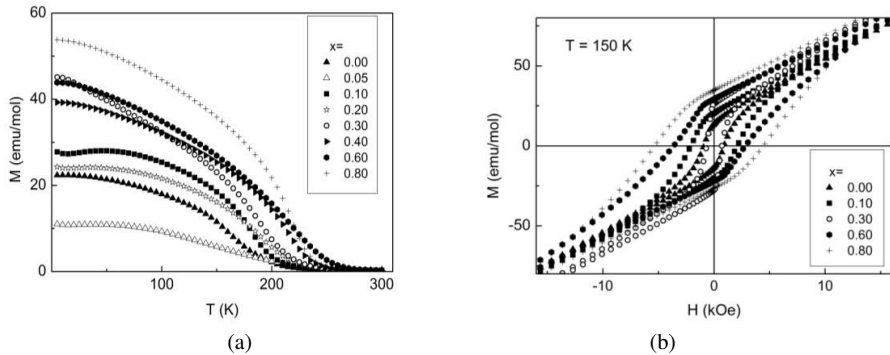


Figure 1. (a) Temperature dependent FC ( $H=100$  Oe) magnetization for the  $\text{Bi}_{1-x}\text{La}_x\text{Fe}_{0.5}\text{Sc}_{0.5}\text{O}_3$  perovskites. The numbers denote the values of  $x$ . (b) Hysteresis loops of the total magnetization of the  $\text{Bi}_{1-x}\text{La}_x\text{Fe}_{0.5}\text{Sc}_{0.5}\text{O}_3$  measured at  $150$  K after zero-field cooling.

The  $\text{Bi}_{1-x}\text{La}_x\text{Fe}_{0.5}\text{Sc}_{0.5}\text{O}_3$  samples demonstrate a small temperature dependent spontaneous magnetic moment,  $(-0.05) - (+0.1)$  emu/g at  $5$  K. Below  $T_N$ , field-dependent magnetization measurements showed well-defined hysteresis loops, which are typical for canted antiferromagnets (Fig. 1b). No saturation of magnetization is observed up to  $H=50$  kOe. A strong magnetic field effect on the properties of the  $\text{Bi}_{0.65}\text{La}_{0.35}\text{Fe}_{0.5}\text{Sc}_{0.5}\text{O}_3$  perovskite, which is close to the compositional transition between antipolar and non-polar phases, has been observed.

This work was supported by the TUMOCs project. This project has received funding from the European Union's Horizon 2020 research and innovation programme under the Marie Skłodowska-Curie grant agreement No 645660. Also this work was supported by the Slovak Grant Agency through grant VEGA 1/0145/13.

[1] D.D. Khalyavin, A.N. Salak, N.M. Olekhovich, A.V. Pushkarev, Yu.V. Radyush, P. Manuel, I.P. Raevski, M.L. Zheludkevich, M.G.S. Ferreira, Polar and antipolar polymorphs of metastable perovskite  $\text{BiFe}_{0.5}\text{Sc}_{0.5}\text{O}_3$ , Phys. Rev. B 89, 174414(1-11) (2014).

[2] D.D. Khalyavin, A.N. Salak, A.B. Lopes, N.M. Olekhovich, A.V. Pushkarev, Yu.V. Radyush, E.L. Fertman, V.A. Desnenko, A.V. Fedorchenko, P. Manuel, A. Feher, J.M. Vieira, M.G.S. Ferreira, Magnetic structure of an incommensurate phase of La-doped  $\text{BiFe}_{0.5}\text{Sc}_{0.5}\text{O}_3$ : Role of antisymmetric exchange interactions, Phys. Rev. B 92, 224428(1-7) (2015).

[3] D.D. Khalyavin, A.N. Salak, P. Manuel, N.M. Olekhovich, A.V. Pushkarev, Yu.V. Radyush, A.V. Fedorchenko, E.L. Fertman, V.A. Desnenko, M.G.S. Ferreira, Antisymmetric exchange in La-substituted  $\text{BiFe}_{0.5}\text{Sc}_{0.5}\text{O}_3$  system: Symmetry adapted distortion modes approach, Z. Kristallogr. Cryst. Mater 230, 767-774 (2015).

## MULTIFERROELECTRICITY OF PEROVSKITE MANGANATES

B. Dabrowski<sup>1</sup>, K. Chapagain<sup>1</sup>, O. Chmaissem<sup>1</sup>, S. Kolesnik<sup>1</sup>, V. Goian<sup>2</sup> and S. Kamba<sup>2</sup>,<sup>1</sup>*Department of Physics, Northern Illinois University, DeKalb, IL, USA;*<sup>2</sup>*Institute of Physics, Academy of Sciences of the Czech Republic*

bdabrowski@niu.edu

Multiferroics that exhibit simultaneous ferroelectric and magnetic orders are a topic of current intense investigation both to understand how these two disparate order parameters interact and because of the promising possibility of controlling the magnetic properties electronically and vice versa [1,2]. Known Type-II or ‘improper’ multiferroics exhibit strong magnetic-ferroelectric coupling, however, the ferroelectric order parameter is more than two orders-of-magnitude smaller than robust nonmagnetic ferroelectrics such as the prototypical  $\text{Ba}^{2+}\text{Ti}^{4+}\text{O}_3$  with  $T_F = 405$  K for which the hybridization of the occupied oxygen  $p$  orbitals to the empty Ti  $d$  orbitals precludes the possibility of magnetic order. The Type-I or ‘proper’ multiferroics with robust displacive-type ferroelectric order are not only rare but also they typically exhibit disparate ordering temperatures and very weak coupling between the order parameters. Recently new promising multiferroics have been discovered with strong coupling. Our earlier work on magnetic  $\text{Sr}_{1-x}\text{Ba}_x\text{Mn}^{4+}\text{O}_3$  materials for  $x \leq 0.2$  did not reveal ferroelectricity predicted for elongated Mn-O bonds [3]; however, expanding the Ba concentrations to higher values ( $x \geq 0.45$ ) succeeded in achieving robust ferroelectricity [4]. These ceramics exhibit unique ferroelectricity ( $T_F > 300$  K) and antiferromagnetism ( $T_N \sim 200$  K) originating exclusively from the  $\text{Mn}^{4+}(d^3)$  cations.

By advancing elaborate synthesis processes, which are necessary to avoid the more stable hexagonal polymorphs, we were able to prepare and study structural, magnetic and ferroelectric properties [5,6] of highly strained multiferroics for  $x = 0.4-0.45$ . The classical displacive-type ferroelectric phase occurs with a polarization of several  $\mu\text{C}/\text{cm}^2$  when the Mn ions move out of the center of the  $\text{MnO}_6$  octahedral units at  $T_F \sim 350$  K. The Mn spins order below  $T_N \sim 210$  K into a simple G-type magnetic structure while the displacive distortions decrease dramatically (80 – 100 %) demonstrating that the two order parameters are strongly coupled. A spin gap of 4.6(5) meV and the magnon density of states peaking at 43 meV characterize the ground state spin dynamics. The ferroelectric phase transition has a signature of a crossover from displacive to order-disorder type. The phonons are coupled with a central mode but contribution to  $\epsilon'$  is rather small. The lowest-frequency polar phonons are overdamped above  $T_N$  and they exhibit pronounced softening on heating towards  $T_C$ .

We have recently extended investigation of manganites to the Ti-substituted  $\text{Sr}_{1-x}\text{Ba}_x\text{Mn}_{1-y}\text{Ti}_y\text{O}_3$  system for which displacive distortions significantly exceed that of  $\text{BaTiO}_3$  and  $T_F \sim 420$  K. The  $T_N$  decreases to below 200 K and the suppression of ferroelectricity below  $T_N$  is reduced to  $\sim 50$  %, i.e., we achieved displacive-type multiferroic with large spontaneous polarization. I will describe unique properties of these materials.

**References:**

- [1] S-W. Cheong and M. Mostovoy, *Nature Mater.* **6**, 13 (2007).
- [2] R. Ramesh and N. A. Spaldin, *Nature Mater.* **6**, 21 (2007).
- [3] O. Chmaissem, et al., *Phys. Rev. B* **64**, 134412 (2001).
- [4] H. Sakai, et al., *Phys. Rev. Lett.* **107**, 137601 (2011).
- [5] K. Pratt, et al., *Phys. Rev. B* **90**, 140401 (2014).
- [6] V. Goian, et al., *Journal of Physics: Condensed Matter* **28**, 175901 (2016).

# Electrophysical properties of PMN-PT-ferrite ceramic composites

D. Bochenek<sup>1</sup>, P. Niemiec<sup>1</sup>, R. Skulski<sup>1</sup>, D. Brzezińska<sup>1</sup>

<sup>1</sup> - University of Silesia, Institute of Technology and Mechatronics, 12 Żytnia Str., 41-200, Sosnowiec, Poland;

Corresponding author: [dariusz.bochenek@us.edu.pl](mailto:dariusz.bochenek@us.edu.pl)

Ferroelectromagnetic composites based on PMN-PT powder and Ni-Zn ferrite powder have been obtained and described. Ferroelectric component of composite i.e.  $(1-x)\text{PMN}-(x)\text{PT}$  (with  $x = 0.25, 0.28, 0.31, 0.34, 0.37, 0.40$ ) was synthesized using sol-gel method and next obtained in the powder form. The magnetic component i.e. nickel-zinc ferrite was obtained using classical ceramic method. Investigated six compositions of PMN-PT have rhombohedral symmetry, tetragonal symmetry and were from morphotropic area. Final composite samples were obtained by classical methods using calcination route and pressureless final sintering (densification). For such obtained ceramic composite samples following investigations have been made: SEM microstructure, dielectric investigations (Fig.1), investigations of electromechanical properties (Fig.2) and DC electric conductivity. Compositions 0.72PMN-0.28PT (with rhombohedral symmetry) and 0.63PMN-0.37PT (with tetragonal symmetry) were obtained and investigated earlier [1]. Magnetic properties will be described in [2].

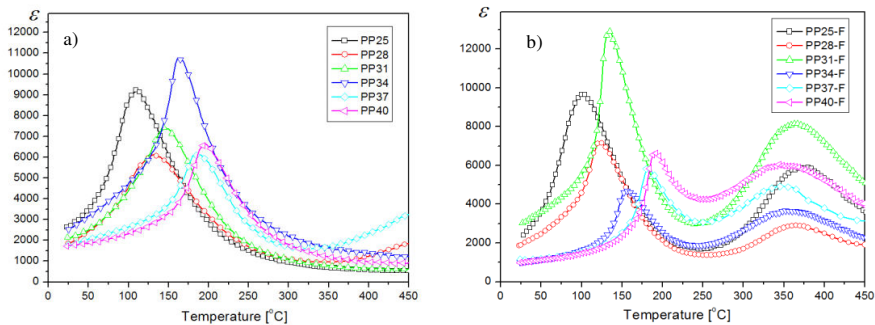


Figure 1 Temperature dependencies of dielectric permittivity for the PMN-PT ceramics (a) and for PP-F ceramic composites (b) (heating cycle, frequency 1 kHz).

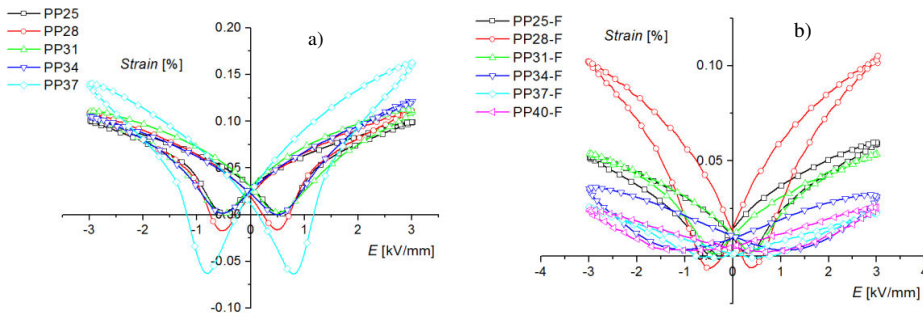


Figure 2 Bipolar strain-electric field loops ( $S-E$ ) for (a) PP ceramics and (b) PP-F composite materials.

The obtained results confirmed ferroelectric and weak ferromagnetic properties at room temperature for the obtained ceramic composite samples.

**Keywords:** PMN-PT-ferrite ceramic composites, electric properties

[1] D. Bochenek, P. Niemiec R. Skulski, A. Chrobak, P. Wawrzala, Ferroelectric and magnetic properties of the PMN-PT-nickel zinc ferrite multiferroic ceramic composite materials, *Materials Chemistry and Physics* 157 (2015) 116-123.

[2] R. Skulski, D. Bochenek, P. Niemiec, A. Chrobak, Technology and main properties of PMN-PT-ferrite multiferroic ceramic composite materials, *Adaptive, Active And Multifunctional Smart Materials Systems*, Book Series Advances in Science and Technology, (2016) in review.

# Modifications of tin thiohypodiphosphate ferroelectrics by doping and indiffusion

**A. A. Grabar, K. E. Glukhov, A. A. Molnar, A.A. Kohutych,  
I. M. Stoika, and Yu. M. Vysochanskii**

*Institute for Solid State Physics and Chemistry of Uzhhorod National University,  
54 Voloshin st., 88000, Uzhhorod, Ukraine*

*alexander.grabar@uzhnu.edu.ua*

Ferroelectric crystals of the tin thiohypodiphosphate ( $\text{Sn}_2\text{P}_2\text{S}_6$ ) family are studied as efficient photorefractive materials which find numerous applications in the schemes of the information processing, dynamic interferometry, phase conjugation and correction of the laser beams on the base of dynamic holography principles. Photorefractive parameters of these materials, which are determined by high values of the linear electrooptic coefficients and photosensitivity in red and near infrared spectral ranges, are characterized by high diffraction efficiency together with short enough (milliseconds) formation times of the photorefractive holograms [1]. The diffusive mechanism of the space-charge grating formation and in result their non-local character in these materials provides a wave mixing between interacting light beams, and this allows their utilizations in the dynamical holographic schemes that are based on the effect of the laser beam interaction and stationary energy transfer.

Optical, dielectric, photoelectric and photorefractive parameters of  $\text{Sn}_2\text{P}_2\text{S}_6$  can be substantially modified by their doping. It was shown earlier [1] that the most efficient is doping of this crystal with Sb, Te and Bi during the growth, that allows to enhance substantially the two-wave mixing coefficients. Nevertheless, further search of the new efficient dopants and other ways of the sample modification is still an important task.

In the communication we present the results of the complex investigations of the optical, photorefractive and dielectric parameters modified by different ways, namely: by the doping at crystal growth by vapor-transport technique, by variation their stoichiometry, and by thermally-induced indiffusion of the various metals (Ag, Cu, Cr) from the surfaces into the bulk of the previously grown  $\text{Sn}_2\text{P}_2\text{S}_6$  samples.

The optimal conditions for the thermally-induced indiffusion process, i.e. temperature, duration and direction relative to crystallographic axes, were determined. It is also found that, among all tested chemical elements, the most efficient is diffusion of copper, that provide almost uniform distribution of the incorporated impurities. A comparison of the optical and dielectric parameters of Cu-doped and Cu-indiffused crystals shows a substantial difference, that can be explained by altered locations of copper atoms in the lattice. Similar peculiarities demonstrate the  $\text{Sn}_2\text{P}_2\text{S}_6$  crystals modified by Ag doping and indiffusion.

The doped and modified by indiffusion crystals were also tested by measurements of their photorefractive parameters. It was found that an impact of the doping and indiffusion on the photorefractive parameters leads to an increasing of the compensative component of the space-charge grating, that is connected with increased dark electric conductivity and screening of the space-charge gratings.

The experimental results are in good correlation with *ab initio* calculations of the electron spectra and defect states in the  $\text{Sn}_2\text{P}_2\text{S}_6$  lattice. These calculations allow to estimate the most probable positions and energy of the various defect levels (impurities, vacancies) in the gap, and also to estimate possible variations of the physical parameters of the crystals. Besides, the model calculations permit to evaluate the local potential barriers for diffusion of various atoms in the  $\text{Sn}_2\text{P}_2\text{S}_6$  lattice. The results demonstrate significantly different values of the barriers heights, depending on both the species and the direction of propagation, that are in good agreement with available experimental data.

[1] A.A. Grabar, M. Jazbinšek, A. N. Shumelyuk, Yu. M. Vysochanskii, G. Montemezzani, P. Günter. Photorefractive Materials and Their Applications, v.2 (Springer Springer Series in Optical Sciences, 114), "Photorefractive effects in  $\text{Sn}_2\text{P}_2\text{S}_6$ ", p. 327-362 (2007).

# ***Ab initio* band electronic structure and molecular dynamics of $(\text{C}_3\text{N}_2\text{H}_5)_2\text{SbF}_5$ crystals**

**B. Andrievskiy<sup>1</sup>, Z. Czapla<sup>2,3</sup>**

1- Faculty of Electronics and Computer Sciences, Koszalin University of Technology, Śniadeckich 2, 75-453, Koszalin, Poland

2- Department of Physics, Opole University of Technology, Ozimska 75, 45-271 Opole, Poland

3- Institute of Experimental Physics, University of Wrocław, M. Borna 9, 50-204 Wrocław, Poland

bohdan.andrievskiy@tu.koszalin.pl

The bis(imidazolium) pentafluoroantimonate(III) crystal  $(\text{C}_3\text{N}_2\text{H}_5)_2\text{SbF}_5$  is one of the known crystal of the general chemical formula  $\text{A}_2\text{SbX}_5$ , where  $\text{A} = \text{NH}_4^+$  and  $\text{C}_3\text{N}_2\text{H}_5^+$  and  $\text{X} = \text{F}$  and  $\text{Cl}$ . In the case of the  $(\text{NH}_4)_2\text{SbF}_5$  a sequence of phase transition was found and ferroelastic properties below 292 K [1, 2]. The  $(\text{C}_3\text{N}_2\text{H}_5)_2\text{SbF}_5$  was found to exhibit first order structural phase transition from orthorhombic room temperature phase (space group  $Pnma$ ) to monoclinic one (space group  $P2_1/c$ ) at about 220 K [3]. Structural studies revealed strong disorder of imidazolium cations at room temperature (phase I). Below phase transitions temperature (phase II) imidazolium cations are totally ordered. Disorder of cations is seen well in phase I, where enhanced values of permittivity (45-55) were observed along the  $a$ - and  $c$ -axes. At the phase transition temperature an abrupt decrease of permittivity connected with freezing of imidazolium cations was observed. Reorientational motion of imidazolium cations were confirmed and described in dielectric dispersion studies in the frequency range 10 kHz-1 MHz [4]. Above room temperature the crystal reveals the properties, which permit to treat it as the ionic conductor [4].

We present results of *ab initio* band electronic structure and equilibrium molecular dynamics studies of  $(\text{C}_3\text{N}_2\text{H}_5)_2\text{SbF}_5$  obtained for the first time.

We have revealed that the characteristic features of partial density of electronic states (PDOS) of the crystal (Fig. 1) are caused by: (1) relatively large number of PDOS valence bands caused by small interatomic interaction in the  $b$ -direction of the crystal, and (2) clear hybridization of the electronic states within separate PDOS band due to the relatively high interatomic interaction within one structural  $b$ -layer of the crystal.

Results of *ab initio* molecular dynamics study of  $(\text{C}_3\text{N}_2\text{H}_5)_2\text{SbF}_5$  have shown that, in the temperature range 190 K - 210 K, the time dependences of mean square displacement (MSD)  $\sigma^2(r)$  are the most growing functions in comparison to the lower and higher temperatures (Fig. 2), that indicates the highest degree of the diffusion like movement of atoms accompanying the rebuilding of crystal structure. Such a rebuilding of crystal structure relates to the experimentally detected phase transition in  $(\text{C}_3\text{N}_2\text{H}_5)_2\text{SbF}_5$ .

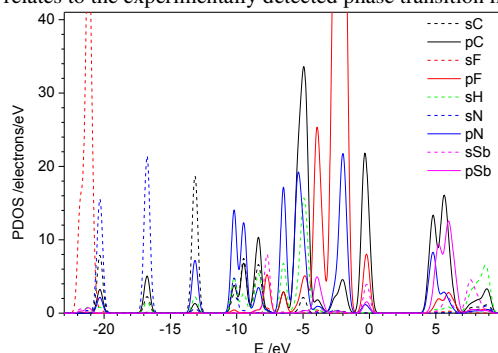


Figure 1 Partial density of electronic states of  $(\text{C}_3\text{N}_2\text{H}_5)_2\text{SbF}_5$  at the monoclinic symmetry group no. 11 for all chemical elements (H, C, N, F, Sb) and different orbital moments ( $s$ ,  $p$ ).

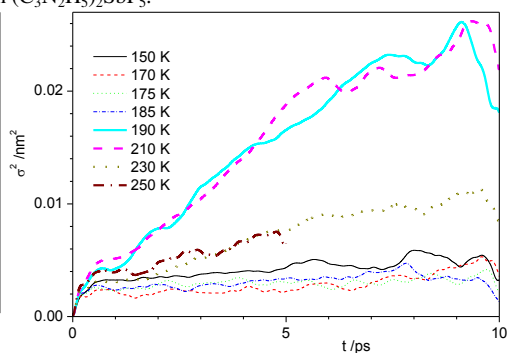


Figure 2 Time evolution of MSD of  $(\text{C}_3\text{N}_2\text{H}_5)_2\text{SbF}_5$  for different temperatures.

- [1] L. Avkutsij, R. Davydovitch, I. Zemnukova, D. Gordienko, V. Urbanovicius, J. Grigas, Phys. Stat. Sol. (b), vol. 116, p. 483, (1983).
- [2] Z. Czapla, S. Dacko, Ferroelectrics 140 (1993) 271-275.
- [3] Z. Czapla, M.K. Krawczyk, A. Ingram, O. Czupiński, J. Phys. Chem. Solids, vol. 87, pp. 233-237, (2015).
- [4] A. Ingram, Z. Czapla, S. Wacke, Curr. Appl. Phys., vol. 16, pp. 278-283, (2016).

# Dielectric Spectroscopy of Barium Strontium Titanate Epitaxial Thin Films

**R. Grigalaitis, R. Mackevičiūtė, M. Ivanov, Š. Bagdzevičius, and J. Banys**

*Vilnius University, Faculty of Physics, Sauletekio av. 3, Vilnius, Lithuania*

*robertas.grigalaitis@ff.vu.lt*

Ferroelectrics are multifunctional materials exhibiting a lot of appealing properties resulting from the presence of the spontaneous polarization, high and tunable dielectric permittivity and attractive piezoelectric activity. Thin films are widely used in electronics, because it is possible to minimize the size of electronic components. Ferroelectrics in thin film form have been used in various radio and microwave frequency (RF) devices and in non-volatile memories. Components based on ferroelectric films are also being developed for various sensor and actuator applications and for tunable microwave circuits.

Most promising to date tunable dielectrics for RF applications are barium strontium titanate (BST) and strontium titanate (ST) because of the unique combination of high tunability and low RF loss in paraelectric phase. BST attracted investigators as a suitable dielectric material for bypass capacitors, IR detectors, and tunable microwave device applications because of its high dielectric constant, low dielectric loss and good thermal stability. Here we present the results of the dielectric permittivity and tunability of BST/LSMO//LSAT heterostructure. Since the main problem hindering the use of ordinary plane capacitor formalism is relatively bad conductivity of the lower electrode, a new theoretical model will be presented which could describe the impedance of such complex heterostructure. Also, based on impedance analysis of BST/SRO//STO heterostructures the strain-dependent anisotropic change of electron/hole mobility will be discussed and the model, which explains changes in the temperature dependence of the conductivity, will be proposed.

# Physical limits of electrocaloric cooling devices

G. Suchaneck

*Solid State Electronics Lab, TU Dresden, 01062 Dresden, Germany*

*Main author email address: Gunnar.Suchaneck@tu-dresden.de*

Electrocaloric (EC) basic research is mainly focused on materials with a first-order phase transition. This provides a large polarization change in a narrow temperature region near the Curie point. In this case, the upper bound of the EC effect established both experimentally and theoretically is 5 to 10 K.

Recently, we have considered an alternative approach: EC device operation at high electric fields  $E$  above the temperature of the maximum dielectric permittivity  $T_m$  [1]. Here, the EC response is determined by the temperature coefficient of dielectric permittivity while dielectric losses are comparably low. Also, the condition that the heat rejected to the sink is larger than the heat absorbed from the load is easily fulfilled.

Since the current estimates of the EC upper bound are related to the presence of a phase transition, we have proposed a new upper bound which is based on the fact that only a certain energy density  $e_{max}$  might be stored in a dielectric - equivalent to a limit in electrostatic pressure:

$$\Delta T_{EC}^{max} < -\frac{T}{2c} \cdot \frac{1}{\varepsilon} \cdot \frac{\partial \varepsilon}{\partial T} \cdot \varepsilon_0 E_{max}^2 \quad (1)$$

where  $\Delta T_{EC}$  is the EC temperature change,  $T$  the temperature,  $c$  the volumetric specific heat,  $\varepsilon$  the relative dielectric permittivity,  $\varepsilon_0$  the vacuum dielectric permittivity, and  $E$  the electric field strength. Our estimation explains the high values of the EC effect previously obtained in relaxor PLZT [2].

For a negligible remanent polarization, the maximum entropy change is then given by:

$$\Delta S_m = -\frac{3\varepsilon_0 [\varepsilon(0)]^2}{2aC} \cdot (1 + \alpha E_m^2)^{1/3} \approx -\frac{3\varepsilon_0 [\varepsilon(0)]^2}{2\alpha^{2/3} C} E_m^{2/3} \quad (2)$$

where  $\varepsilon(0)$  is the low field value of  $\varepsilon$ ,  $C$  the Curie constant derived from its temperature dependence, and  $\alpha$  an empirical coefficient describing the field dependence of  $\varepsilon$  for a second-order phase transition [3]:

$$\varepsilon(E) \approx \frac{\varepsilon(0)}{(1 + \alpha E^2)^{1/3}} \quad (3)$$

Consequently, the EC effect will be increased at lower  $C$ , i.e., by means of introducing disorder or doping with larger-sized isovalent atoms.

A figure of merit of EC materials performance might be derived of considering the coefficient of performance of the refrigeration cycle, the refrigeration capacity and the Fourier number per cycle time [1]:

$$FoM = \frac{c \cdot \Delta T_{EC}^2 \cdot \delta T \cdot \kappa}{\varepsilon_0 \cdot \tan \delta} \cdot \frac{1}{T \cdot E^2 \cdot d^2} \quad (4)$$

with  $\delta T$  the full width at half maximum of the entropy versus temperature curve,  $\kappa$  the thermal conductivity,  $\tan \delta$  the dielectric loss tangent, and  $d$  the thickness of the EC material. With regard to our upper bound of the electrocaloric effect, relaxor ferroelectrics are the best choice for EC application.

Optimized lead-free EC relaxor materials possess an isovalent B-site substitution at the crossover from ferroelectric to relaxor behavior at a critical dopant fraction of about 0.23 corresponding to the 3D site percolation limit of the dopant bonds [4].

EC relaxor materials is characterized by different time scales, two electronic ones due to (i) polarization response and (ii) polar nanoregion dynamics and two thermal ones, (i) the thermal transit time during which the sample reaches internal thermal equilibrium (called by us the acoustic limit) and (ii) the time constant of the material's volume during which thermal equilibrium with the environment is established. In order to provide adiabatic depolarization during the cooling step, the decay time of the applied electric field should not exceed the acoustic limit. On the other hand, the performance of EC cooling elements is limited by the thermal time constants of heat switches or by the heat transfer coefficient to the gaseous or liquid heat transfer agent of active EC regenerators.

Thus, cooling power densities of a few W/cm<sup>2</sup> and temperature spans in the order of a 20 K (in regeneration systems) are gainable at a cycle time of 100 ms using lead-free relaxor EC elements.

[1] G. Suchaneck, G. Gerlach, Lead-free relaxor ferroelectrics for electrocaloric cooling, *Materials Today: Proceedings*, 3, 622-631 (2016).

[2] S. G. Lu, B. Rožič, Q. M. Zhang, Z. Kutnjak, X. Li, E. Furman, L.J. Gorny, M. Lin, B. Malič, M. Kosec, R. Blinc, R. Pirc, Organic and inorganic relaxor ferroelectrics with giant electrocaloric effect, *Appl. Phys. Lett.*, 97, 162904 (2010).

[3] V.L. Ginzburg, The theory of ferroelectric phenomena (in Russian), *Usp. Fiz. Nauk* 38, 490-525 (1949).

[4] J. Wang, Z. Zhou, W. Zhang, T.M. Garoni, Y. Deng, Bond and site percolation in three dimensions, *Phys. Rev. E*, 87, 052107 (2013).

# Hysteresis Loop of Electrocaloric Effect in Ferroelectricity

**Tongqing Yang, Jinfei Wang**

*Functional Materials Research Laboratory, College of Materials Science and Engineering, Tongji University,  
4800 Cao'an Road, 201804, Shanghai, China*

*E-mail: yangtongqing@tongji.edu.cn*

It is well known, the polarization of polar domain in ferroelectric materials is orientated and reversed with the alternating electric field, and the hysteresis loops of polarization-electric field (  $P$ - $E$  ) and strain-electric field (  $S$ - $E$  ) are observed. For electrocaloric effect ( EC ), the temperature change with the application and removal of electric field is also attributed to the change of polarization with the applied field. In most report for EC, the temperature change is shown as an abrupt jump or slump due to the applied electric field that is a pulsed wave. Obviously, it is impossible to observe the hysteresis loop of EC. In our research, both sine wave and pulsed wave electric field are applied to samples in direct measurement, and temperature-electric field hysteresis loop (  $T$ - $E$  ) is observed only in measurement of sine wave. The  $T$ - $E$  hysteresis loop display a shape of butterfly, just like the shape of  $S$ - $E$ . The frequency and electric field dependence of EC are also given. The obtained results will be helpful for us to know the electrocaloric effect further.

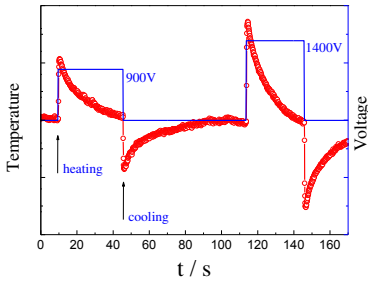


Fig. 1 Electrocaloric effect response measured directly with an applied field of pulsed wave

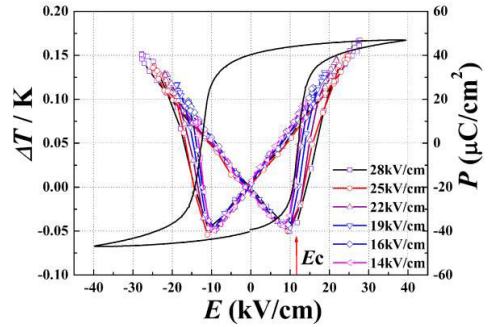


Fig. 2 Temperature-electric field hysteresis loop of electrocaloric effect and polarization-electric field hysteresis loop

- [1] A. S. Mischenko, Q. Zhang, J. F. Scott, R. W. Whatmore, and N. D. Mathur, Giant Electrocaloric Effect in Thin-Film  $\text{PbZr}_{0.95}\text{Ti}_{0.05}\text{O}_3$ , *Science*, vol.311, 1270-1271, 2006
- [2] Jinfei Wang, Tongqing Yang, Shengchen Chen, Gang Li, Qingfeng Zhang, Xi Yao, Nonadiabatic direct measurement electrocaloric effect in lead-free  $\text{Ba,Ca}(\text{Zr,Ti})\text{O}_3$  ceramics, *Journal of Alloys and Compounds*, 550, 561–563, 2013
- [3] Jinfei Wang, Tongqing Yang, Kun Wei, and Xi Yao, Temperature-electric field hysteresis loop of electrocaloric effect in ferroelectricity-  
-Direct measurement and analysis of electrocaloric effect. I, *Appl. Phys. Lett.*, 102, 152907, 2013



# Polarization switching kinetics in composite ferroelectrics: case studies on porous and fatigued ceramics

**Y.A. Genenko<sup>1</sup>, S. Zhukov<sup>1</sup>, R. Khachatryan<sup>1</sup>, C. Galassi<sup>2</sup>, J. Glaum<sup>3</sup>, H. Kungl<sup>4</sup>, J. Koruza<sup>1</sup>, J. Schultheiß<sup>1</sup>, H. von Seggern<sup>1</sup>**

<sup>1</sup> Institute of Materials Science, Technische Universität Darmstadt, Jovanka-Bontschits-Str. 2, 64287 Darmstadt, Germany

<sup>2</sup> CNR-ISTEC National Research Council, Institute of Science and Technology for Ceramics, Via Granarolo 64, I-48018 Faenza (RA), Italy

<sup>3</sup> Department of Materials Science and Engineering, Norwegian University of Science and Technology, Trondheim, Norway

<sup>4</sup> Forschungszentrum Jülich, Institut für Energie- und Klimaforschung IEK-9, 52425 Jülich, Germany

genenko@mm.tu-darmstadt.de

Switching of spontaneous polarization in ferroelectrics subject to an external pulse electric field is a key process for many applications. In perfectly ordered crystals this dynamic property may be described in terms of the classic Kolmogorov-Avrami-Ishibashi (KAI) nucleation and growth theory [1] exploiting a single characteristic switching time  $\tau$ . In heterogeneous ferroelectric materials, such as polycrystalline thin films or bulk ceramics, polarization switching becomes dispersive, i.e., exhibits a wide spectrum of switching times related to different regions in a sample and may be described as superposition of polarization reversal in different regions [2]:

$$\Delta P(E_m, t) = \Delta P_{\max} \int_{-\infty}^{\infty} d(\ln \tau) G(\ln \tau) \left\{ 1 - \exp\left(-\left(t/\tau\right)^{\beta}\right) \right\} \quad (1)$$

where  $\Delta P_{\max}$  is the maximum total polarization reached at infinite time  $t$ ,  $\beta$  is the so called Avrami index dependent on the dimensionality of the nucleating reversed polarization domain and  $G(\ln \tau)$  is the statistical distribution function of the switching times. Based on the hypothesis that the spatial distribution of the switching times is caused by the spatial distribution of the local electric field values the Inhomogeneous Field Mechanism

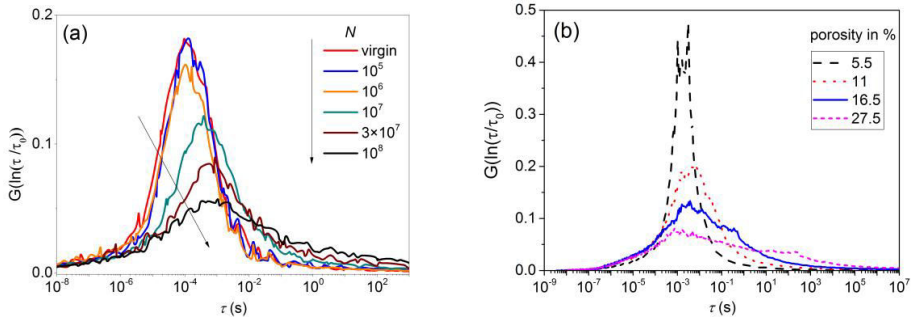


Figure 1. (a) Evolution of the statistical distribution of switching times during bipolar electric cycling of a commercial PZT material PIC 151; the number of cycles  $N$  is indicated on the plot. (b) Simulated statistical distributions of switching times in porous materials with spherical pores for different values of the total porosity as indicated on the plot.

(IFM) model [3] allows determination of the statistical distributions of local field values and switching times as well as the local relation of the switching time on the field  $\tau(E)$ .

When exposed to bipolar electric cycling, ferroelectric materials exhibit degradation of different properties, particularly, they demonstrate loss of saturation and remanent polarizations and slowing down of the polarization reversal response. Thereby numerical regions of a ferroelectric material become unswitchable reminding of the ferroelectric-dielectric composite. The IFM analysis reveals widening and shifting to the larger times of the statistical switching time distributions in the course of fatigue as shown in the Figure 1(a). Porous ceramics present another sort of composite materials which allow control over their properties by introducing a certain amount of air filled pores. Their polarization dynamics can be particularly affected by the presence of oriented pores of anisotropic shapes. FEM simulations of such systems were performed (Figure 1(b)) and compared with the IFM analysis of the response of porous PZT with isotropic and oriented anisotropic pores.

[1] Y. Ishibashi and Y. Takagi, Note on Ferroelectric Domain Switching, J. Phys. Soc. Jap. 31, pp. 506-510 (1971).

[2] A.K. Tagantsev, I. Stolichnov, N. Setter, J.S. Cross, and M. Tsukada, Non-Kolmogorov-Avrami switching kinetics in ferroelectric thin films, Phys. Rev. B 66, 214109/1-6 (2002).

[3] Y.A. Genenko, S. Zhukov, S.V. Yampolskii, J. Schütrumpf, R. Dittmer, W. Jo, H. Kungl, M.J. Hoffmann, and H. von Seggern, Universal Polarization Switching Behavior of Disordered Ferroelectrics, Adv. Funct. Mater. 22, pp. 2058-2066 (2012).



**ABSTRACTS OF ORAL PRESENTATIONS**  
**8<sup>th</sup> September**

# Phase transitions, ferroelasticity, possible ferroelectricity and antiferroelectricity in $[(C_2H_5)_4N(CH_3)_4NMeX_4]$ crystals

Z. Czapla

*Department of Physics, Opole University of Technology, Ozimska 75,  
45-370 Opole, Poland*

*z. czapla@po.opole.pl*

The crystals of the formula  $[(C_2H_5)_4N(CH_3)_4NMeX_4]$  belong to large family of hybrid organic-inorganic materials. We studied properties of the crystals with a formula  $[(C_2H_5)_4N(CH_3)_4NZnBr_4]$ ,  $[(C_2H_5)_4N(CH_3)_4NMnBr_4]$  and  $[(C_2H_5)_4N(CH_3)_4NZnCl_4]$ . In the paper thermal, structural, dilatometric, dielectric, and polarized microscopic observation are presented. The studies revealed reversible first order phase transition of ferroelastic type in  $[(C_2H_5)_4N(CH_3)_4NMnBr_4]$  at 484/482 K on heating and cooling, respectively. At room temperature phase crystal is tetragonal with the space group  $P\bar{4}2_1m$  and above the phase transition temperature it is orthorhombic with the space group  $P2_12_12$ . This change of symmetry is characteristic for ferroelastic type of phase transition. The transition belongs to Aizu species  $\bar{4}2mF222$  and the change of symmetry was confirmed in domain structure appearance in (110) and  $(\bar{1}10)$  planes of tetragonal phase. The transition fulfils group-subgroup relation but symmetry is reduced on heating. We can classified the transition as reverse Landau type transition. The phase transition exhibiting such features has not been presented so far. In the  $[(C_2H_5)_4N(CH_3)_4NZnBr_4]$  crystal analogous transition is observed at 490/488 K on heating and cooling, respectively. In both crystals dielectric studies revealed significant increase of losses above 450 K connected with ionic conductivity. Dielectric studies of the  $(C_2H_5)_4N(CH_3)_4NZnBr_4$  revealed low temperature phase transitions seen as two anomalies of electric permittivity at 105 K and 90 K. The low temperature phases show ferroelectric and antiferroelectric features.

# Anomalous Magnetoelectric Effect in Multiferroic $\text{Pb}(\text{Fe}_{1/2}\text{Nb}_{1/2})\text{O}_3$ and its Solid Solution with $\text{PbTiO}_3$

V. V. Laguta<sup>1,2</sup>, A. N. Morozovska<sup>3</sup>, E. A. Eliseev<sup>1</sup>, I. P. Raevski<sup>4</sup>, S. I. Raevskaya<sup>4</sup>, E. I. Sitalo<sup>4</sup>, S. A. Prosandeev<sup>4,5</sup>, and L. Bellaiche<sup>5</sup>

1- Institute for Problems of Materials Science, National Academy of Sciences of Ukraine, Krjijanovskogo 3, 03142 Kyiv, Ukraine

2- Institute of Physics AS CR, Cukrovarnicka 10, 162 53 Prague, Czech Republic

3- Institute of Physics, National Academy of Sciences of Ukraine, 46, pr. Nauky, 03028 Kyiv, Ukraine

4- Research Institute of Physics, Southern Federal University, Stachki Ave. 194, 344090, Rostov-on-Don, Russia

5- Physics Department and Institute for Nanoscience and Engineering, University of Arkansas, Fayetteville, Arkansas 72701, USA

laguta@materials.kiev.ua; laguta@fzu.cz

Multiferroics are materials having two or more order parameters (for instance, magnetic, electric or elastic) coexisting in the same phase. They have emerged as an important topic in condensed matter physics due to both their intriguing physical behaviors and a broad variety of novel physical applications they enable. The unique physical properties of multiferroics originate from the complex interactions among the structural, polar and magnetic long-range order parameters [1]. In magnetoelectric (ME) multiferroic materials, besides of the linear and biquadratic couplings of magnetic and electric order parameters, quadratic paramagnetoelectric (PME) effect should exist in the paramagnetic phase below the  $T_C$  temperature of the paraelectric-to-ferroelectric phase transition, where the electric polarization is non-zero. In general, the quadratic ME coupling is much less studied in magnetoelectrics than the linear coupling while the former one can be even larger than its linear counterpart in antiferromagnetic (AFM) materials.

In the present work, we report results of detailed study of the quadratic ME effect of single crystals and high-resistive ceramics of  $\text{Pb}(\text{Fe}_{1/2}\text{Nb}_{1/2})\text{O}_3$  (PFN) and  $(1-x)\text{PFN}-x\text{PbTiO}_3$  (PFN-PT). The ceramics enabled performing measurements of dielectric properties and ME response up to the temperatures of 400-450 K without marked influence of conductivity. The ME coefficient was determined by a dynamic method as a function of

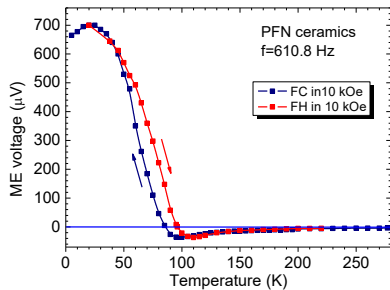


Figure 1 Temperature dependence of the magnetoelectric voltage in PFN ceramics in the magnetic field 10 kOe.

bias magnetic field  $H_{dc}$  at small ac field  $h_{ac}=1-5$  Oe and frequencies 0.2-1 kHz by measuring the voltage across the sample. The concentration of PT addition to PFN varied from  $x=0$  up to 0.2. All samples were characterized by standard X-ray diffraction, dielectric and magnetic measurements [2].

We have found that PME coefficient shows a pronounced maximum near the ferroelectric phase transition temperature and then decreases sharply down to zero on a subsequent temperature increase. Its temperature dependence correlates well with the ones of the piezoelectric coefficient or dielectric permittivity in the ferroelectric paramagnetic phase. The ME coefficient is sufficiently small at room and higher temperatures,  $(1-6)\times 10^{-18}$  s/A. However, it essentially increases at low temperatures (up to  $10^{-16}$  s/A) and shows a sign reversal around the Neel temperature (Fig. 1). In the AFM phase

the quadratic ME effect related to the long-range AFM order competes with the PME effect. In PFN-PT solid solution, the temperature interval of the PME effect is extended to higher temperatures in accordance with the shift of the paraelectric-to-ferroelectric phase transition temperature with adding  $\text{PbTiO}_3$ . In 0.8PFN-0.2PT composition only the PME effect exists to the lowest temperatures as the long-range AFM order is destroyed by Ti dilution.

The theoretical description of the quadratic ME effect in the framework of the Landau theory of phase transitions, describes qualitatively well its temperature behavior. In particular, the Landau theory predicts that the PME coefficient is equal to the product of the spontaneous polarization, dielectric permittivity, square of magnetic susceptibility and the coefficient of biquadratic ME coupling.

[1] A.P. Pyatakov, A.K. Zvezdin, Magnetoelectric and multiferroic media. *Physics-Uspeski* **55**, 557-581 (2012).

[2] V.V. Laguta, M.D. Glinchuk, M. Maryško, R.O. Kuzian, S.A. Prosandeev, S.I. Raevskaya, V.G. Smotrakov, V.V. Eremkin, I.P. Raevski, Effect of Ba and Ti doping on magnetic properties of multiferroic  $\text{Pb}(\text{Fe}_{1/2}\text{Nb}_{1/2})\text{O}_3$ . *Phys Rev B* **87**, 064403 (2013).

The support of the GA CR under project No. 13-11473S is gratefully acknowledged.

# Ferroelectric and antiferroelectric generators of electric current

**Ryszard Poprawski<sup>1</sup>**, Ewa, Beata Radojewska<sup>1</sup>, Wojciech Poprawski<sup>2</sup>

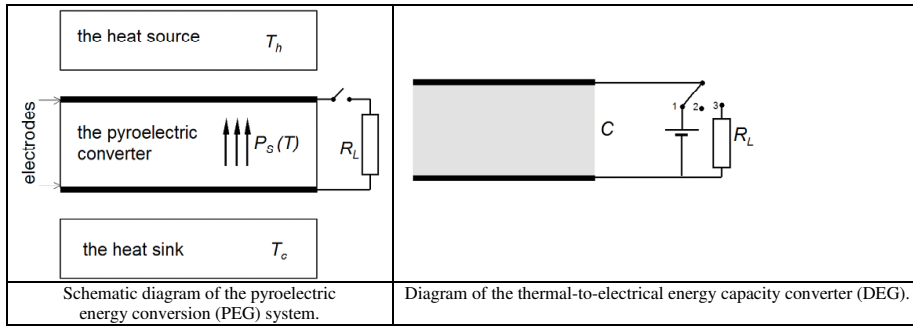
*1 - Department of Experimental Physics, Faculty of Fundamental Problems of Technology  
Wrocław University of Science and Technology, Wybrzeże Wyspiańskiego 27, 50-370 Wrocław, Poland*

*2 - Faculty of Mechanical and Power Engineering, Wrocław University of Science and Technology  
Wybrzeże Wyspiańskiego 27, 50-370 Wrocław, Poland*

*ryszard.poprawski@pwr.edu.pl*

The pyroelectric effect is usually used to construct infrared radiation detectors, while piezoelectric properties of ferroelectrics are used to build force, pressure and acceleration sensors and mechanical to electrical energy transducer. In this presentation we want to pay attention to a possibility of the pyroelectric effect employment along with the temperature dependence of the dielectric permittivity into a direct conversion of the time-alternating heat flux and the electromagnetic radiation to the electric energy. Converters making use of the mentioned phenomena can be applied in the low-power electric energy generators mounted in autonomous electronic devices.

Operation principles for pyroelectric and dielectric generators (PEG and DEG) of the electric energy are presented in this presentation together with a brief review on ferro- and antiferroelectric materials suitable for the generators.



The presentation reports figure of merit of materials used for pyroelectric energy harvesting [1], [2]

$$Z_{pyro} = \frac{\gamma^2}{C_v \epsilon'}, \quad (1)$$

where:  $\gamma$  is the pyroelectric coefficient,  $C_v$  denotes the specific heat of the unit volume and  $\epsilon'$  – real part of the dielectric permittivity.

It was shown that for the ferroelectrics with the second-order phase transition the conversion efficiency of PEGs did not depend on temperature in a wide temperature range, and ferroelectrics showing an order-disorder phase transition together with composites and heterostructures based on these ferroelectrics had high conversion efficiency. For the first time ferro- and antiferroelectric materials were extensively reviewed with regard to their applicability in PEGs. It was also shown that ferro- and antiferroelectrics with translation-type phase transition, quantum ferroelectrics, ferro- and antiferroelectric relaxors were good materials for DEGs.

Considering literature data the efficiency for the thermal-to-electrical energy conversion was estimated for a few typical material groups. Advantages and disadvantages of the individual groups were presented along with their possible limitations for PEG and DEG usage.

[1] W. Poprawski, Z. Gnutek, J. Radojewska, R. Poprawski, Pyroelectric and dielectric energy conversion e A new view of the old problem, *Applied Thermal Engineering* 90, 858 (2015).

[2] C.R. Bowen, J.Taylor, E. Le. Boulbar, D. Zabek, V. Yu. Topolov, A modified figure of merit for pyroelectric energy harvesting, *Materials Letters*, 138, 243 (2015)

# Multiferroic properties and order-disorder phase transition in the ammonium templated metal-organic frameworks

A. Ciupa, M. Mączka, M. Ptak

*Institute of Low Temperature and Structure Research, Polish Academy of Sciences, 50-422, Wrocław, Poland*

*a.ciupa@int.pan.wroc.pl*

Metal-organic frameworks (MOFs) are known for a very wide spectrum of functionalities, properties and possible applications arising from them. Their high porosity and flexible structures have afforded excellent gas separation and sorption ability, catalytic activity and more [1]. However, it should be remembered that MOFs exhibit also magnificent electric, magnetic, dielectric and even multiferroic attributes, which can be achieved by the incorporation of short formate  $\text{HCOO}^-$  ions as ligands and H-bonding acceptors, (magnetic) metal ions and ammonium or alkylammonium cations as templates and H-bonding donors [2]. The good examples are compounds of general formula  $[\text{NH}_4][\text{M}(\text{HCOO})_3]$  ( $\text{M} = \text{Ni}, \text{Mg}, \text{Fe}, \text{Mn}, \text{Co}, \text{Zn}$ ) with the smallest ammonium cations ( $\text{NH}_4^+$ ) located in the cavities of the framework [3-5]. These formates crystallize at room temperature in  $P6_322$  space group and possess chiral framework of  $4^9\cdot6^6$  topology. The previously published data showed coexistence of magnetic and electric orders in this class of MOFs. For the magnetic members weak ferromagnetism was observed at low temperatures with  $T_c$  in the range 8 – 36 K [3]. On the other hand, the ferroelectric phase transition ( $T_c = 191\text{-}254$  K) in these ammonium templated metal formates has been associated with the ordering of  $\text{NH}_4^+$  cations. As a consequence, the decrease of symmetry to  $P6_3$  is observed [3-5]. The mechanism of observed phase transitions in  $[\text{NH}_4][\text{M}(\text{HCOO})_3]$  is still not very well explained. For instance, Xu et al. has discussed the dependence between the phase transition temperature and size of the used  $\text{M}^{2+}$  ions. It was suggested that for smaller metal ions the framework becomes smaller and thus the phase transition temperature decreases due to the higher internal pressure for 1D liquid-solid transition. This dependence is correct for  $[\text{NH}_4][\text{M}(\text{HCOO})_3]$  with  $\text{M} = \text{Ni}, \text{Fe}, \text{Mn}, \text{Co}$  and  $\text{Zn}$ , whereas the magnesium analogue diverges [3,4].

To better understand the mechanism of observed phase transitions in this class of dense MOFs, we have decided to use the vibrational spectroscopic techniques which are known to be very sensitive to even the tiniest structural changes. Our studies have showed that the deformation of host framework, together with the dynamic transitions of templated cations between ordered and disordered states result in the phase transitions [6].

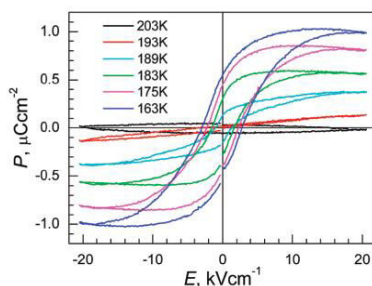


Figure 1. Dielectric hysteresis loops of  $[\text{NH}_4][\text{Zn}(\text{HCOO})_3]$  with  $E \parallel c$  at various temperatures. (Reprinted from reference [5]).

- [1] C. Janiak, J. K. Vieth, MOFs, MILs and more: concepts, properties and applications for porous coordination networks (PCNs), *New J. Chem.* 34, pp. 2366-2388, (2010).
- [2] G. Rogez, N. Viart, M. Drillon, Multiferroic materials: the attractive approach of metal-organic frameworks (MOFs), *Angew. Chem. Int. Ed.* 49, pp. 1921 – 1923, (2010).
- [3] G.-C. Xu, W. Zhang, X.-M. Ma, Y.-H. Chen, L. Zhang, H.-L. Cai, Z.-M. Wang, R.-G. Xiong, S. Gao, Coexistence of magnetic and electric orderings in the metal-formate frameworks of  $[\text{NH}_4][\text{M}(\text{HCOO})_3]$ , *J. Am. Chem. Soc.* 133, pp. 14948 – 14951, (2011).
- [4] R. Shang, G.-C. Xu, Z.-M. Wang, S. Gao, Phase transitions, prominent dielectric anomalies, and negative thermal expansion in three high thermally stable ammonium magnesium-formate frameworks, *Chem. Eur. J.* 20, pp. 1146-1158, (2014).
- [5] G.-C. Xu, Z.-M. Ma, L. Zhang, Z.-M. Wang, S. Gao, Disorder-order ferroelectric transition in the metal formate framework of  $[\text{NH}_4][\text{Zn}(\text{HCOO})_3]$ , *J. Am. Chem. Soc.* 132, pp. 9588 – 9590, (2010).
- [6] M. Mączka, K. Szyborka – Małek, A. Ciupa, J. Hanuza, Comparative studies of vibrational properties and phase transitions in metal-organic frameworks of  $[\text{NH}_4][\text{M}(\text{HCOO})_3]$  with  $\text{M} = \text{Mg}, \text{Zn}, \text{Ni}, \text{Fe}, \text{Mn}$ , *Vib. Spectrosc.* 77, pp. 17-24, (2015).

## Synthesis and characterization of 2-amino-3-nitropyridinium hydrogen sulfate

T. J. Bednarchuk<sup>1</sup>, **D. Komornicka**<sup>1</sup>, V. Kinzhybalov<sup>1</sup>, P. Monasterski<sup>2</sup>,  
A. Sieradzki<sup>2</sup>, M. Wołczyrz<sup>1</sup>, A. Pietraszko<sup>1</sup>

1- Institute of Low Temperature and Structure Research, Polish Academy of Sciences, Okólna 2, 50-422 Wrocław, Poland

2- Wrocław University of Technology, Wybrzeże St. Wyspiańskiego 27, 50-370 Wrocław

d.komornicka@int.pan.wroc.pl

Wide variety of interesting supramolecular networks oftentimes discovered in compounds that consist of organic cations and inorganic anions evoke pronounced scientific attention. The non-centrosymmetric packing in these materials is one of the major challenges in the design of functional materials exhibiting non-trivial physical properties and (or) second-order optical nonlinearities.

Novel anhydrous proton conducting organic-inorganic hybrid salt named 2-amino-3-nitropyridinium hydrogen sulfate (2A3NP-HS) was obtained and characterized by means of DSC, TG-DTA, dielectric and electric measurements and X-ray diffraction. The results of DSC studies reveal the presence of reversible phase transition at 300/297 K (**II**↔**I**) for heating/cooling cycles, respectively. At room temperature 2A3NP-HS crystallizes in non-centrosymmetric orthorhombic space group *Pna*2<sub>1</sub>. Additionally, for the latter, high-temperature modification (HT, **I** phase), diffuse scattering was found present in the shape of streaks elongated parallel to the *a*\* crystallographic direction.

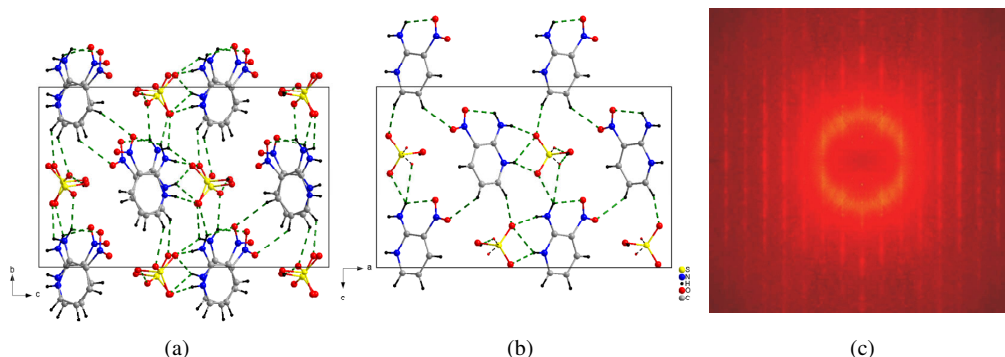


Figure 1 (a) The molecular arrangement in LT phase (projection along [100]). (b) The packing diagram for HT phase viewed along [010], the disordered anions are shown with thin black dashed bonds. Hydrogen bonds are denoted by green dashed lines ((a) and (b)). (c) The *h*0.5*l* section of reciprocal space with the streaks of diffuse scattering extended along *a*\* direction.

The occurrence of the mentioned phenomena can be associated with the structural disorder existing in this phase. The model of the local structure has been proposed. There are strong correlations within (100) atom layers and weaker correlations between them. Careful analysis of diffraction pattern showed that diffuse scattering streaks are modulated with increase of intensity in the midway between Bragg peaks. That suggested the occurrence of additional correlations to the nearest neighbour and to the next-near neighbour in the (100) atom layers, which causes local doubling of the unit cell in *a* and *b* directions.

While cooling 2A3NP-HS the symmetry tends to decrease to monoclinic non-centrosymmetric space group *P*2<sub>1</sub> (LT, **II** phase). This transition may be classified as of 'order-disorder' type. In the crystal cations and anions are linked in each layer by strong hydrogen bonds. These layers are connected by weaker C-H⋯O hydrogen-bonding interactions.

Furthermore, results of dielectric response and electric conductivity for 2A3NP-HS will be presented and discussed.

- [1] T. J. Lukianova, V. Kinzhybalov, A. Pietraszko, Crystal structure of tris(piperidinium) hydrogen sulfate, *Acta Cryst. E*, 71, 1444-1446, (2015).
- [2] Y. L. Fur, R. Masse, J.-F. Nicoud, 2-Amino-3-nitropyridinium hydrogensulfate hydrate: a nonlinear optical crystal engineered with a two-dimensional hyperpolarisable chromophore, *New J. Chem.* 22, 159-163, (1998).
- [3] P. Czarnecki and H. Małuszyńska, Structure and dielectric properties of ferroelectric pyridinium perhenate crystals, *J. Phys.: Condens. Matter.*, 12, 4881-4892, (2000).



**ABSTRACTS OF ORAL PRESENTATIONS**  
**9<sup>th</sup> September**

# Peculiar polarization domains in the layered ferroelectric $\text{CuInP}_2\text{Se}_6$

**A. Dziaugys<sup>1</sup>, M. Chyasnachyus<sup>2</sup>, A. N. Morozovska<sup>3</sup>, E. A. Eliseev<sup>4</sup>, J. Banys<sup>1</sup>, Y. Vysochanskii<sup>5</sup>, P. Maksymovych<sup>2</sup>**

*1-Faculty of Physics, Vilnius University, Vilnius, LT-01513 Lithuania*

*2-The Institute for Functional Imaging of Materials and the Center for Nanophase Materials Sciences, Oak Ridge National Laboratory, Oak Ridge, Tennessee 37831, United States*

*3-Institute of Physics, National Academy of Sciences of Ukraine, Prospect Nauky 46, Kyiv-28, 03680, Ukraine*

*4-Institute for Problems of Materials Science, National Academy of Sciences of Ukraine, Krjijanovskogo 3, 03142 Kyiv, Ukraine*

*5-Institute of Solid State Physics and Chemistry, Uzhgorod University, 88000 Uzhgorod, Ukraine*

*andrius.dziaugys@ff.vu.lt*

Chalcogenophosphates, which belong to layered 2D multiferroics, are attractive in term of fundamental science of physics and applications in electronic, and energy harvesting devices. Most extensively studied chalcogenophosphate is a room temperature layered ferroelectric  $\text{CuInP}_2\text{S}_6$ . This compound has a unique characteristics and shows interesting physical properties when In is doped with Cr [1-2] or S with Se.  $\text{CuInP}_2\text{Se}_6$  is a new member of the prospective chalcogenophosphate materials with interesting and sometimes puzzling properties. There is an open question what processes happen in  $\text{CuInP}_2\text{Se}_6$  in the temperature range from 200 K to 240 K and what theoretical model could be applied to explain experimental results. For this reason we focused our attention on the observation of domain structure temperature dependence and repolarization processes in  $\text{CuInP}_2\text{Se}_6$  crystals by piezoresponse force microscopy (PFM) in UHV. Experimental results revealed that puzzling temperature evolution of ferroelectric domains, at least two types of domain of different (primary ferroelectric or ferroelastic) origin coexist in the temperature range (210 – 230) K. Theoretical modelling indicate that the experimentally observed phenomena take place in the morphotropic region between the spatially-modulated ferroelectric antiferrodistortive phase stability and metastability.

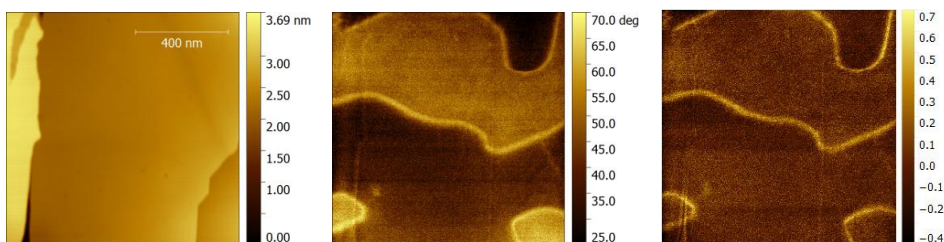


Fig. 1. UHV results of the  $\text{CuInP}_2\text{Se}_6$  surface at 170 K. A) 1x1 um contact AFM image; b) PFM image (piezoresponse phase) c) PFM image (piezoresponse amplitude)

[1] A. Dziaugys, V. Shvartsman, J. Macutkevicius, J. Banys, Yu. Vysochanskii, W. Kleemann. Phys. Rev. B, 2012, v. 85, p. 134105-1 - 134105-6.

[2] W. Kleemann, V. V. Shvartsman, P. Borisov, J. Banys, Yu. M. Vysochanskii. Phys. Rev. B, 2011, v. 84, p. 094411-1 - 094411-8.

# Amorphous, nano- and microcrystalline phases of lithium germanate oxides

O. Nesterov, M. Trubitsyn, S. Plyaka, M. Volnyanskii

*Solid state physics and optoelectronics dept, Oles' Honchar Dnipropetrovsk National University, prosp. Gagarina 72, Dnipropetrovsk, 49010, Ukraine*

*email: trubitsyn\_m@ua.fm*

Devitrification of glasses and electrical properties of amorphous, nano- and microcrystalline phases of  $\text{Li}_2\text{O}-x(\text{GeO}_2)$  compounds were studied. Influence of phase composition and morphology on charge transfer and space-charge polarization phenomena is discussed. It is shown that thermal treatment of glass allows to obtain the compounds in intermediate nanocrystalline state with high electrical conductivity. It is demonstrated that creating nano-dispersed media could be an effective approach to increase ionic conductance in dielectrics.

The structure, morphology, thermal and electric properties of amorphous, glassceramic and polycrystalline  $\text{Li}_2\text{O}-x(\text{GeO}_2)$  compounds were studied by differential scanning calorimetry, X-ray diffraction, atomic force microscopy (AFM), dielectric, impedance and NMR spectroscopies.  $\text{Li}_2\text{O}-x(\text{GeO}_2)$  glasses, where  $x=2.7, 7, 11.5$  and 18, were obtained by the melts quenching. It is shown that on heating amorphous phases with  $x=7, 11.5, 18$  crystallized in stages (Fig.1a) through an intermediate metastable state, where lithium tetragermanate  $\text{Li}_2\text{Ge}_4\text{O}_9$  ( $x=4$ ) and lithium heptagermanate  $\text{Li}_2\text{Ge}_7\text{O}_{15}$  ( $x=7$ ) ordered regions appear. On further heating metastable regions with  $\text{Li}_2\text{Ge}_4\text{O}_9$  structure recrystallised into thermodynamically favourable  $\text{Li}_2\text{Ge}_7\text{O}_{15}$  crystallites. In accord with AFM data, the average size of the nuclei in the intermediate state was about 75 nm and after total crystallization of  $\text{Li}_2\text{Ge}_7\text{O}_{15}$  phase the size of crystallites increased to micrometer range (0.3  $\mu\text{m}$ ). Variation of heat treatment regime allowed to show that crystallization of  $\text{Li}_2\text{O}-x(\text{GeO}_2)$  glasses occurred in the bulk of the medium and was suppressed near the surface.

Measuring  $\sigma(T)$  through glasses devitrification shown that conductivity of the intermediate nanocrystalline state was sufficiently higher than in amorphous and microcrystalline phases (Fig.1b).

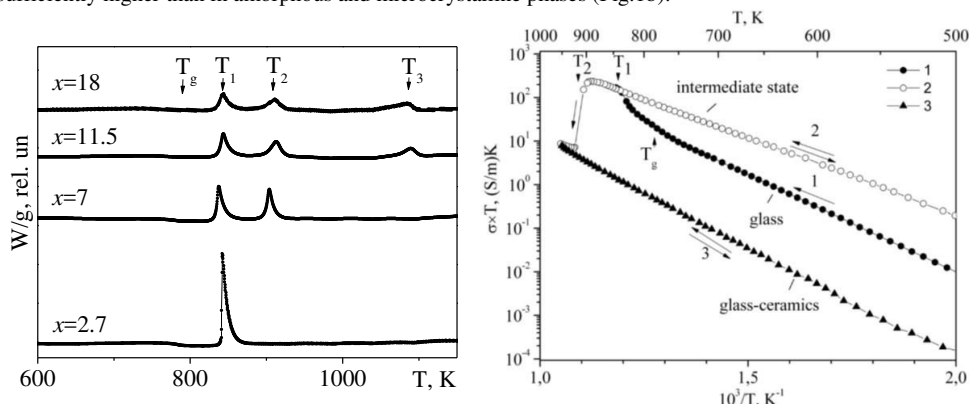


Figure 1 (a) DSC curves, obtained on heating  $\text{Li}_2\text{O}-x(\text{GeO}_2)$  glasses. (b)  $\sigma(1/T)$  dependencies measured in AC field ( $f=1\text{kHz}$ ) on different heating and cooling regimes and showing  $\text{Li}_2\text{O}-11.5(\text{GeO}_2)$  amorphous phase crystallization: 1 - original glass; 2 - intermediate nanocrystalline state; 3 - glass ceramics consisting of  $\text{Li}_2\text{Ge}_7\text{O}_{15}$  microcrystals and  $\text{GeO}_2$  glass.

Mechanism of charge transfer in amorphous, nano- and microcrystalline  $\text{Li}_2\text{O}-x(\text{GeO}_2)$  phases was investigated by complex impedance  $\rho^*(\omega)$  and NMR spectroscopies. The data obtained testify for hopping mechanism of charge transfer and reflect spatial distribution of Li ions in the bulk of multiphase samples. Increase of  $\sigma$  in the intermediate state is the result of high mobility of Li ions in comparison with glass and microcrystalline states. Studying AFM, electrical properties and NMR indicates that high conductivity of the intermediate state is determined by nanometer size of crystalline nuclei. Increasing the nuclei size to micrometer range leads to sharp decrease of carrier mobility and conductivity (Fig.1b).

[1] M. Volnyanskii, O. Nesterov, M. Trubitsyn, Devitrification of the  $\text{Li}_2\text{O}-x(\text{GeO}_2)$  glass, *Ferroelectrics*, vol.462, 126-130 (2014).

[2] O. Nesterov, M. Trubitsyn, D. Volnyanskii, Metastable state of the  $\text{Li}_2\text{O}-11.5\text{GeO}_2$  glass-ceramics with a high electrical conductivity, *Phys.of the Solid State*, vol.57, 683-688 (2015).

[3] O. Nesterov, M. Trubitsyn, S. Plyaka, D. Volnyanskii, Spectra of complex impedance of  $\text{Li}_2\text{O}-11.5\text{GeO}_2$  glass and glass ceramics, *Phys.of the Solid State*, vol.57, 1715-1719 (2015).

# Dielectric properties and the phase diagram of $(\text{Bi}_x\text{Na}_{1-x})(\text{Mn}_y\text{Nb}_{1-y})\text{O}_3$ ceramics

**J. Macutkevic<sup>1</sup>, A. Molak<sup>2</sup>, J. Banys<sup>1</sup>**

*1- Faculty of Physics, Vilnius university, Sauletekio al. 9, LT-10222 Vilnius, Lithuania*

*2- Institute of Physics, University of Silesia, ul. Uniwersytecka 4, PL-40-007 Katowice, Poland*

*Main author email address: jan.macutkevic@gmail.com*

Sodium niobate ( $\text{NaNbO}_3$ ) is an oxygen perovskite with the largest number of phase transitions [1]. The material gained new attention in the last years due the increased interest in environmental protection, since it is an end member of a number of solid solutions with good piezoelectric properties (for example  $\text{Na}_{0.5}\text{K}_{0.5}\text{NbO}_3$ ) which could replace the widely used lead-based perovskites.  $\text{NaNbO}_3$  co-doped with N and Mn ions attracts attention for photocatalytic studies [2].  $\text{BiMnO}_3$  is well known antipolar ferromagnet, earlier claimed as multiferroic [3]. In this presentation results of broadband dielectric investigations of mixed  $(\text{Bi}_x\text{Na}_{1-x})(\text{Mn}_y\text{Nb}_{1-y})\text{O}_3$  ( $x=0$ ,  $y=0$ ;  $x=1$ ,  $y=1$ , and  $x=0.06$ ,  $y=0.04$ ) ceramics in wide temperature region (25-730 K) are presented. Five phase transitions were observed in  $\text{NaNbO}_3$  ceramics on cooling by broadband dielectric investigations in temperature range from 25 K to 1000 K. Despite that  $T_1$ - $T_2$  and  $S$ - $T_1$  phase transitions are non polar, they are clearly expressed in dielectric properties of ceramics due the corresponding conductivity anomalies. At higher temperature (above 600 K) the electrical conductivity dominates in the dielectric spectra of ceramics. The electrical conductivity have peculiarities close to  $T_1$ - $T_2$ ,  $S$ - $T_1$ ,  $P$ - $R$  phase transitions temperatures. In mixed  $(\text{Bi}_x\text{Na}_{1-x})(\text{Mn}_y\text{Nb}_{1-y})\text{O}_3$  with  $x=0.06$  and  $y=0.04$  the antiferroelectric phase transitions  $P$ - $Q$  and  $Q$ - $R$  are clearly expressed in dielectric properties. The microscopic origin of phase transition will be discussed in presentation. The dielectric properties of  $\text{BiMnO}_3$  are dominated by the huge electrical conductivity and Maxwell-Wagner relaxation. The conductivity activation energy non evenly decreases on heating and due substitution  $\text{Na} \rightarrow \text{Bi}$  and  $\text{Nb} \rightarrow \text{Mn}$ . The variation in activation energy relates to the level of ionization of oxygen vacancies and to effects of the high temperature annealing. The small polaron mechanism of conduction is proposed.

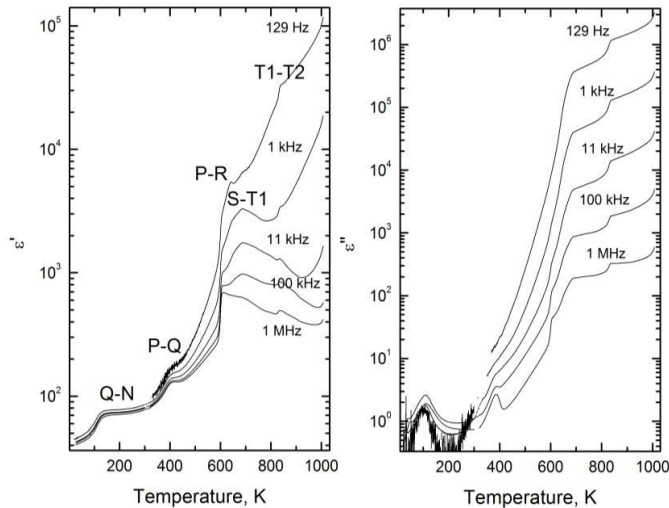


Figure 1 Temperature dependence of complex dielectric permittivity  $\varepsilon^*$  for  $\text{NaNbO}_3$  ceramics at different frequencies (on cooling).

[1] H. D. Megaw, 7 Phase of Sodium Niobate, *Ferroelectrics* 7, 87-89 (1974).

[2] A. Molak, M. Pilch, Visible light absorbance enhanced by nitrogen embedded in the surface layer of Mn-doped sodium niobate crystals, detected by ultra violet – visible spectroscopy, x-ray photoelectron spectroscopy, and electric conductivity tests, *Journal of Applied Physics* 119, 204901-1-10 (2016).

[3] V. Goian, S. Kamba, M. Savinov, D. Nuzhnyy, F. Borodavka, P. Vanek, A. A. Belik, Absence of ferroelectricity in  $\text{BiMnO}_3$  ceramics, *Journal of Applied Physics* 112, 074112 (2012).

[4] J. Macutkevic, A. Molak, J. Banys, Dielectric properties of  $\text{NaNbO}_3$  ceramics, *Ferroelectrics* 479, 48–55, (2015).

# CARS spectroscopy and imaging of graphene layers and nanoplatelets

A. Dementjev<sup>1</sup>, A. Cataldo<sup>2</sup>, F. Micciulla<sup>2</sup>, S. Bistarelli<sup>2</sup>, S. Bellucci<sup>2</sup>, T. Kaplas<sup>3</sup>, D. Pidgirniy<sup>4</sup>, O. Posudievsky<sup>5</sup>, G. Dovbeshko<sup>4</sup>

<sup>1</sup>*Institute of Physics, Center for Physical Sciences and Technology, A. Goštauto 11, Vilnius LT-01108, Lithuania*

<sup>2</sup>*INFN, Laboratori Nazionali di Frascati, P.O. Box 13, I-00044 Frascati, Italy*

<sup>3</sup>*Institute of Photonics, University of Eastern Finland, Yliopistokatu 7, P.O. Box 111, Joensuu FI-80101, Finland*

<sup>4</sup>*Institute of Physics, National Academy of Sciences of Ukraine, 46 Nauki Ave, Kyiv 03680, Ukraine*

<sup>5</sup>*L.V. Pisarzhevsky Institute of<sup>3</sup>Physical Chemistry National Academy of Science of Ukraine*

gd@iop.kiev.ua

Graphene being a new material with unique chemical and physical property attracts much attention by scientists and engineers. Characterization of the graphene single (double, triple) layers and graphene nanoplatelets (GNP) are conventionally done by electron or atomic force microscopy and Raman scattering (RS) spectroscopy. However, sometimes these methods are not enough. Here we apply one of the microspectroscopy method, namely, Coherent anti-stokes Raman scattering (CARS) for imaging and spectroscopy of graphene materials: graphene single (double, triple) layers on SiO<sub>2</sub> obtained by CVD and transferred from Cu foil on SiO<sub>2</sub> and GNP obtained by 2 different methods: mechanochemical and microwave exfoliation.

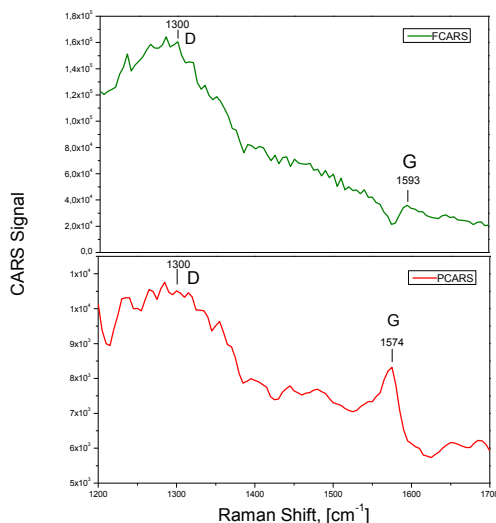


Figure 1 CARS spectrum of GNP in the region 1200 – 1700 cm<sup>-1</sup> FCARS (green, top)) and PCARS (red, bottom): probe power at 1064 nm – 150 uW, pump power – 50 uW. Signals value from FCARS and photoluminescence – 50/50 %

The characteristics of CARS spectra of GNP are shift of G-mode in low frequency range up to 7 cm<sup>-1</sup>, appearance of new modes in the 1400-1500 cm<sup>-1</sup> and many modes of second and higher orders, widening of D-mode. The CARS spectra of graphene nanostructures have features of resonant and non-resonant electronic and vibrational contributions overlapped by luminescence caused by defects on the edges of the particles or layer islands. It confirms by FCARS and PCARS of GNP (Fig.1) and imaging of structure at marker vibrational modes. Application of CARS spectroscopy and mapping for graphene structures is analysed and discussed.

**ACKNOWLEDGEMENT:** We thank to PIRSES-2012-318617 FAEMCAR, STCU-2016 6175, Graphene Core 1 H2020-Adhoc-2014-20 projects for financial support .

# Dielectric and shielding properties of Ni@C/ polydimethylsiloxane composites

A. Plyushch<sup>1</sup>, J. Macutkevič<sup>1</sup>, P.Kuzhir<sup>2</sup>, O. Shenderova<sup>3</sup>

1- Faculty of Physics, Vilnius University, Sauletekio 9, Vilnius LT-10222, Lithuania

2- Research Institute for Nuclear problems of Belarusian State University, Bobruiskaya Str., 11 Minsk 220030 Belarus

3- International Technology Center, Raleigh, NC 27715, USA

artyom.plyushch@gmail.com

New class of EMI absorbing composite materials combining Ohmic (carbon) and magnetic (nickel) losses has been studied in wide frequency and temperature ranges. Ni@C nanocomposites were prepared by evaporation of overheated liquid drop of Ni in the flow of inert gas containing a hydrocarbon. The resulting carbon-coated nickel nanoparticles contain metal cores of about 5 nm in size that are wrapped in a few layers of graphene-like carbon [1]. The polydimethylsiloxane (Sylgard, Dow-Corning) was utilized as a composite matrix. An intermediate solvent (isopropanol (IPA)) was employed as a dispersion medium for the nanoparticles. The nanoparticles were dispersed in the solvent and sonicated to break up large agglomerates, then the suspension was combined with uncured PDMS and the IPA solvent subsequently removed by vacuum. Curing of the Ni@C / PDMS mixture at 60 °C for 2 h and 40 °C over-night resulted in films with good nanoparticle dispersion.

Figure 1 presents the temperature dependence of the dielectric permittivity on cooling to 25K. It is clearly seen, that pure PDMS matrix demonstrates anomalous behaviour at low temperatures that may correspond to the glass transition effect. Even smallest (1 vol. %) addition of the Ni@C particles leads to significant changes in the temperature behaviour of the dielectric losses. The position of the dielectric losses maximum is frequency dependent. The peak increases and shifts to higher temperatures with the frequency. The shift can be characterized by the Vogel–Fulcher relation as

$$f = f_0 \exp\left[\frac{-E_{VF}}{kb(T_{max} - T_{ref})}\right] \quad (1)$$

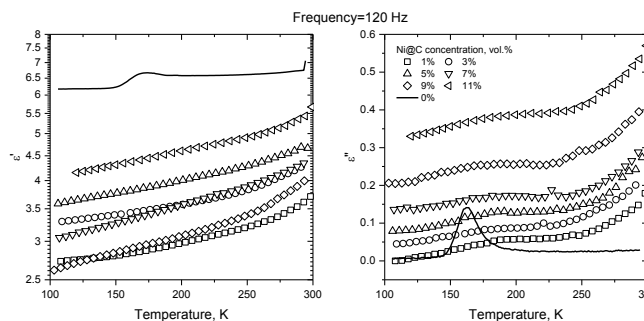


Figure 1. Temperature dependence of complex dielectric permittivity at 120 Hz

The freezing temperature in composites is found to be Ni@C concentration – independent and significantly lower than for the pure PDMS.

We can conclude that the addition of Ni@C particles has huge impacts on dielectric properties of PDMS.

[1] A.V. Erokhin, E.S. Lokteva, A.Ye. Yermakov, D.W. Boukhalov, K.I. Maslakov, E.V. Golubina, M.A. Uimin, A. Author and B. Phenylacetylene hydrogenation on Fe@C and Ni@C core-shell nanoparticles: About intrinsic activity of graphene-like carbon layer in H<sub>2</sub> activation, CARBON 74, 291 – 301, (2014).

## LIST OF POSTER PRESENTATIONS

### Poster session I: September 6<sup>th</sup>

P1-01	<b>Ieva Kranauskaitė</b>	Electrical properties of MWCNT, GNP and hybrid MWCNT/GNP composites
P1-02	<b>Ewa Cwikiel</b>	Ferroelectric ceramics how it's made?
P1-03	<b>Tamara Bednarchuk</b>	Phase transitions in two new organically templated metal sulfates with 4-aminopyridinium
P1-04	<b>Oksana Mys</b>	Acoustic properties of new chalcogenide type crystals
P1-05	<b>Oksana Mys</b>	Topological reactions of electrically induced defects of optical indicatrix orientation in crystals
P1-06	<b>Volodymyr Khrustalov</b>	High magnetic field induced electric polarization of antiferromagnets $\text{LiCoPO}_4$ and $\text{LiNiPO}_4$
P1-07	<b>Katarzyna Pasińska</b>	Effect of Nd and Sc substitution on structural, magnetic and dielectric properties of $\text{SrFe}_{12}\text{O}_{19}$ hexaferrite
P1-08	<b>Anna Dyachenko</b>	Photoluminescence and photoconductivity of $\text{Bi}_{12}\text{SiO}_{20}$ crystals doped by AL, Ga, Sn
P1-09	<b>Katarzyna Matyjasek</b>	Domain switching in TGS and DTGS crystals near the phase transition
P1-10	<b>Dorota Sitko</b>	Effect of Cu doping on the mechanical properties of $\text{Ba}_{0.95}\text{Pb}_{0.05}\text{TiO}_3$ ceramics
P1-11	<b>Dagmara Brzezińska</b>	The properties of $(1-x)(0.5\text{PZT}-0.5\text{PFW})-x\text{PFN}$ ceramics
P1-12	<b>Jan Macutkevič</b>	Dielectric properties of sodium bismuth titanate ceramics
P1-13	<b>Vidmantas Kalendra</b>	Functional properties of $\text{BaTiO}_3$ ceramics: the influence of iron addition
P1-14	<b>Andrzej Osak</b>	Raman spectroscopy study of the phase transition in ferroelectric PZT+PFS
P1-15	<b>Marek Kostrzewa</b>	On the structural phase transition in a perovskite type Diaminopropanetetraclorocuprate (II) - $\text{NH}_3(\text{CH}_2)_3\text{NH}_3\text{CuCl}_4$ crystal
P1-16	<b>Mantas Šimėnas</b>	EPR of structural phase transitions in formate metal-organic frameworks
P1-17	<b>Džiugas Jablonskas</b>	Dielectric Spectroscopy of $\text{Pyr}_{14}\text{TFSI}$ and $\text{Pyr}_{12}\text{O}_1\text{TFSI}$ Ionic Liquids
P1-18	<b>Adam Ingram</b>	Structural phase transition in ammonium hydrogen fumarate
P1-19	<b>Aliaksandr Shylin</b>	Effect of High-Power Sonication on Formation of the $\text{Bi}_{1-x}\text{La}_x\text{Fe}_{0.5}\text{Sc}_{0.5}\text{O}_3$ Perovskite Phases
P1-20	<b>Erazm Maria Dutkiewicz</b>	Electrical transport in lead-free $(\text{Na}_{0.5}\text{Bi}_{0.5})_{1-x}\text{Sr}_x\text{TiO}_3$ ceramics ( $x=0, 0.01$ and $0.02$ )
P1-21	<b>Monika Karpierz</b>	Effects of $\text{PbTiO}_3$ doping on electric properties of $\text{K}_{0.5}\text{Bi}_{0.5}\text{TiO}_3$ ceramics

## Poster session II: September 7<sup>th</sup>

P2-01	<b>Dawid M. Nalecz</b>	Origin of the $\lambda$ -type anomaly in $\text{SrMnO}_3$ and $\text{EuTiO}_3$ : Magnetic contribution to the specific heat
P2-02	<b>Sylwester Wacke</b>	Dielectric dispersion studies in $(\text{N}_2\text{H}_5)_2\text{CdCl}_4$ crystal
P2-03	<b>Urszula Lewczuk-Jodłowiec</b>	Thermal and pyroelectric properties of NBT-BT systems
P2-04	<b>Sergejus Balčiūnas</b>	Dielectric Properties of BTKN Composites
P2-05	<b>Ihor P. Studenyak</b>	Influence of grain size effect on physical properties of $\text{Cu}_6\text{PS}_5\text{I}$ micro- and nanocrystals
P2-06	<b>Vitalii Yu. Izai</b>	Electrical conductivity in the range of phase transitions in $\text{Cu}_6\text{PS}_5\text{I}$ crystals
P2-07	<b>Yuri Potapovich</b>	Phase compositions of $\text{Na}_{0.5}\text{Bi}_{0.5}\text{TiO}_3$ thin films deposited in various working gas mixtures
P2-08	<b>Przemysław Niemiec</b>	Dielectric properties of the multicomponent PZT-type ceramic for actuator applications
P2-09	<b>Krzysztof Cwikiel</b>	New forms of TGS crystals
P2-10	<b>Krzysztof Konieczny</b>	Electrical, thermoelectric and thermal properties of $\text{Li}_x\text{Na}_{1-x}\text{NbO}_3$ solid solution for $x=0$ to $0.1$
P2-11	<b>Edita Palaimiene</b>	Dielectric properties of $\text{Ba}_6\text{MnNb}_9\text{O}_{30}$ ( $\text{M} = \text{Ga}, \text{Sc}$ ) tungsten bronze ceramics
P2-12	<b>Jan Suchanicz</b>	Dielectric and ferroelectric properties of lead-free $(\text{Na}_{0.5}\text{Bi}_{0.5})_{1-x}\text{Sr}_x\text{TiO}_3$ ceramics ( $x=0-0.04$ )
P2-13	<b>Vasyl Sidak</b>	Photoluminescence and Optical Absorption of $\text{Na}_{0.5}\text{Bi}_{0.5}\text{TiO}_3$ Crystals
P2-14	<b>Andrius Džiaugys</b>	Ferroelectricity and Semiconductor – Metal Transition in $\text{Sn}(\text{Pb})_2\text{P}_2\text{S}_6$ Compounds with Valence Fluctuations
P2-15	<b>Andrius Laurikėnas</b>	Hybrid inorganic-organic compounds as promising ferroelectric materials
P2-16	<b>Krzysztof Pytel</b>	Basic characterization of ferroelectric lead lanthanum zirconate titanate based on correlation coefficients
P2-17	<b>Monika Krawczyk</b>	Phase transitions in $[\text{NEt}_4][\text{NMe}_4][\text{ZnBr}_4]$ crystal
P2-18	<b>Dorota Podsiadla</b>	Properties of $(\text{C}_3\text{H}_4\text{N}_2)\text{HClO}_4$ crystal: structural, Infrared and thermal studies
P2-19	<b>Julius Važgėla</b>	Reduced Bimolecular Recombination in a Ternary Silole-Based Polymer:P3HT:PCBM Solar Cell
P2-20	<b>Saulius Rudys</b>	Carbon fiber material defectoscopy using mm wave near field microscopy methods
P2-21	<b>Alexander Grabar</b>	Dynamic interferometer based on photorefractive effect in Sb-doped $\text{Sn}_2\text{P}_2\text{S}_6$ ferroelectric



## **ABSTRACTS OF POSTER PRESENTATIONS**

**6<sup>th</sup> September**

# Electrical properties of MWCNT, GNP and hybrid MWCNT/GNP composites

**I. Kranauskaite<sup>1</sup>, J. Macutkevici<sup>1</sup>, A. Borisova<sup>2</sup>, A. Martone<sup>3</sup>, M. Zarrelli<sup>3</sup>, A. Aniskevich<sup>2</sup>, J. Banys, M. Giordano<sup>3</sup>**

*1- Vilnius University, Physics Faculty, Radiophysics Department, Vilnius, Lithuania*

*2- Institute of Polymer Mechanics, University of Latvia, Riga, Latvia*

*3- Institute for Composite and Biomedical Materials, National Research Council of Italy, Portici, Italy*

*Main author email address: ieva.kranauskaite@ff.vu.lt*

Polymer composites with various carbon inclusions like multiwalled carbon nanotubes (MWCNT), carbon black (CB), graphite or graphene are interesting for fundamental research and are attractive for various applications [1]. The electrical percolation threshold of these composites could be very low and it is important to obtain as low percolation threshold as possible in order to reach optimal mechanical properties of composites and to use minimal concentration of expensive fillers. Adding several different fillers in the matrix the percolation threshold can decrease in comparison with single filler composites due to synergy effect between the different components [2].

In this contribution the dielectric/electrical properties of epoxy resin composites filled with different nanofillers were investigated. The composites were filled with MWCNT (filler content 0.015 – 0.3% wt.), graphene nanoplatelets (GNP) (filler content 0.015 – 3% wt.) and hybrid MWCNT/GNP filler with total contents 0.03 and 0.3% wt. and in different ratios. The dielectric measurement were performed in frequency range from 20 Hz to 3 GHz at room temperature and at low frequencies (20 Hz – 1 MHz) in temperature range from 30 K to 300 K. The quantitative synergy effect on the material electrical conductivity was obtained due to combination of both carbon fillers at filler content 0.3% wt. The electrical conductivity of hybrid filler composites, containing 0.25 wt% of MWCNT and small amount of GNP 0.05 wt% was 4 times higher than the conductivity of composites containing only MWCNT with total 0.3 wt% content.

In this presentation the results of electrical investigations of epoxy resin matrix composites filled with MWCNT, GNP and hybrid MWCNT/GNP composites will be presented and discussed in wide frequency and temperature range.

[1] W. Bauhofer, J. Z. Kovacs, Composite science and technology 69, 1486 (2009).

[2] J. Chen, X. Ch. Du, W. B. Zhang, J. H. Yang, N. Zhang, T. Huang, Y. Wang, Composite science and technology 81, 1-8 (2013).

## **Ferroelectric ceramics how it's made?**

**E. Ćwikiel**

*University of Silesia, Faculty of Computer Science and Materials Science, 2 Śnieżna St., 41-200 Sosnowiec, Poland*

*ewa.cwikiel@us.edu.pl*

Materials showing ferroelectric behaviour are being used in many applications in electronics. A large number of applications of ferroelectric ceramics also exploit properties that are an indirect consequence of ferroelectricity, such as piezoelectric or pyroelectric properties.

The final properties of ferroelectric ceramic greatly depend upon the processing conditions. Each step of processing has to be carefully controlled to get the best product. During the calcination step the solid phase reaction takes place giving the ferroelectric phase. Proper calcination at the right temperature is necessary to obtain the best mechanical and electrical properties. The sintering temperature and time should be optimum for proper densification. For lead containing ferroelectric ceramics (PZT, PLZT, etc.) lead loss occurs at temperatures above 800°C. When the ferroelectric ceramic is cooled after sintering, it does not show any piezoelectricity or pyroelectricity because of the random orientations of the ferroelectric domains in the ceramic. Piezoelectric behaviour can be induced in a ferroelectric ceramic by poling.

# Phase transitions in two new organically templated metal sulfates with 4-aminopyridinium

**Tamara J. Bednarchuk<sup>1</sup>, Vasyl Kinzhybalov<sup>1</sup>, Adam Pietraszko<sup>1</sup>**

<sup>1</sup> Institute of Low Temperature and Structure Research, PAS, Wrocław, Poland

*T.Bednarchuk@int.pan.wroc.pl*

4-Aminopyridine forms a series of inorganic-organic hybrids with different halogen salts which exhibit ferroelectric, ferroelastic and interesting magnetic properties [1-3]. The only representative of double 4-aminopyridinium metal sulfate was nickel analog described by T. Sahbani [4]. During the course of our investigations on sulfate materials, aluminium and iron(III) sulfates templated by 4-aminopyridinium (**4ap**) have been prepared and characterized by vibrational spectroscopy (IR and Raman), single crystal X-ray diffraction and magnetic measurement studies (for compound with Fe<sup>III</sup>). Additionally, Hirshfeld surface analysis have been used to compare the intermolecular interactions in the investigated crystals.

Crystals with Fe<sup>III</sup> in room temperature (RT) are characterized by metal coordination octahedra disordered into two equivalent positions. **4ap** cations in this compound play a role of structure directing agents, they form  $\pi$ - $\pi$  interacting columns of oriented antiparallel in respect to each other cations, which are involved in the pattern of strong hydrogen bonds of N-H $\cdots$ O type.

Two phase transitions were observed in these crystals (Fig. 1): first from a disordered RT phase to incommensurately modulated intermediate phase (with  $\mathbf{q}_1 = 0.270, 0, 0.550$ ) at 265 K, and second around 175 K to the commensurate superstructure (with  $\mathbf{q}_2 = \frac{1}{2}, \frac{1}{2}, \frac{1}{2}$ ).

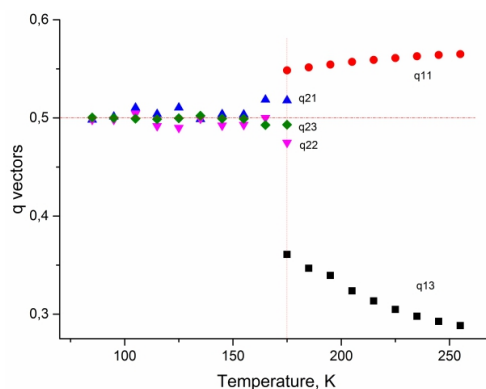


Figure 1 The changes of modulation wavevector  $\mathbf{q}$  with temperature.

The compound with aluminium is characterized by disordered **4ap** cations (at RT). Below  $T_c = 185$  K the **4ap** cations become ordered and oriented antiparallel to each other what results in doubling of the cell in  $b$  axis direction. In the diffraction pattern it is being manifested by the appearance of the weak superstructure reflections.

The mechanism of phase transitions and the physical properties of new 4-aminopyridinium aluminium and iron(III) sulfates will be presented.

[1] R. Jakubas, Z. Ciunik, G. Bator, Ferroelectric properties of  $[4\text{-NH}_2\text{C}_5\text{H}_4\text{NH}][\text{SbCl}_6]$ , Phys. Rev. B, 67, 241031-241036, (2003).

[2] B. Kulicka, R. Jakubas, A. Pietraszko, W. Medycki, J. Świergiel, Structure, phase transitions and molecular dynamics in 4-aminopyridinium hexachloroantimonate(V),  $[4\text{-NH}_2\text{C}_5\text{H}_4\text{NH}][\text{SbCl}_6]$ , J. Mol. Struct., 783, 88-95, (2006).

[3] P. Román, J. Sertucha, A. Luque, L. Lezama, T. Rojo, Structure, phase transitions and molecular dynamics in 4-aminopyridinium hexachloroantimonate(V),  $[4\text{-NH}_2\text{C}_5\text{H}_4\text{NH}][\text{SbCl}_6]$ , J. Mol. Struct., 783, 88-95, (2006).

[4] T. Sahbani, W.S. Sta, M. Rzaigui, Bis(4-aminopyridinium) hexaaquanickel(II) bis(sulfate), Acta Cryst. E, 70, m6, (2014).

# Acoustic properties of new chalcogenide type crystals

**I. Martynyuk-Lototska<sup>1</sup>, B. Zapeka<sup>1</sup>, O. Mys<sup>1</sup>, O. Kokhan<sup>2</sup>, O. Parasyuk<sup>3</sup>, R. Vlokh<sup>1</sup>**

*1- Vlokh institute of Physical Optics, 23 Dragomanov Str., 79005, Lviv, Ukraine, mys@ifio.lviv.ua*

*2- Uzhgorod National University, 46 Pidgorna Street, 88000 Uzhgorod, Ukraine*

*3- Eastern European National University, 13 Voli Ave., 43025 Lutsk, Ukraine*

We present comprehensive experimental measurements and analysis of anisotropy of the acoustic wave (AW) velocities for a number of chalcogenide crystals. We have studied the acoustic properties of the  $\text{Ti}_3\text{AsS}_4$  crystals, including the AW velocities, obliquity and nonorthogonality of the AW, and the deviations from purely longitudinal and transverse polarization types [1]. We have found that the crystals under analysis are characterized by rather low transverse wave velocities  $v_{23}$  and  $v_{32}$ , which are both equal to 630 m/s. It is shown that the efficiency of acoustooptic (AO) interactions in  $\text{Ti}_3\text{AsS}_4$  can be notably increased when providing anisotropic interaction with the slowest transverse AW. Under the previously mentioned conditions, the AO figure of merit can be estimated to be extremely high, i.e., approximately  $3 \times 10^{-12} \text{ s}^3/\text{kg}$ .

We have experimentally studied AW velocities in  $\text{Ti}_3\text{AsSe}_3$  crystals [2]. Basing on these results, the matrices of elastic stiffness and compliance coefficients are obtained and the cross sections of the AW velocity surfaces by the principal crystallographic planes are constructed. We have revealed a phenomenon termed as an acoustic isotropic point. We have found that, at the room temperature and the AW frequency equal to 10 MHz, the  $\text{Ti}_3\text{AsSe}_3$  crystals are close to the conditions of acoustic isotropy, which are analogous to the isotropic point known in crystal optics. Namely, the cross sections of the AW velocity surfaces under these conditions are almost circular and the difference between the velocities of transverse AWs with mutually orthogonal polarizations is very small. Then the specific relations among the elastic stiffness tensor components hold true, which are peculiar for the isotropic glass materials:  $C_{11} \approx C_{33}$ ,  $C_{12} \approx C_{13}$ ,  $C_{44} \approx C_{66} \approx (C_{11} - C_{12})/2$ , and  $C_{14} \approx 0$ . We have revealed that the  $\text{Ti}_3\text{AsSe}_3$  crystals exhibit very small obliquity of the acoustic energy flow with respect to the wave vector of the AW, as well as negligibly small angles of deviation of acoustic polarization from the purely transverse or longitudinal types. The acoustooptic figures of merit calculated for the interaction of waves propagating close to the principal crystallographic axes are as high as  $3068 \times 10^{-15}$  and  $3262 \times 10^{-15} \text{ s}^3/\text{kg}$ , respectively for the isotropic and anisotropic types of acoustooptic interactions.

We present the studies of anisotropy of AW propagation in  $\text{AgGaGe}_3\text{Se}_8$  crystals [3]. Complete matrices of mechanical stiffness and compliance coefficients are determined basing on the experimental values of AW velocities. Cross sections of AW velocity surfaces by the principal crystallographic planes are obtained. We have found that the velocities of quasi-transverse and quasi-longitudinal AWs propagating in the  $\text{AgGaGe}_3\text{Se}_8$  crystals can be very low, thus facilitating potentially high acoustooptic figures of merit.

[1] I. Martynyuk-Lototska, M. Kushnirivych, B. Zapeka, O. Krupych, O. Kokhan, A. Pogodin, E. Peresh, O. Mys, R. Vlokh, Acoustic anisotropy of acoustooptic  $\text{Ti}_3\text{AsS}_4$  crystals, *Applied Optics*, vol. 54, pp. 1302-1308 (2015).

[2] I. Martynyuk-Lototska, O. Mys, B. Zapeka, A. Solomon, O. Kokhan and R. Vlokh, Acoustic, elastic and acoustooptic properties of  $\text{Ti}_3\text{AsSe}_3$  crystals: acoustic isotropic point, *Ukr. J. Phys. Opt.* vol. 16, pp. 178-186 (2015).

[3] I. Martynyuk-Lototska, M. Kushnirivych, G. Myronchuk, O. Parasyuk and R. Vlokh, Acoustic anisotropy of  $\text{AgGaGe}_3\text{Se}_8$  crystals and their acoustooptic applications, *Ukr. J. Phys. Opt.* vol. 16, pp. 77-84 (2015).

# Topological reactions of electrically induced defects of optical indicatrix orientation in crystals

Yu. Vasylykiv, I. Skab, T. Kryvyy, O. Mys, R. Vlokh

*Vlokh institute of Physical Optics, 23 Dragomanov Str., 79005, Lviv, Ukraine, mys@ifp.lviv.ua*

We study the behaviour of topological defects (TDs) of optical indicatrix orientation under the conditions when electrooptic Pockels and Kerr nonlinearities coexist (crossover regime) in the crystals belonging to cubic, hexagonal, trigonal and tetragonal systems [1, 2]. The conically shaped electric field was applied along the principal crystallographic axis or along [111] direction in crystals of cubic system. We have found that increases in the electric voltage applied to a crystal induce neither topological defects, with the strengths being not multiples of  $\frac{1}{2}$ , or the optical vortices with fractional charges. Instead, there appear some additional topological defects of the optical indicatrix orientation, the behavior of which we have studied in detail. The topological reactions accompanying the processes of birth, addition, division and annihilation of the TDs of optical indicatrix orientation were observed under electric field variations. It is shown that the conservation law for the strength of TDs holds true under these topological reactions and the behaviour of the TDs can be exhaustively described by four different scenarios. For example in crystals of cubic system we have found that the electric voltage leads to a birth of three pairs of TDs. They are characterized by half-integer magnitudes of their strength and the opposite signs of that strength within the pairs. The above pairs of TDs annihilate with decreasing voltage. We have also shown that the total charge of relevant optical vortices is not conserved under topological reactions.

- [1].Yu.Vasylykiv, T.Kryvyy, I.Skab and R. Vlokh, Behavior of topological defects of optical indicatrix orientation in cubic single crystals under conically distributed electric field. 1. The electric field and the optical beam parallel to the three-fold symmetry axis , Ukr. J. Phys. Opt. vol. 15, pp.184-194 (2014).
- [2] Yu.Vasylykiv, T.Kryvyy, I. Skab and R.Vlokh, Behaviour of topological defects of optical indicatrix orientation in cubic, hexagonal, trigonal and tetragonal crystals under conically distributed electric field. 2. The electric field and the optical beam parallel to the principal crystallographic directions, Ukr. J. Phys. Opt. vol. 16, pp. 1-16 (2015).
- [3] Yu. Vasylykiv, I. Skab, and R. Vlokh Crossover regime of optical vortices generation via electro-optic nonlinearity: the problem of optical vortices with the fractional charge generated by crystals J. Opt. Soc. Am. A, vol. 31, pp. 1936-1945, (2014).

# High magnetic field induced electric polarization of antiferromagnets $\text{LiCoPO}_4$ and $\text{LiNiPO}_4$

**V. Khrustal'ov, V. Savitsky, M. Kharchenko**

*B.Verkin Institute for Low Temperature Physics and Engineering NAS of Ukraine,  
47 Nauky Ave., 61103 Kharkiv, Ukraine*

*khrustal'ov@ilt.kharkov.ua*

In this report the results of measurements of electrical polarization of well-known magneto-electric antiferromagnetic crystals  $\text{LiCoPO}_4$  ( $T_N = 21.6$  K) and  $\text{LiNiPO}_4$  ( $T_N = 20.8$  K) under the influence of strong pulsed magnetic field are represented.

The experiments were carried out with single crystal samples at the liquid helium temperatures in a pulse magnetic field aligned along an easy magnetic axis (axis  $b$  for  $\text{LiCoPO}_4$  and axis  $c$  for  $\text{LiNiPO}_4$ ). The electric polarizations of the crystals were measured along crystallographic axes  $a$ . It was found in  $\text{LiCoPO}_4$  the electric polarization vanishes at the first magnetic phase transition in the field  $H_1 = 121$  kOe and reverts at the second phase transition in the field  $H_2 = 226$  kOe. The transition to the saturated paramagnetic state ( $H_3 = 276$  kOe) leads to disappearance of polarization again. The electric polarization in  $\text{LiNiPO}_4$  has the similar behavior, but in low field region it has the large nonlinear component. The polarization also vanishes when magnetic field reaches value of the first transition field  $H_1 = 130$  kOe and reappears in the field 226 kOe. But in this case polarization has opposite sign. At transition to saturated paramagnetic state ( $H = 215$  kOe) electric polarization disappears.

As it seen from the figure the linear extrapolation of reentrant electric polarization to zero fields for  $\text{LiNiPO}_4$  gives zero value of polarization in contrast with  $\text{LiCoPO}_4$ , where reentrant polarization decreases with increasing magnetic field. One can assume that in  $\text{LiNiPO}_4$  the electric polarization in high-field phase is a result of the magneto-electric effect. Reducing reentrant polarization with increasing field in  $\text{LiCoPO}_4$  confirms the assumption that high-field phase is the incommensurate strongly anisotropic ferrimagnetic one in which the number of antiferromagnetic coupled pairs decreases with increasing field. The occurrence of reentrant polarization indicates that the spatial inversion as the symmetry operation is recovered in high-field magnetic phases in both crystals.

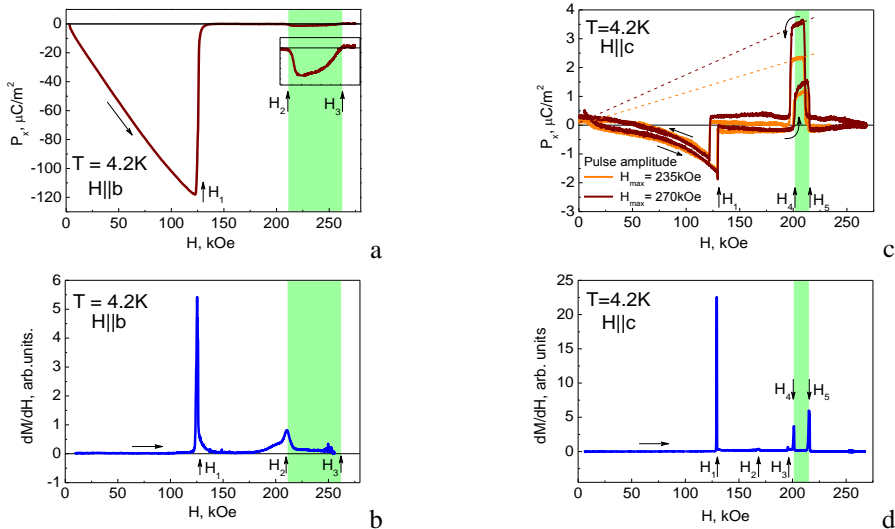


Fig.1. Electric polarization and differential magnetic susceptibility, (a,b) – for  $\text{LiCoPO}_4$  and (c,d) – for  $\text{LiNiPO}_4$ .

Recent research in this area was done in the network of project TUMOCS. This project has received funding from the European Union's Horizon 2020 research and innovation programme under the Marie Skłodowska-Curie grant agreement No 645660.

# Effect of Nd and Sc substitution on structural, magnetic and dielectric properties of $\text{SrFe}_{12}\text{O}_{19}$ hexaferrite

**K. Pasińska<sup>1</sup>, A. Hilczer<sup>2</sup>, B. Andrzejewski<sup>2</sup>, Ewa Markiewicz<sup>2</sup>, V. Kinzhybalo<sup>1</sup>, A. Pietraszko<sup>1</sup>**

1- Institute of Low Temperature and Structure Research, PAS, Wrocław, Poland

2- Institute of Molecular Physics, PAS, Poznań, Poland

*k.pasinska@int.pan.wroc.pl*

M-type hexaferrites ( $\text{SrFe}_{12}\text{O}_{19}$ , denoted as SrM), with  $P6_3/mmc$  space group and  $Z = 2$ , can be considered as containing five magnetic sublattices coupled by superexchange interactions through the  $\text{O}^{2-}$  ions [1,2]. They have recently become of great interest since the discovery of multiferroic behaviour in the barium hexaferrites (denoted as BaM).

The substitution of Fe-site may induce the conical magnetic spin structure. The longitudinal conical structure was observed for Sc substituted BaM,  $\text{BaFe}_{12-x}\text{Sc}_x\text{O}_{19}$  [3]. Moreover, using rare earth metals as dopants has been reported as a method that promotes increased Fe–O–Fe interaction, which would result in changed magnetic properties in the doped SrM particles [4].

In the present study  $\text{Sr}_{0.95}\text{Nd}_{0.05}\text{Fe}_{12-x}\text{Sc}_x\text{O}_{19}$  series with different substitution ratios ( $x = 0.01, 0.03, 0.05, 0.07, 0.09$ ) were obtained by the citric sol-gel method. The structure of the samples was controlled by X-ray diffraction (X'Pert PANalytical,  $\text{CuK}\alpha$ , Bragg-Brentano geometry) and the microstructure by scanning electron microscopy (FEI Nova NanoSEM). Magnetic properties were studied using PPMS (Quantum Design) with VSM probe in 10 - 310 K temperature range. The structure of the samples was refined using the Rietveld method (HighScore Plus, standard setting  $P6_3/mmc$  space group No 194) and the results are shown in Figure 1.

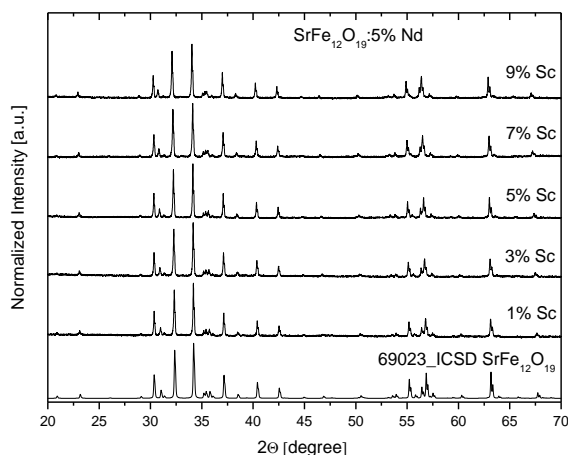


Figure 1 XRD diffraction patterns of  $\text{Sr}_{0.95}\text{Nd}_{0.05}\text{Fe}_{12-x}\text{Sc}_x\text{O}_{19}$ .

[1] K. Kimura, M. Ohgaki, K. Tanaka, H. Morikawa, F. Marumo, Study of the bipyramidal site in magnetoplumbite-like compounds,  $\text{SrM}_{12}\text{O}_{19}$  ( $M = \text{Al, Fe, Ga}$ ), *J. Solid State Chem.*, **87**, 186-194, (1990).

[2] J. Park, Y.-K. Hong, S.-G. Kim, S. Kim, L.S.I. Liyanage, J. Lee, W. Lee, G.S. Abo, K.-H. Hur, S.-Y. An, Maximum energy product at elevated temperatures for hexagonal strontium ferrite ( $\text{SrFe}_{12}\text{O}_{19}$ ) magnet, *J. Magn. Magn. Mater.*, **355**, 1-6, (2014).

[3] Y. Tokuda, Y. Kaneko, D. Okuyama, S. Ishiwata, T. Arima, S. Wakimoto, K. Kakurai, Y. Taguchi, Y. Tokura, Multiferroic M-Type Hexaferrites with a Room-Temperature Conical State and Magnetically Controllable Spin Helicity, *Phys. Rev. Lett.*, 1-4 (2010).

[4] J. F. Wang, C. B. Ponton, I. R. Harris, A study of the magnetic properties of hydrothermally synthesised Sr hexaferrite with Sm substitution, *J. Magn. Magn. Mater.*, **234**, 233-240, (2001).



# PHOTOLUMINESCENCE and PHOTOCONDUCTIVITY of $\text{Bi}_{12}\text{SiO}_{20}$ CRYSTALS DOPED by Al, Ga and Sn

**A. A. Dyachenko<sup>1</sup>, T. V. Panchenko<sup>2</sup>**

<sup>1,2</sup> *Department of Physics, Electronics and Computer Science, Oles Honchar Dnepropetrovsk National University, 72 Gagarin Avenue, Dnepropetrovsk, Ukraine*

*Main author email address: anna.diachenko@mail.ru*

Noncentro-symmetrical crystals with sillenite structure  $\text{Bi}_{12}\text{MO}_{20}$  (BMO, where M = Si, Ge, Ti) combine the properties of active dielectrics and wide-gap semiconductors ( $\Delta E_g \approx 3.4$  eV). These crystals are widely used as functional media in different types of light-modulating devices. So, the study of photoinduced processes and their modification by doping is very important in these applications.

It is shown, in particular, that Al, Ga- ions considerably reduce the photoconductivity (PC) and optical absorption, decrease photochromic effect in the visible range of spectra, influence on some characteristics of spatial-time modulating devices [1, 2]. Nevertheless, changes in the structure of local energy levels of the band gap in sillenites and schemes of electron transitions in the impurity centers are still not quite clear. It seems that unifies investigations of photoluminescence (PL) can provide useful information in solving this problem. In the present work, the results of investigations of PL in  $\text{Bi}_{12}\text{SiO}_{20}$  (BSO) doped by Al, Ga, Sn ions (BSO:Al, BSO:Ga, BSO:Sn) are represented in parallel with investigations of PC spectra.

Crystals of BSO, BSO:Al, BSO:Ga and BSO:Sn were grown by Czochralski method. PL was excited from the sample bulk by radiation of a xenon lamp DKsEl-1000. The measurements were carried out at  $T = 4.2 \pm 0.2$  and 80 K. PC was studied using a SPM-2 monochromator, a synchronic detection instrument, and a B7-30 voltmeter-electrometer. Measurements were carried out under constant electric field; the light was modulated with frequency 12 Hz at  $T = 80$  K.

Photoluminescence of BSO crystals was observed in the range  $h\nu = 1.0 - 2.9$  eV under excitation with  $h\nu^{exc} \geq 3.3$  eV at  $T = 4.2$  K. The spectra  $I^{PL}(h\nu)$  are broad structured and consist of five components with half-width  $\Delta h\nu \approx 0.01 - 0.024$  eV and positions of maxima  $h\nu_{max} = 1.72, 1.9, 2.1, 2.36, 2.52$  eV. The similar  $I^{PL}(h\nu)$  spectra was observed also in [3]. Doping of BSO by Al, Ga, and Sn ions causes the transformation of  $I^{PL}(h\nu)$  spectral contours with occurring new short wavelength bands  $h\nu_{max} = 2.62$  and 2.76 eV. The large width of  $I^{PL}(h\nu)$  spectrum points to the presence of several recombination levels in the band gap. Increasing the temperature up to 80 K results in dropping the intensity and narrowing the spectral range to 1.75 – 2.5 eV; the shape of the envelope of  $I^{PL}(h\nu)$  spectral components becomes close to symmetric.

Spectra of selective excitation,  $I^{PLE}(h\nu)$ , of one of general for investigated crystals intensive component of  $I^{PL}(h\nu)$  emission spectra with  $h\nu_{max} = 2.1$  eV have a shape of intensive narrow bands in the area of the edge of fundamental absorption for BSO. For pure crystals, spectral positions of the maximum of this band  $h\nu_{max} = 3.4$  and 3.25 eV at  $T = 4.2$  and 80 K correspond to the positions of the intrinsic PC peak and to steep increase of optical absorption. For BSO:Al, BSO:Ga and BSO:Sn crystals, such accordance is absent.

So, on the base of the spectra of PL and PC in crystals BSO:Al, BSO:Ga, BSO:Sn simultaneously recombination and intracenter mechanism of the luminescence was revealed. We assume that the recombination centers in investigated crystals are  $\text{Bi}^{3+}_{\text{Si}} - \text{O}^-$  complexes as well as impurity centers  $\text{Al}^{3+}_{\text{Si}}$ ,  $\text{Ga}^{3+}_{\text{Si}}$ ,  $\text{Sn}^{4+}_{\text{Si}}$ .

## References

- [1] S.L. Hou, R.B. Lauer, R.E. Aldrich, Journal of Applied Physics, vol. 6, p. 2654-2658 (1971)
- [2] T.V. Panchenko, Physical Solid State, vol. 40, p. 454 – 457 (1998)
- [3] V.K. Malinovsky, O.A. Gudayev, V.A. Gusev, Photoinduced phenomena in sillenites, Novosibirsk: Nauka, p. 40 – 68 (1990)

# DOMAIN SWITCHING IN TGS and DTGS CRYSTALS NEAR THE PHASE TRANSITION

**K. Matyjasek**

*Institute of Physics, Faculty of Mechanical Engineering and Mechatronics, West Pomeranian University of Technology Al. Piastów 48, 70-310 Szczecin, Poland*

Ferroelectric crystals of the triglycine sulphate group are characterized by high pyroelectric coefficient and are applied in high sensitivity IR detectors. They are primarily interesting as model materials for analyzing the influence of defects on the dynamics of the domain structure during polarization switching. In this report we investigate the microscopic features of  $180^\circ$  domain wall dynamics and relate its dynamics to the defect structure in triglycine sulphate (TGS) and deuterated triglycine sulphate (DTGS) crystals. An analysis of the domain structure evolution with a change in temperature and under electric field has been studied by means of nematic liquid crystal method. The stabilization of the domain structure appears to be strongly dependent on the defect structure in DTGS crystals. In this crystals structural disordering and composition fluctuations, induce local symmetry distortions, and internal fields. Microscale studies of switching process in conjunction with electric measurements allowed us to establish a relationship between local properties of domain dynamics and macroscopic response such as polarization and switching currents. The effect of lattice defects on the crystal properties is observed near the phase transition, where the crystalline structure can be easily reconstructed by external forces. As a result of local inhomogeneities, there is observed the distribution of the transition temperatures in the local regions of the examined DTGS crystal samples.

# Effect of Cu doping on the mechanical properties of $\text{Ba}_{0.95}\text{Pb}_{0.05}\text{TiO}_3$ ceramics.

**D Sitko<sup>1</sup>, K Konieczny<sup>2</sup>, W Piekarczyk<sup>3</sup>, A Kalvane<sup>4</sup>, P. Czaja<sup>2</sup> and J Suchanicz<sup>2</sup>**

*Institute of Physics, Pedagogical University, Podchorążych 2, 30-084, Kraków, Poland*

*Institute of Technology, Pedagogical University, Podchorążych 2, 30-084, Kraków, Poland*

*Faculty of Materials Science and Ceramics, AGH-University of Science and Technology, Mickiewicza 30, 30-059, Kraków, Poland*

*Institute of Solid State Physics, University of Latvia, 8 Kengaraga*

*Str., LV-1063, Riga, Latvia*

*dsitko@up.krakow.pl*

Recently more interest have been focused on mechanical properties ferroelectrics ceramics. This is because, these materials would be exposed to mechanical stress. We investigated the mechanical properties of  $\text{Ba}_{0.95}\text{Pb}_{0.05}\text{TiO}_3 + X\% \text{CuO}$  ( $X=0, 0.05, 0.1, 1, 3$ ) (BPTCX) samples were made by a conventional method.

The investigations of microstructure of the ceramics were performed on fractures sections. They were carried out by means of an electron scanning microscope with field emission Hitachi S4700.

The SEM analysis showed that the samples are perfectly sintered. The surface of the fracture goes along grains as well as along boundaries between grains. The fracture has a fragile nature and in grains the crystalline structures are observed. They indicate that the growth of grains has occurred according to the layer mechanism, probably the screw dislocation mechanism.

The EDS was applied to determine the homogeneity of the studied material. The obtained „mappings” confirmed the qualitative composition of the examined samples. Using an ultrasonic method and the INCO-VERITAS ultrasonic measuring set UZP-1 main material constants of the BPTCX were determined. The investigation of elastic properties was performed in order to determine the influence of the crystalline structure, structural anisotropy and the material microstructure on mechanical properties of this material. For all samples the Young's modulus ( $E$ ), the shear modulus ( $G$ ), bulk modulus ( $K$ ) as well as Poisson's coefficient ( $\nu$ ) were calculated on the basis of the longitudinal and transverse wave velocities. The mechanical properties showed that the elastic modules are correlated to the microstructure of the material. The Young's modulus exhibits non-linear compositional dependencies. While the shear modulus, over a range of concentration is stable. Moreover, Poisson's ratio  $\nu$  is  $\sim 0.25$ . The obtained values of elastic modules indicate, that the tested ceramics materials are the dense and stiff[2].

[1] J. Piekarczyk, H.W. Henniscke, R. Pampuch, The determining the elastic constants of porous zinc ferrite materials. *cfi/Ber.D.K.G.* 59 227-232 (1982).

[2] W. Śmiga, D. Sitko, W. Piekarczyk, I. Jankowska-Sumara and M. Kalvane. Composition-related structural, thermal and mechanical properties of  $\text{Ba}_{1-x}\text{Sr}_x\text{TiO}_3$  ceramics ( $0 \leq x \leq 0.4$ ), *Phase Transitions* (2015)87;992-1001.

# The properties of $(1-x)(0.5\text{PZT}-0.5\text{PFW})-x\text{PFN}$ ceramics

**D. Brzezińska<sup>1</sup>, R. Skulski<sup>1</sup>, D. Bochenek<sup>1</sup>, P. Niemiec<sup>1</sup>, A. Chrobak<sup>2</sup>**

*1 - University of Silesia, Institute of Technology and Mechatronics, 12 Żytnia Str., 41-200, Sosnowiec, Poland;*

*2 - University of Silesia, A. Chelkowski Institute of Physics, 4, Uniwersytecka St., 40-007 Katowice, Poland*

*Corresponding author: dagmara.brzezinska@us.edu.pl*

The ceramic samples of solid solution  $(1-x)[0.5(\text{PbZr}_{0.53}\text{Ti}_{0.47}\text{O}_3)-0.5(\text{PbFe}_{2/3}\text{W}_{1/3}\text{O}_3)]-x(\text{PbFe}_{1/2}\text{Nb}_{1/2}\text{O}_3)$  [i.e.  $(1-x)[0.5(\text{PZT}-\text{PFW})]-x\text{PFN}$  with  $x=0; 0.1; 0.2$ ] have been obtained by conventional ceramic technology from oxides  $\text{PbO}$ ,  $\text{ZrO}_2$ ,  $\text{TiO}_2$ ,  $\text{Fe}_2\text{O}_3$ ,  $\text{WO}_3$ ,  $\text{Nb}_2\text{O}_5$ . The calcined powders were crushed and next pressed into discs and sintered using free sintering (FS) method. Basing on the literature data for individual components it can be expected that this material should have interesting multiferroic properties. In our previous work [1] we described details of the technology and main dielectric properties of obtained samples. The presented work is the next step in investigations of this solid solution and concerns the magnetic properties. We present obtained results of investigations of magnetic hysteresis loops (Fig.1) and the dependency of magnetic susceptibility on temperature (Fig.2).

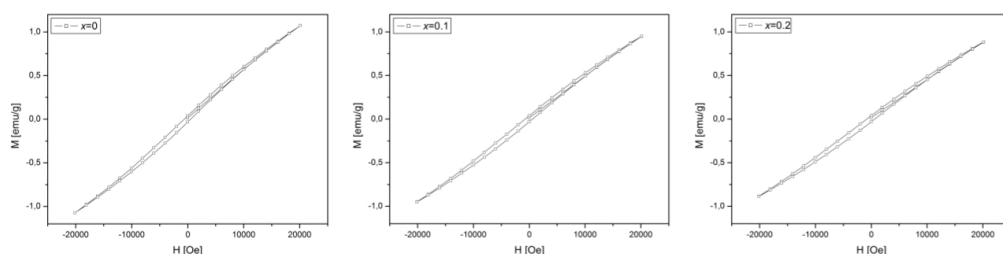


Figure 1 Magnetic hysteresis loops  $M(H)$  for  $(1-x)[0.5(\text{PbZr}_{0.53}\text{Ti}_{0.47}\text{O}_3)-0.5(\text{PbFe}_{2/3}\text{W}_{1/3}\text{O}_3)]-x(\text{PbFe}_{1/2}\text{Nb}_{1/2}\text{O}_3)$  ceramics with  $x=0, 0.1$  and  $0.2$ . Temperature 2K.

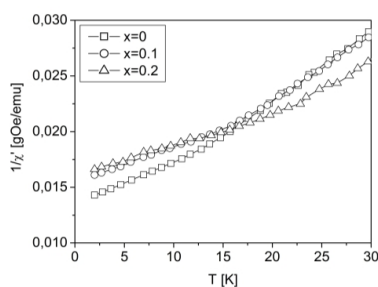


Figure 2 The dependency of magnetic susceptibility on temperature for all investigated compositions.  $H=1000\text{Oe}$ .

**Keywords:** PZT-PFW and PZT-PFW-PFN ceramics, magnetic properties

[1] D. Brzezińska, R. Skulski, D. Bochenek, P. Niemiec, The properties of  $(1-x)(0.5\text{PZT}-0.5\text{PFW})-x\text{PFN}$  ceramics, Integrated Ferroelectrics, DOI: 10.1080/10584587.2016.1185320.

# Dielectric properties of sodium bismuth titanate ceramics

**J. Macutkevici<sup>1</sup>, J. Banys<sup>1</sup>, I. Gruszka<sup>2</sup>, A. Kania<sup>2</sup>**

*1- Faculty of Physics, Vilnius university, Sauletekio al. 9, LT-10222 Vilnius, Lithuania*

*2- Institute of Physics, University of Silesia, ul. Uniwersytecka 4, PL-40-007 Katowice, Poland*

*Main author email address: jan.macutkevici@gmail.com*

The mixed ferroelectric-relaxor systems close to morphotropic boundary demonstrate very attractive dielectric and piezoelectric properties. Recently, sodium bismuth titanate ( $\text{Na}_{0.5}\text{Bi}_{0.5}\text{TiO}_3$ , NBT) based ceramics pay attention due their attractive piezoelectric properties [1]. The traditional view of the structure and phase behaviour of NBT is follows  $R3c \rightarrow 523 \text{ K} \rightarrow R3c+P4bm \rightarrow 670 \text{ K} \rightarrow P4bm \rightarrow 813 \text{ K} \rightarrow Pm3m$ , however recently was reported a ferroelectric (R3c) – ferroelectric (Cc) phase coexistence at room temperature [2]. In this work broadband dielectric properties of NBT ceramics in wide temperature region (25-750 K) are presented (Fig. 1). The frequency dependent dielectric anomaly close to 400 K is caused by different symmetry ferroelectric domains dynamics and the mean relaxation time follows the Vogel-Fulcher law in this temperature region. At higher temperature (above 600 K) the ferroelectric phase transition is expressed in the temperature dependence of the complex dielectric permittivity. The evidence for relaxational soft mode existence in NBT will be presented and discussed. Therefore, the ferroelectric phase transition is mixed one “order-disorder” and displacive. At very high temperatures (above 650 K) the electrical conductivity effects becomes very important in dielectric properties of NBT ceramics. Conductivity mechanism will be also discussed in the presentation.

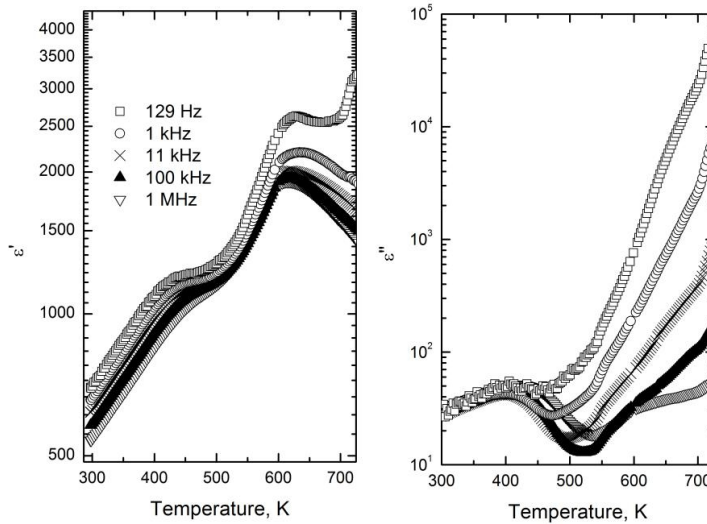


Fig. 1 Temperature dependence of complex dielectric permittivity at different frequencies for NBT ceramics.

1. H. Nagata, M. Yoshida, Y. Makiuchi, T. Takenaka, Large piezoelectric constant and high Curie temperature of lead – free piezoelectric ceramic ternary system based on bismuth sodium titanate – bismuth potassium titanate near the morphotropic phase boundary Jap. J. Appl. Phys. 111, pp. 024107 (2012).
2. B. N. Rao, A. N. Fitch, R. Ranjan, Ferroelectric-ferroelectric phase coexistence in  $\text{Na}_{1/2}\text{Bi}_{1/2}\text{TiO}_3$ . Phys. Rev. B 87, 060102 (R) (2013).

# Functional properties of BaTiO<sub>3</sub> ceramics: the influence of iron addition

**Vidmantas Kalendra<sup>1</sup>, Mantas Simenas<sup>1</sup>, Felicia Gheorghiu<sup>2</sup>, Cristina Ciomaga<sup>3</sup>, Nadejda Horchidan<sup>3</sup>, Liliana Mitoseriu<sup>3</sup> and Juras Banys<sup>1</sup>**

<sup>1</sup> *Lab. of Microwave Spectroscopy, Radio Physics Department, Faculty of Physics, Vilnius University, Sauletekio av. 9, LT-10222 Vilnius, Lithuania*

<sup>2</sup> *Research Center on Advanced Materials and Technologies, Sciences Department, Alexandru Ioan Cuza University of Iasi, Blvd. Carol I, nr. 11, 700506 Iasi, Romania*

<sup>3</sup> *Dielectrics, Ferroelectrics & Multiferroics Group, Department of Physics, Alexandru Ioan Cuza University of Iasi, Blvd. Carol I, nr. 11, 700506 Iasi, Romania*

*e-mail address: vidmantas.kalendra@ff.vu.lt*

The research field of dilute magnetic oxides (DMO) has a great interest in the last years as attractive materials for spintronics and different magnetoelectric devices [1,2]. In the present study, BaTi<sub>1-x</sub>Fe<sub>x</sub>O<sub>3</sub> (0 ≤ x ≤ 0.5) ceramics have been synthesized by solid state reaction technique. The structural, microstructural and functional properties of BaTi<sub>1-x</sub>Fe<sub>x</sub>O<sub>3</sub> ceramics were investigated and discussed. X-ray diffraction analysis indicated that higher doping level of Fe, higher sintering temperature and longer sintering time promoted the formation of hexagonal phases in Fe-doped BaTiO<sub>3</sub> ceramics. The composition with x=0.015 presents a tetragonal crystalline symmetry, while a superposition of tetragonal and hexagonal phases was found for x=0.018 and 0.02. SEM analysis indicates a heterogeneous microstructure with a small degree of porosity (relative densities are above 94% for all samples) and a bimodal grain size distribution, consisting of larger grains with an equivalent grain size of ~15-18 μm and of smaller grains of ~4-8 μm. Dielectric properties in the frequency range (20Hz-2MHz) showed that all the Fe-doped BaTiO<sub>3</sub> ceramics have some anomalies. The dielectric permittivity maximum vs. temperature presents a decrease around the ferroelectric-paraelectric phase transition from 127°C for pure BaTiO<sub>3</sub> to ~85°C for x=0.02. Using impedance spectroscopy, we can easily separate the contribution from the grain or grain-boundary. It was observed that by Fe doping, the complex impedance plot indicates more than one semi-circle, demonstrating that ceramics have a local electrical heterogeneity, even they look homogeneous from structural and compositional point of view. The EPR analysis for the composition x=0.005 supports the X-ray diffraction results, since the observed Fe<sup>3+</sup> spectrum corresponds to tetragonal Fe-doped BaTiO<sub>3</sub>. It was found that paramagnetic Fe<sup>3+</sup> ions reside at the Ti lattice sites.

The presented results have indicated that the BaTi<sub>1-x</sub>Fe<sub>x</sub>O<sub>3</sub> system can be considered as a possible candidate for modern electronics applications and functionalized materials.

## References:

1. T. Chakraborty, S. Ray, M. Itoh, Phys Rev B 83, 144407 (2011)
2. I. Mikulska, M. Valant, I. Arčon, D. Lisjak, J. Am. Ceram. Soc., 98 [4] 1156–1161 (2015)

## **A Raman spectroscopy study of the phase transition in ferroelectric PZT+PFS**

**A. Osak**

*Cracow University of Technology, ul. Podchorążych 1, 30-084 Kraków, Poland*

*puosak@cyfronet.pl*

The Raman spectra in  $\text{Pb}[(\text{Fe}_{1/3}\text{Sb}_{2/3})_x\text{Ti}_y\text{Zr}_z]\text{O}_3$  ferroelectric ceramics with  $x=0.1$ ,  $y=0.43$ ,  $0.44$ ,  $0.47$  and  $x+y+z=1$  has been studied. The samples with the morphotropic ( $y=0.43$  and  $0.44$ ) and non-morphotropic ( $y=0.47$ ) content have been measured. The results of Raman study was compared and discussed with results of X ray diffraction studies of the phase transition and dielectric spectroscopy. Raman spectra have been carried out in the temperature range 298-623K.

# On the structural phase transition in a perovskite-type Diaminopropanetetrachlorocuprate (II) - $\text{NH}_3(\text{CH}_2)_3\text{NH}_3\text{CuCl}_4$ crystal

M. Kostrzewa<sup>1</sup>, O. Czupiński<sup>2</sup>, A. Ingram<sup>1</sup>, Janczak<sup>3</sup>, J. Przesławski<sup>4</sup> and Z. Czapla<sup>1</sup>

*1- Department of Physics, Opole University of Technology, Ozimska 75,  
45-370 Opole, Poland*

*2- Faculty of Chemistry, University of Wrocław, F. Joliot-Curie 14,  
50-383 Wrocław, Poland*

*3- Institute of Low Temperature and Structure INTBiS PAN Wrocław, Okólna 2,  
50-422 Wrocław*

*4- Institute of Experimental Physics, University of Wrocław, M. Born'a 9,  
50-204 Wrocław, Poland*

*m.kostrzewa@po.opole.pl*

Chemical preparation, DSC studies, thermal stability (TGA studies), X-ray powder studies, PAL investigations, optical studies (polarization microscopy observation, linear birefringence studies) and electric properties of  $\text{NH}_3(\text{CH}_2)_3\text{NH}_3\text{CuCl}_4$  crystal are presented. On a ground of DSC studies the structural phase transition of the first order was observed at 436 K. The enthalpy and entropy of the phase transition are equal to 1120 J/mol and 2.57 J/molK, respectively. DTA and TGA studies confirmed the phase transition at 436 K and give evidence of chemical and thermal stability of the compound up to about 480 K. X-ray studies revealed the change of symmetry from orthorhombic room temperature phase to monoclinic above the phase transition temperature. The change of symmetry was confirmed in optical polarization microscopy observation as appearance of domain structure in the (010) plane. Birefringence measurement show clearly the first order phase transition at 436 K. Dielectric measurements showed significant increase of conductivity on approaching of phase transitions region and its further significant increase above the phase transition temperature. An activation energy obtained from measurement of complex impedance activation is dependent on the temperature range and different for particular phases.



# EPR of structural phase transitions in formate metal-organic frameworks

**M. Šimėnas<sup>1</sup>, A. Ciupa<sup>2</sup>, K. Aidas<sup>1</sup>, M. Maczka<sup>2</sup>, A. Pöppl<sup>3</sup>, J. Banys<sup>1</sup>**

*1- Faculty of Physics, Vilnius University, Sauletekio 9, LT-10222 Vilnius, Lithuania*

*2- Institute of Low Temperature and Structure Research, Polish Academy of Sciences, P.O. Box 1410, PL-50-950 Wrocław 2, Poland*

*3- Faculty of Physics and Earth Sciences, Universität Leipzig, Linnestrasse 5, D-04103 Leipzig, Germany*

*mantas.simenas@ff.vu.lt*

Lately, novel porous materials called metal-organic frameworks (MOFs) emerged and immediately attracted attention of the scientific community. These crystalline compounds are unique due to the high degree of porosity which can be utilized for gas adsorption related applications. Additionally, many MOFs containing paramagnetic transition-metal ions exhibit peculiar magnetic properties. The organic part in several of such compounds consists of polar molecules which below a certain phase transition temperature order into a ferroelectric-type phase, making these materials single-phase hybrid multiferroics.

We use continuous-wave (CW) and pulse EPR as well as pulse ENDOR spectroscopic techniques to investigate and characterize structural phase transitions in manganese and copper doped MOFs with general chemical formula  $[A][Zn(HCOO)_3]_n$  (where  $n = 1, 2$  and  $A^{n+}$  is molecular cation such as  $NH_4^+$ ,  $(CH_3)_2NH_2^+$  or  $NH_3(CH_2)_4NH_3^{2+}$ ) (Figure 1). The temperature dependent CW EPR spectra reveal that the local paramagnetic ion-probes are indeed sensitive to the local structural changes occurring at the phase transitions. Spectral simulations are used to obtain the  $g$ , hyperfine  $A$  and fine structure  $D$  tensors and temperature dependencies of their components allowing to characterize the observed phase transitions. Pulse EPR and ENDOR measurements are performed to study structure of the frameworks in the low temperature phase. The experimentally obtained structural information is supported by the density functional theory calculations.

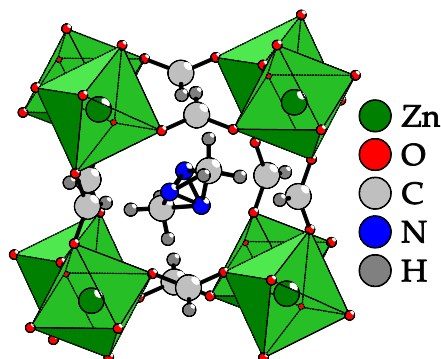


Figure 1. High temperature phase of  $[(CH_3)_2NH_2][Zn(HCOO)_3]$  MOF.

# Dielectric Spectroscopy of Pyr<sub>14</sub>TFSI and Pyr<sub>12</sub>O<sub>1</sub>TFSI Ionic Liquids

**D. Jablonskas,<sup>1,\*</sup> M. Ivanov<sup>1</sup>, J. Banys<sup>1</sup>, G. A. Giffin<sup>2,3</sup> and S. Passerini<sup>2,3</sup>**

<sup>1</sup>*Faculty of Physics, Vilnius University, Sauletekio av. 9/IIIb, Vilnius, Lithuania*

<sup>2</sup>*Helmholtz Institute Ulm, Helmholtzstrasse 11, 89081 Ulm, Germany*

<sup>3</sup>*Karlsruhe Institute of Technology (KIT), P.O. Box 3640, 76021 Karlsruhe, Germany*

*\*Corresponding Author: dziugas.jablonskas@ff.stud.vu.lt*

The ionic liquids are known to have a wide application spectrum. To name a few, they are used as solvents, as a good choice to dissolve carbon nano particles, and as electrolytes for lithium batteries as well – a good alternative to organic liquid electrolytes. Strictly speaking, this is a family of salts that exist in a liquid state at room temperature [1].

This work is concentrated on dielectric properties of N-butyl-N-methylpyrrolidinium bis(trifluoromethanesulfonyl)imide (Pyr<sub>14</sub>TFSI) and N-methoxyethyl-N-methylpyrrolidinium bis(trifluoromethanesulfonyl)imide (Pyr<sub>12</sub>O<sub>1</sub>TFSI) ionic liquids. TFSI anion is a promising material to be used in Lithium ion batteries [2], thus it drew our attention to investigate the dielectric response of TFSI-based ionic liquids.

The dielectric permittivity of Pyr<sub>14</sub>TFSI and Pyr<sub>12</sub>O<sub>1</sub>TFSI was measured in frequency range of 40 MHz to 20 GHz and temperature range of 298 K to 370 K. The measurements were performed during heating cycle with 0.75 K/min temperature change rate. It is known that Pyr<sub>14</sub>TFSI and Pyr<sub>12</sub>O<sub>1</sub>TFSI are hygroscopic ionic liquids. In order to prevent the influence of water, the samples were handled in dry room and were kept in vacuum bags until the experiment. We believe that the influence of water during the measurement was minor if any, because results of heating and cooling cycles are similar. The dielectric spectra of both ionic liquids show clearly conductive behavior, i.e. the complex dielectric permittivity increases with decrease of frequency. This phenomenon obscures any traces of dielectric dispersion caused by dipoles of the material. In order to be able to extract any useful data, we recalculated the dielectric spectra to specific resistivity spectra. The obtained form of spectra was found out to be of Havriliak – Negami (H-N) type (fig. 1). The fitting of spectra allowed to calculate the temperature dependence of the mean relaxation time [3], which is Vogel – Fulcher – Talmann (VFT) type for both materials. The obtained results and comparison of both ionic liquids will be presented.

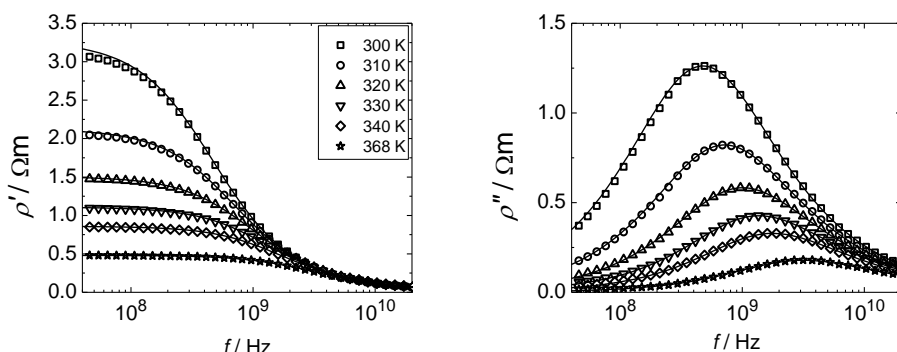


Fig. 1 Frequency dependence of specific resistivity of Pyr<sub>14</sub>TFSI ionic liquid. The curves show Havriliak – Negami approximations

## References

- [1] M. Armand, F. Endres, D. R. MacFarlane, H. Ohno, B. Scrosati, *Nat. Mater.*, 8, 621 – 629 (2009)
- [2] A. Balducci, S. S. Jeong, G. T. Kim, S. Passerini, M. Winter, M. Schmuck, G. B. Appetecchi, R. Marcilla, D. Mecerreyes, V. Barsukov, V. Khomenko, I. Cantero, I. De Meatza, M. Holzapfel, N. Tran, *J. Power Sources*, 196, 9719-9730 (2011)
- [3] R. Zorn, *J. Chem. Phys.*, 116, 3204 – 3209 (2002)

## Structural phase transition in ammonium hydrogen fumarate

**A. Ingram<sup>1</sup>, V. Kizhibalo<sup>2</sup>, Z. Czapl<sup>1</sup> and A. Kozdraś<sup>1</sup>**

*1 - Department of Physics, Opole University of Technology, Ozimska 75,  
45-370 Opole, Poland*

*2 - Institute of Low Temperature and Structure INTBiS PAN Wrocław, Okólna 2,  
50-422 Wrocław, Poland*

*a.ingram@po.opole.pl*

Structural, DSC, optical and dielectric studies are presented for ammoniumbisfumarate. X-ray structural studies confirmed triclinic symmetry of crystal. DSC studies showed reversible structural phase transition of the first order with the transition entropy equal to 6.7 J/molK. The entropy change evidenced the order-disorder type of phase transition. It is assumed that the transition is connected with ordering of protons in hydrogen bonds. Optical microscopic observation showed destructive character of phase transition. During the phase transition crystalline samples are crushed into pieces both on cooling and heating runs. Successive cooling/heating runs give further destruction of samples into smaller pieces. The destruction is connected with significant deformation of lattice parameters at the phase transition region. The destruction of crystalline sample observed by means of microscope resembles small “earthquake”. Dielectric measurements confirm the presence of phase transition as a significant decrease of permittivity in three crystallographic direction  $a^*$ ,  $b^*$  and  $c$ . The permittivity measured on heating is smaller above the phase transition in comparison to its starting value. It is connected with destruction of crystalline sample into polycrystalline one. The important features is relatively big value of permittivity (more than 50) measured along the  $c$ -crystallographic direction. It comes from disorder of protons. The motion of protons between two equilibrium positions gives the large change of dipole moment along the  $c$ -direction.

# Effect of High-Power Sonication on Formation of the $\text{Bi}_{1-x}\text{La}_x\text{Fe}_{0.5}\text{Sc}_{0.5}\text{O}_3$ Perovskite Phases

Yu.V. Radyush<sup>1</sup>, A.V. Pushkarev<sup>1</sup>, N.M. Olekhovich<sup>1</sup>, A. Stanulis<sup>2</sup>, A. Kareiva<sup>2</sup>,  
A.D. Shvlin<sup>3</sup>, V.V. Rubanik<sup>3</sup>, D.D. Khalyavin<sup>4</sup>, A.N. Salak<sup>5</sup>

<sup>1</sup>Scientific-Practical Materials Research Centre of NAS of Belarus, 220072 Minsk, Belarus

<sup>2</sup>Department of Inorganic Chemistry, Faculty of Chemistry, Vilnius University, Naugarduko Street, 24, LT-03225, Vilnius, Lithuania

<sup>3</sup>Institute of Technical Acoustics of NAS of Belarus, General Lyudnikov Avenue, 13, 210023 Vitebsk, Belarus

<sup>4</sup>ISIS Facility, Rutherford Appleton Laboratory, Chilton, OX11 0QX Didcot, UK

<sup>5</sup>Department of Materials and Ceramic Engineering/CICECO, University of Aveiro, 3810-193 Aveiro, Portugal

[ita@vitebsk.by](mailto:ita@vitebsk.by)

The quasi quadruple  $\text{BiFeO}_3\text{--BiScO}_3\text{--LaFeO}_3\text{--LaScO}_3$  perovskite system is under study. Three end members of this system,  $\text{BiFeO}_3$ ,  $\text{LaFeO}_3$  and  $\text{LaScO}_3$ , can be obtained using the conventional methods (in particular, the standard ceramic technique), while a bulk perovskite  $\text{BiScO}_3$  phase can be synthesized under the high-pressure conditions only [1]. Bismuth ferrite is a multiferroic perovskite compound with the high-temperature magnetic ( $T_N=643$  K) and polar ( $T_C=1083$  K) orderings. The main idea of the exploration of the  $\text{Bi}_{1-x}\text{La}_x\text{Fe}_{1-y}\text{Sc}_y\text{O}_3$  system is to control (adjust) the temperatures of the magnetic and the polar transitions through substitutions in the Fe-sites and the Bi-sites, respectively.

In this work, some particular compositions of the  $\text{Bi}_{1-x}\text{La}_x\text{Fe}_{0.5}\text{Sc}_{0.5}\text{O}_3$  section of the system where the iron-to-scandium ratio is 1:1 were considered. It has earlier been shown that single-phase perovskite ceramics of this section can be prepared using the conventional route, only when the lanthanum substitution rate is at least 80 mol.%, while application of the high-pressure synthesis is needed for the rest of compositions. The temperature of magnetic transition for the compositions of the  $\text{Bi}_{1-x}\text{La}_x\text{Fe}_{0.5}\text{Sc}_{0.5}\text{O}_3$  section is about 220 K [2-4]. At room temperature, the perovskite phase of the solid solutions in the range of about  $0.10 \leq x \leq 0.31$  is antipolar with the incommensurate modulation applied to Bi/La and oxygen displacements [3], while when  $x \geq 0.35$ , the phase is non-polar [4]. In the range of  $0.31 < x < 0.35$ , a compositional transitions between the antipolar and the non-polar phases occurs and some solid solutions from this range have  $T_C$  close to  $T_N$ . Since the crystal structure and properties of the perovskite phases in this range are very sensitive to the chemical composition, the advanced preparation methods were applied. The powders prepared using a sol-gel method followed by calcination at 600°C instead of a stoichiometric mixture of the oxides were used as precursors for the high-pressure synthesis/sintering of the ceramics with  $x$  from 0.31 to 0.35 (step 0.01). The calcined product was found to be a single phase perovskite although poorly crystallized. The powders were then sonicated in ethanol media at 0.5 kW for 20 min. It was found that such treatment results in further crystallization: the diffraction reflections of the perovskite phase became sharper and better resolved. Besides, the sonication was revealed to decrease the optimal sintering temperature under high pressure.

Here we report on a systematic study of effects of the sonication power and the treatment duration on the morphological properties of the high-pressure sintered ceramics.

This work was supported by project TUMOCS. This project has received funding from the European Union's Horizon 2020 research and innovation programme under the Marie Skłodowska-Curie grant agreement No 645660. Financial support of the Belarusian Republican Foundation for Fundamental Research (Project No T15VT-008) is gratefully acknowledged as well.

[1] A.A. Belik, S. Iikubo, K. Kodama, N. Igawa, S. Shamoto, M. Maie, T. Nagai, Y. Matsui, S.Yu. Stefanovich, B.I. Lazoryak, E. Takayama-Muromachi,  $\text{BiScO}_3$ : centrosymmetric  $\text{BiMnO}_3$ -type oxide, *J. Amer. Chem. Soc.* 128, 706-707 (2006).

[2] D.D. Khalyavin, A.N. Salak, N.M. Olekhovich, A.V. Pushkarev, Yu.V. Radyush, P. Manuel, I.P. Raevski, M.L. Zheludkevich, M.G.S. Ferreira, Polar and antipolar polymorphs of metastable perovskite  $\text{BiFe}_{0.5}\text{Sc}_{0.5}\text{O}_3$ , *Phys. Rev. B* 89, Art. No 174414 (2014).

[3] D.D. Khalyavin, A.N. Salak, A.B. Lopes, N.M. Olekhovich, A.V. Pushkarev, Yu.V. Radyush, E.L. Fertman, V.A. Desnenko, A.V. Fedorchenko, P. Manuel, A. Feher, J.M. Vieira, M.G.S. Ferreira, Magnetic structure of an incommensurate phase of La-doped  $\text{BiFe}_{0.5}\text{Sc}_{0.5}\text{O}_3$ : Role of antisymmetric exchange interactions, *Phys. Rev. B* 92, Art. No 224428 (2015).

[4] D.D. Khalyavin, A.N. Salak, P. Manuel, N.M. Olekhovich, A.V. Pushkarev, Yu.V. Radyush, A.V. Fedorchenko, E.L. Fertman, V.A. Desnenko, M.G.S. Ferreira, Antisymmetric exchange in La-substituted  $\text{BiFe}_{0.5}\text{Sc}_{0.5}\text{O}_3$  system: Symmetry adapted distortion modes approach, *Z. Kristallogr. Cryst. Mater* 230, 767-774 (2015).

# Electrical transport in lead-free $(\text{Na}_{0.5}\text{Bi}_{0.5})_{1-x}\text{Sr}_x\text{TiO}_3$ ceramics ( $x=0, 0.01$ and $0.02$ )

**E.M.Dutkiewicz<sup>1,2</sup>, J.Suchanicz<sup>3</sup>, K.Konieczny<sup>3</sup>, M.Antonova<sup>4</sup>, A.Sternberg<sup>4</sup>**

<sup>1</sup>*Institute of Physics, Pedagogical University, ul. Podchorążych 2, 30-084 Krakow, Poland*

<sup>2</sup>*Institute of Nuclear Physics PAN, ul.Radzikowskiego 152, 31-342 Krakow, Poland*

<sup>3</sup>*Institute of Technics, Pedagogical University, ul Podchorążych 2, 30-084 Krakow, Poland*

<sup>4</sup>*Institute of Solid State Physics, University of Latvia, LV-1063 Riga, Latvia*

Multifunctional materials are becoming increasingly important in technological devices since they enable coupling between electrical, magnetic, mechanical and optical properties. Lead zirconate titanate  $\text{Pb}(\text{Zr,Ti})\text{O}_3$  (PZT) and their solid solutions are utilized in a broad variety of devices, such sensors, actuators, motors, transducers and nonvolatile random access memory chips [1, 2]. However, Pb and PbO were identified as toxic for human health and the environment. Therefore, there has been a growing research interest in developing alternative lead-free materials, which can replace the current lead-based materials. Among various lead-free systems, the  $\text{Na}_{0.5}\text{Bi}_{0.5}\text{TiO}_3$  (NBT) and NBT-based solid solutions are promising compounds.

Lead-free  $(\text{Na}_{0.5}\text{Bi}_{0.5})_{1-x}\text{Sr}_x\text{TiO}_3$  ( $x=0, 0.01$  and  $0.02$ ) ceramics were manufactured through a solid-state mixed oxide method and their ac ( $\sigma_{ac}$ ) and dc ( $\sigma_{dc}$ ) electric conductivity were studied. It is shown that the low-frequency (100 Hz-1 MHz) ac conductivity obeys a power law  $\sigma_{ac} \sim \omega^s$  characteristic for disordered materials. The frequency exponent  $s$  is a decrease function of temperature and tends to zero at high temperatures. The dc conductivity has thermally activated character and possesses four linear parts with four different activation energies and some discontinuous changes. However,  $\sigma_{ac}(T)$  possesses three linear parts with three different activation energies and some discontinuous changes. The results was interpreted by a correlated hopping model. The NBT-ST system is expected to be a new promising candidate for lead-free electronic materials.

[1] Lines ME, Glass AM. Principles and applications of ferroelectrics and related materials. Oxford: Clarendon Press; 2001.

[2] Randall CA, Kelnberger A, Yang GY, Eitel RE, Shrout TR. High strain piezoelectric multilayer actuators- A materials science and Engineering Challenge. J.Electrocer. 2005;14:177-191.

# EFFECTS OF $\text{PbTiO}_3$ DOPING ON ELECTRIC PROPERTIES OF $\text{K}_{0.5}\text{Bi}_{0.5}\text{TiO}_3$ CERAMICS

**M. Karpierz<sup>1</sup>, J. Suchanicz<sup>2</sup>, K. Konieczny<sup>2</sup>**

<sup>1</sup> Institute of Physics, Pedagogical University, ul. Podchorążych 2, 30-084 Krakow, Poland

<sup>2</sup> Institute of Technology, Pedagogical University, ul. Podchorążych 2, 30-084 Krakow, Poland

Main author email address: [mkarpierz@outlook.com](mailto:mkarpierz@outlook.com)

Lead titanate ( $\text{PbTiO}_3$ ) and lead titanate - based ceramics are very attractive due to the possibility of using them for production of transducers, actuators or other electromechanical devices [1]. The downside of these ceramics is the toxicity of lead and its high vapour pressure during processing. Low-lead and lead-free ceramics can be used instead of lead-based materials if their properties are promising [2].

$\text{K}_{0.5}\text{Bi}_{0.5}\text{TiO}_3$  (KBT) and  $(1-x)\text{K}_{0.5}\text{Bi}_{0.5}\text{TiO}_3$ - $x\text{PbTiO}_3$  (KBT-PT) have received significant attention as a prospective piezoelectric materials [3-5].

The  $(1-x)\text{KBT}$ - $x\text{PT}$  ( $x = 0.18$  and  $0.5$ ) ceramics were fabricated by a conventional solid-phase synthesis method. Both compositions show complete perovskite solid solutions. Their  $dc$ ,  $ac$  conductivity, electric and thermoelectric properties were investigated. We also calculate the Seebeck coefficient  $\alpha$ , the concentration  $n$  and mobility  $\mu$  of charge carriers for the investigated samples. The possible origin of the observed effects is discussed. We suggest that the KBT-PT solid solutions can be good electronic materials.

## References

- [1] K. Uchino, *Ferroelectric devices*. New York (NY): Marcel Dekker; 2000.
- [2] S. Zhang, R. Xia, T.R. Shrout, Lead-free piezoelectric ceramics vs. PZT? *J. Electroceram.*, 19, 251-257, (2007).
- [3] O. Elkechai, P. Marchet, J.P. Mercurio, Structural and dielectric study of the  $\text{Na}_{0.5}\text{Bi}_{0.5}\text{TiO}_3$ - $\text{PbTiO}_3$  and  $\text{K}_{0.5}\text{Bi}_{0.5}\text{TiO}_3$ - $\text{PbTiO}_3$  systems, *J. Mat. Chem.*, 7, 91-97 (1997).
- [4] M. Karpierz, J. Suchanicz, R. Bujakiewicz-Koronska, D. Sitko, A. Niewiadomski, M. Sokolowski, Dielectric and ferroelectric properties of  $0.82\text{K}_{0.5}\text{Bi}_{0.5}\text{TiO}_3$ - $0.18\text{PbTiO}_3$  ceramic: effect of uniaxial pressure, *Phase Transitions*, 88, 811-816 (2015).
- [5] M. Karpierz, J. Suchanicz, K. Konieczny, D. Sitko, P. Marchet, U. Lewczuk, Thermal, Raman and dielectric study of  $0.5\text{K}_{0.5}\text{Bi}_{0.5}\text{TiO}_3$ - $0.5\text{PbTiO}_3$  ceramics, *Phase Transitions*, 88, 662-667 (2015).

## **ABSTRACTS OF POSTER PRESENTATIONS**

**7<sup>th</sup> September**

# Origin of the $\lambda$ -type anomaly in $\text{SrMnO}_3$ and $\text{EuTiO}_3$ : Magnetic contribution to the specific heat.

**D. M. Nalecz<sup>1</sup>, R. J. Radwanski<sup>1,2</sup> and Z. Ropka<sup>2</sup>**

<sup>1</sup>*Institute of Physics, Pedagogical University, ul. Podchorążych 2, 30-084 Krakow, Poland*

<sup>2</sup>*Center of Solid State Physics, S<sup>mi</sup> Filip 5, 31-150 Krakow, Poland  
sfnalecz@cyf-kr.edu.pl*

Perovskites are known to form the biggest group of ferroelectrics. Oxides like  $\text{BaTiO}_3$ ,  $\text{CaTiO}_3$ ,  $\text{SrTiO}_3$ ,  $\text{PbTiO}_3$ ,  $\text{LiNbO}_3$  have only core closed electronic shells.

In this contribution we would like to analyze magnetic phase transitions in  $\text{EuTiO}_3$  and in  $\text{SrMnO}_3$ . In these perovskite oxides there are magnetically active ions, Eu and Mn, which have an incomplete  $3d$  shell. They exhibit the magnetic order at 5.5 K [1] and 233-286 K (depending on the polymorph type) [2, 3], respectively.

The detailed specific-heat measurements presented in Ref. 1 allows for unambiguous determination of the entropy related with the magnetic phase transition in  $\text{EuTiO}_3$  owing to the low temperature of the transition - then the lattice contribution is small. The  $\text{Eu}^{2+}$  and  $\text{Mn}^{4+}$  ions are somehow similar in the respect that in the magnetic phase transition practically only the spin degree of freedom are released. We have calculated temperature dependence of the specific heat including the  $\lambda$ -type peak [4] and of the low-energy atomic-like electronic structure at the sub-meV energy scale [4,5]. In the magnetic state there exists the discrete atomic-like electronic structure at the 0.05 meV scale. Our studies establish that the realized valency of the  $\text{Eu}^{2+}$  and  $\text{Mn}^{4+}$  in these oxides is exactly the same as the formal valency.

- [1] A. Bussmann-Holder, J. Kohler, R. K. Kremer, and J. M. Law, Relation between structural instabilities in  $\text{EuTiO}_3$  and  $\text{SrTiO}_3$ , Phys. Rev. B 83, 212102 (2011).
- [2] O. Chmaissem, B. Dabrowski, S. Kolesnik, J. Mais, D. E. Brown, R. Kruk, P. Prior, B. Pyles, and J. D. Jorgensen, Relationship between structural parameters and the Neel temperature in  $\text{Sr}_{1-x}\text{Ca}_x\text{MnO}_3$  and  $\text{Sr}_{1-x}\text{Ba}_x\text{MnO}_3$ , Phys.Rev. B 64, 134412 (2001).
- [3] A. Daoud-Aladine, C. Martin, L. C. Chapon, M. Hervieu, K. S. Knight, M. Brunelli, P. G. Radaelli, Structural phase transition and magnetism in hexagonal  $\text{SrMnO}_3$  by magnetization measurements and by electron, x-ray, and neutron diffraction studies, Phys. Rev. B 75, 104417 (2007).
- [4] R. J. Radwanski, R. Michalski, Z. Ropka, From Atomic Physics to Solid-State Physics: Magnetism and Electronic Structure of  $\text{PrNi}_5$ ,  $\text{ErNi}_5$ ,  $\text{LaCoO}_3$  and  $\text{UPd}_2\text{Al}_3$ , Acta Physica Pol. B 31, 307 (2000).
- [5] Z. Ropka and R. J. Radwanski,  $^5\text{D}$  term origin of the excited triplet in  $\text{LaCoO}_3$ , Phys. Rev. B 67, 172401 (2003).



## Dielectric dispersion studies in $(\text{N}_2\text{H}_5)_2\text{CdCl}_4$ crystal

S. Wacke<sup>1</sup>, Z. Czapla<sup>1</sup>, O. Czupiński<sup>2</sup>, A. Ingram<sup>1</sup> and J. Janczak<sup>3</sup>

*1- Department of Physics, Opole University of Technology, Ozimska 75,  
45-370 Opole, Poland*

*2- Faculty of Chemistry, University of Wrocław, F. Joliot-Curie 14,  
50-383 Wrocław, Poland*

*3- Institute of Low Temperature and Structure Research, Polish Academy of Sciences, Okólna 2,  
50-422 Wrocław*

*s.wacke@po.opole.pl*

Cadmium chloride and bromide to large family of complex salts with organic and inorganic cations. The paper presents the dielectric studies of new crystalline material, namely  $(\text{N}_2\text{H}_5)_2\text{CdCl}_4$ . The crystal exhibits a sequence of structural phase transition discovered in DSC studies [1] at  $T_1 = 357$  K,  $T_2 = 436$  K and  $T_3 = 448$  K on heating and at  $T_1 = 333$  K,  $T_2 = 435$  K and  $T_3 = 446$  K on cooling. Interesting features is found in the case of transition at  $T_1$  where large temperature hysteresis is observed [1] and the change of symmetry from monoclinic to orthorhombic one [2]. Our dielectric studies were done in a frequency range of 42 Hz – 5 MHz and temperature range 300 – 380 K. Dielectric studies revealed dielectric dispersion in the studied frequency range that most probably connected with conductivity. The activation energy estimated from frequency dependences of permittivity and losses are different for particular phases.

# Thermal and pyroelectric properties of NBT-BT systems

**U. Lewczuk-Jodłowiec<sup>1</sup>, J. Suchanicz<sup>2</sup>, D. Sitko<sup>1</sup>, K. Konieczny<sup>2</sup>;**

<sup>1</sup>*Institute of Physics, Pedagogical University, ul. Podchorążych 2, 30-084 Krakow, Poland*

<sup>2</sup>*Institute of Technology, Pedagogical University, ul. Podchorążych 2, 30-084 Krakow, Poland*

*e-mail: urszula.lewczuk@gmail.com*

Due to their impressive dielectric and piezoelectric properties lead-based perovskites, like  $\text{PbTiO}_3$ - $\text{PbZrO}_3$  (PZT) have been used in many electronic devices. Serious environmental pollution caused by lead-based materials has become the reason for the search for alternatives [1]. Previous study shows that  $\text{Na}_{0.5}\text{Bi}_{0.5}\text{TiO}_3$  (NBT) and  $\text{Na}_{0.5}\text{Bi}_{0.5}\text{TiO}_3$ - $x\text{BaTiO}_3$  (NBT-BT) ceramics are interesting for future applications [2-5].

A conventional solid phase sintering process was used to fabricate the  $\text{Na}_{0.5}\text{Bi}_{0.5}\text{TiO}_3$ - $x\text{BaTiO}_3$  ceramics ( $x=0, 0.04, 0.06, 0.08$  and  $0.1$ ). X-ray measurements showed that all samples have a perovskite structure. The bulk density of the obtained samples exceeds 95% of the theoretical density. The thermal (DSC, dilatometry), dielectric and pyroelectric properties of these ceramics were investigated in a wide temperature range. The relaxor behavior of the investigated ceramics was revealed. The transition temperatures observed by means of dielectric studies are in good agreement with those obtained from thermal and pyroelectric measurements.

[1] Parija B: Study of structural, electrical and optical properties of lead-free ( $\text{Bi}_{0.5}\text{Na}_{0.5}\text{TiO}_3$ ) based ceramic systems. Department of Physics National Institute of Technology: Rourkela, 769008; 2012.

[2] Lewczuk U, Suchanicz J: Properties of  $\text{Na}_{0.5}\text{Bi}_{0.5}\text{TiO}_3$  ceramics after  $\text{Ba}^{2+}$  doping. *Integrated Ferroelectrics*. 2016; 173:1, 53-58.

[3] Lewczuk U, Suchanicz J, Karpierz M, Stachowski G: Dielectric and ferroelectric properties of NBT-BT systems. To be published in *Phase Transitions*.

[4] Suchanicz J, Lewczuk U, Konieczny K, Dutkiewicz EM: Effect of Ba addition on the structural, dielectric and ferroelectric properties of  $\text{Na}_{0.5}\text{Bi}_{0.5}\text{TiO}_3$  ceramics. *Mat. Sci.-Poland*. 2015; 33(2): 414-417.

[5] Suchanicz J, Lewczuk U, Konieczny K: Effect of Ba doping on the structural, dielectric and ferroelectric properties of  $\text{Na}_{0.5}\text{Bi}_{0.5}\text{TiO}_3$  ceramics. *Ferroelectrics*. 2016; 497:1, 85-91.

# Dielectric Properties of BaTiO<sub>3</sub>-KNbO<sub>3</sub> Composites

**Sergejus Balčiūnas<sup>1</sup>, Maksim Ivanov<sup>1</sup>, Jūras Banyš<sup>1</sup>, Satoshi Wada<sup>2</sup>**

<sup>1</sup> Faculty of Physics, Vilnius University, Sauletekio 9/3 817k., LT10222 Vilnius, Lithuania.

<sup>2</sup> Interdisciplinary Graduate School of Medical and Engineering, University of Yamanashi, Kofu, Yamanashi 400-8510, Japan.

e-mail: [sergejus.balciunas@ff.vu.lt](mailto:sergejus.balciunas@ff.vu.lt)

For the past 40-50 years, lead based perovskite Pb(Zr<sub>x</sub>Ti<sub>1-x</sub>)O<sub>3</sub> (PZT) piezoelectric ceramics have dominated the commercial market of piezoelectric devices due to their remarkable dielectric and piezoelectric properties and ability to operate in wide temperature range.

BaTiO<sub>3</sub> (BT) is perhaps the most widely researched perovskite in the last decades. Inserting potassium niobate (KN) into BT structure creates stresses that increase domain wall count and in result piezoelectric coefficient [1]. KNBT has comparable piezoelectric coefficient with PZT, thus making it a great substitute. The fact that KNBT is lead free ceramic makes it of high interest for both researchers and engineers due to environmental concerns.

KNBT composites were prepared in two steps: compact BT particles were heated up to 1000°C and heat-treated at that temperature for 2h to create low-density ceramics, then KN were epitaxially deposited into BT structure. [2].

In this presentation dielectric properties of KNBT with different KN/BT molar ratios will be presented. From figure 1 we can observe that the bigger the KN/BT ratio is, the more obscured phase transitions of BaTiO<sub>3</sub> become. Low dielectric permittivities in KN/BT with molar ratios of 0.22 and 0.5 can be explained by its low relative density.

Furthermore, experimental data of the frequency dependences were approximated by superposition of 3 Cole-Cole equations (Fig 2). Three relaxation processes were distinguished: Maxwell – Wagner relaxation (1), domain wall motion (2) and electro – mechanical resonance (3). Additionally we can see that relaxation times of the third relaxation process has no temperature dependence and it contributes to dielectric permittivity the most.

Lastly, the model proposed by Arlt [3] was used to calculate spontaneous polarization from electro – mechanical resonance contribution to dielectric permittivity and showed promising results. Also, theoretical models of electro – mechanical resonance will be presented.

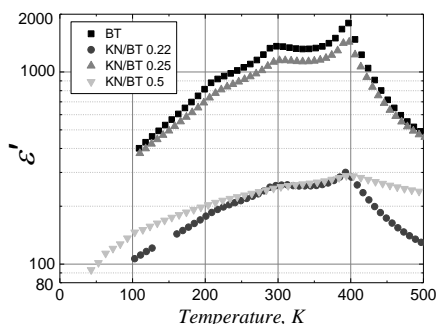


Fig. 1: Temperature dependence of the real part of dielectric permittivity at 1MHz, for: BT, KN/BT 0.22, KN/BT 0.25, KN/BT 0.5 respectively with 60%, 53% 79%, 60% relative densities.

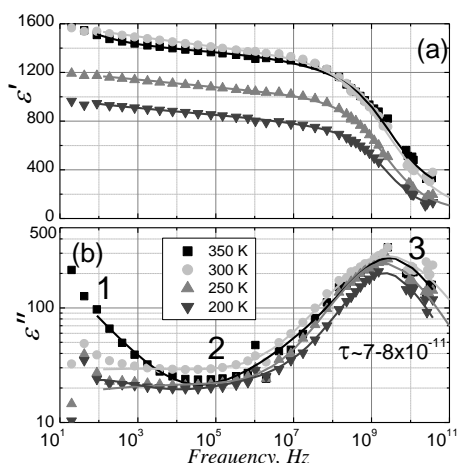


Fig. 2: Frequency dependence of real (a) and imaginary (b) part of dielectric permittivity for BT with 60% relative density.

[1] T. Higuchi, Journal of mechanical science and technology, vol. 24, pp. 13-18, 2010

[2] I. Fujii, S. Shimizu, K. Yamashita, K. Nakashima, N. Kumada, C. Moriyoshi, et al., Applied Physics Letters, vol. 99, p. 202902, 2011

[3] G. Arlt, U. Böttger, S. Witte, Annalen der Physik, vol. 506, pp. 578-588, 1994.

# Influence of grain size effect on physical properties of $\text{Cu}_6\text{PS}_5\text{I}$ micro- and nanocrystals

**I. Studenyak<sup>1</sup>, V. Izai<sup>1</sup>, T. Salkus<sup>2</sup>, A. Orliukas<sup>2</sup>, Il'kovič S.<sup>3</sup>, Reiffers M.<sup>3,4</sup>, Timko M.<sup>4</sup>**

*1 - Faculty of Physics, Uzhhorod National University, 3 Narodna Sq., 88000 Uzhhorod, Ukraine*

*2 - Faculty of Physics, Vilnius University, 9 Saulėtekio Al., LT-10222 Vilnius, Lithuania*

*3 - Faculty of Humanities and Natural Sciences, Prešov University, ul. 17. novembra 1, Prešov, Slovakia*

*4 - Institute of Experimental Physics, Watsonova 47, Košice, Slovakia*

*E-mail: studenyak@dr.com*

$\text{Cu}_6\text{PS}_5\text{I}$  superionic-ferroelastic belongs to the compounds with argyrodite crystal structure and is characterized by high electrical conductivity. It is well-known that in the few recent decades, superionic conductors are being widely studied due to their promising applications as new materials for future energy technologies, for development of new types of solid-state batteries, supercapacitors, electrochemical sensors, and thermoelectric devices.

$\text{Cu}_6\text{PS}_5\text{I}$  crystals at a room temperature belong to cubic syngony (space group  $F43m$ ). There are two low-temperature phase transitions (PT) in  $\text{Cu}_6\text{PS}_5\text{I}$  crystal, one of which at  $T_{II}$  is structural second-order PT which is accompanied by the change of symmetry  $F43m \rightarrow F43c$ , and the other at  $T_I$  is the first-order PT which is simultaneously a superionic and ferroelastic, and it is accompanied by the change of symmetry  $F43c \rightarrow Cc$ .

$\text{Cu}_6\text{PS}_5\text{I}$  single crystals were grown using chemical vapour transport method. The microcrystalline powder with the average grain size of 50  $\mu\text{m}$  were obtained by grinding of the synthesized material in an agate mortar.  $\text{Cu}_6\text{PS}_5\text{I}$  nanocrystalline powders were obtained by ball milling the material in a stainless steel cylindrical vial with hardened steel balls. The average grain size were determined from the XRD patterns; for the material under investigation the average grain size were 98 nm, 53 nm and 24 nm. Pellets of 8 mm in diameter and 0.2–2 mm thick were pressed at 250 MPa and were placed in an evacuated ampoule of quartz glass. The ampoule was heated at a rate 100 K/h to the temperatures of 600°C and kept at this temperature during 24 h. Then the ampoule was cooled to room temperature. Structural studies were performed using scanning electron microscopy, the chemical composition is controlled by energy-dispersive X-ray spectroscopy investigations.

The measurements of complex electrical conductivity ( $\sigma = \sigma' + i\sigma''$ ) were carried out in the frequency range of 10 Hz – 3 GHz in the temperature interval 300–400 K by a coaxial impedance spectrometer set-up and a custom impedance spectrometer operating by voltmeter-ammeter method. With the average grain size decrease the total electric conductivity at room temperature and frequency of  $10^3$  Hz increases from  $3.8 \times 10^{-2}$  S/m ( $d=98$  nm) to  $5.2 \times 10^{-2}$  S/m ( $d=53$  nm) and to  $1.0 \times 10^{-1}$  S/m ( $d=24$  nm). The high value of the total electric conductivity in  $\text{Cu}_6\text{PS}_5\text{I}$  ceramics prepared from nanocrystalline powder with the average grain size of 24 nm is observed and it is very close to the conductivity value of the single crystal. This effect is attributed to the predominance of grain-boundary conduction in the nanostructured materials, coupled with an increase in the grain-boundary ionic diffusivity with decreasing grain size.

Frequency studies of the complex electrical conductivity have shown the two dispersion regions caused by the ion transport in the grain boundaries and the bulk of the  $\text{Cu}_6\text{PS}_5\text{I}$  superionic ceramics. The high frequency parts of the spectra were attributed to the relaxation in bulk, while the lower parts corresponded to the grain boundary processes. The temperature studies have shown that with temperature growth the electrical conductivity increase according to Arrhenius law in the temperature interval  $T=300\text{--}400$  K.

Heat capacity measurements were performed in the temperature range 50–300 K by a Versalab commercial device (Quantum Design). The two- $\tau$  model of the standard relaxation method was used. It is shown that for  $\text{Cu}_6\text{PS}_5\text{I}$  single crystal a step-like anomaly at the second-order PT at  $T_{II}=272.6$  K and a weak smeared anomaly at the superionic-and-ferroelastic first-order PT at  $T_I=147.5$  K are observed. For the powdered  $\text{Cu}_6\text{PS}_5\text{I}$ , in addition to the anomalies in the temperature dependence of specific heat corresponding to the PTs in the bulk material, an anomaly at a higher temperature is observed which is related to the "surface" PT. Based on calorimetric studies, it is shown that the ferroelastic-and-superionic first-order PT and the structural second-order PT shift towards higher temperatures with the average grain size reduction. At the transition to the nanometric scale, smearing of the anomaly at the second-order PT is revealed as well as the appearance of a new feature at a higher temperature which is assigned to a "surface" PT. It is supposed that the "surface" PT observed in micro- and nanocrystalline powders results from the high concentration of the copper and sulfur vacancies.

# Electrical conductivity in the range of phase transitions in $\text{Cu}_6\text{PS}_5\text{I}$ crystals

V. Izai<sup>1</sup>, I. Studenyak<sup>1</sup>, T. Šalkus<sup>2</sup>, J. Banys<sup>2</sup>

1- Faculty of Physics, Uzhhorod National University, 3 Narodna Sq., 88000 Uzhhorod, Ukraine

2- Faculty of Physics, Vilnius University, 9 Saulėtekio Al., LT-10222 Vilnius, Lithuania

E-mail: vital.babaj@gmail.com

Superionic ferroelastics  $\text{Cu}_6\text{PS}_5\text{I}$  belong to the family of compounds with argyrodite structure [1]. Electrical studies of  $\text{Cu}_6\text{PS}_5\text{I}$  crystals show that they possess high value of electrical conductivity at room temperature, which comparable with the conductivity of best solid electrolytes [2]. At room temperature they belong to the cubic syngony  $F\bar{4}3m$ . With temperature decrease two phase transitions occur, first of them at  $T_{II}=(269\pm 2)$  K is the structural second-order phase transition (accompanied by the change of symmetry  $F\bar{4}3m \rightarrow F\bar{4}3c$ ), and the second – at  $T_I=(144\pm 1)$  K is at the same time superionic and ferroelastic first-order phase transition (accompanied by the change of symmetry  $F\bar{4}3c \rightarrow Cc$ ) [3].

$\text{Cu}_6\text{PS}_5\text{I}$  crystals were grown using chemical vapour transport method. Measurements of complex electrical conductivity of  $\text{Cu}_6\text{PS}_5\text{I}$  superionic crystals were carried out in the range of frequencies from 10 Hz to – 1 MHz in a temperature interval 140–300 K by a coaxial impedance spectrometer [4].

In the range of the second-order phase transition at  $T=T_{II}$  the knee at the temperature dependence  $\sigma'(T)$  and change of activation energy  $\Delta E_a$  is observed as well as in the range of superionic and ferroelastic first-order phase transition at  $T=T_I$  the small maximum at high frequencies is revealed. It is shown that at  $T < 250$  K in the frequency range of 20 Hz to – 1 MHz the dispersion of electrical conductivity takes place. The transition from low-frequency conductivity to high-frequency conductivity is clearly seen from Figure 1. It should be noted that maximum at  $T=T_I$  is frequency-dependent.

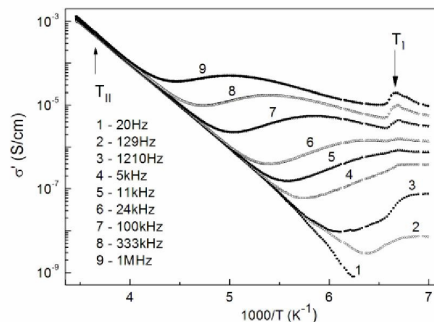


Figure 1 Temperature dependences of electrical conductivity  $\sigma'$  for  $\text{Cu}_6\text{PS}_5\text{I}$  crystals at different frequencies.

[1] W. F. Kuhs, R. Nitsche, K. Scheunemann, The argyrodites – a new family of the tetrahedrally close-packed structures, Mat. Res. Bull., 14, 241-248, (1979).

[2] I.P. Studenyak, M. Kranjčec, M.V. Kurik, Urbach rule and disordering processes in  $\text{Cu}_6\text{P}(\text{S}_{1-x}\text{Se}_x)_5\text{Br}_{1-y}\text{I}_y$  superionic conductors, J. Phys. Chem. Solids, 67, 807-817, (2006).

[3] A. Gabor, A. Pietraszko, D. Kaynts, Diffusion paths formation for  $\text{Cu}^+$  ions in superionic  $\text{Cu}_6\text{PS}_5\text{I}$  single crystals studied in terms of structural phase transition, J. Solid State Chem., 178, 3366-3375, (2005).

[4] A.F. Orliukas, A. Kezionis, E. Kazakevicius, Impedance spectroscopy of solid electrolytes in the radio frequency range, Solid State Ionics, 176, 2037- 2043 (2005).

# Phase compositions of $\text{Na}_{0.5}\text{Bi}_{0.5}\text{TiO}_3$ thin films deposited in various working gas mixtures

S.A. Popov, Yu.N. Potapovich, T.V.Kruzina, M.P. Trubitsyn, A. S. Rutskiy, M.M. Koptev

*Oles' Honchar Dnipropetrovsk National University, prosp. Gagarina 72, Dnipropetrovsk, 49010, Ukraine*

*Main author email address: potap@meta.ua*

High piezoelectric parameters stimulate growing interest to ferroelectric  $\text{Na}_{0.5}\text{Bi}_{0.5}\text{TiO}_3$  (NBT) and solid solutions based on it. Perspectives of applications in micropumps, ultrasonic motors, hi-frequency transducers, energy harvesting cause essential efforts on developing technology of the NBT thin films deposition and studying the size effects. Pt/Ti( $\text{TiO}_2$ )/ $\text{SiO}_2$ /Si(100) hetero-structure substrates are most often used for NBT ferroelectric thin film deposition [1]. Thin films are prepared by ex-situ high-temperature treatment. However, NBT thin films deposition conditions are not enough elaborated. In particular, it is difficult to prepare films with high-quality structure and reproducible electro-physical properties. It requires further researches and developing NBT thin films deposition technology.

In the abstract, we report influence of working gas (Ar/ $\text{O}_2$  mixture) and thicknesses of hetero-structure substrate layers on the phase composition of NBT thin films prepared by RF magnetron sputtering. Our investigations showed that thickness of Ti layer on Pt/Ti/ $\text{SiO}_2$ /Si substrate had significant impact on the further deposition of Pt (111) layer which determined orientation of  $\text{Na}_{0.5}\text{Bi}_{0.5}\text{TiO}_3$  film. When the thickness of the adhesive Ti layer exceeded 50 nm, the surface of the Pt layer became heterogeneous. Under the influence of temperature, an activity of Ti increases and it diffuses into the Pt layer and the process of its oxidation continues [2]. Interpenetration of Ti and Pt layers leads to local exfoliation of the layers and destruction of their integrity. Investigation of electro-physical properties of NBT films on such substrates did not give reproducible results. Our investigation showed that it was preferable to use  $\text{TiO}_2$  as the adhesive layer instead of active Ti. The layer of  $\text{TiO}_2$  was obtained by RF magnetron sputtering of Ti target in Ar and  $\text{O}_2$  (1:1) atmosphere,  $P = 40\text{mTorr}$ , on a  $\text{SiO}_2$ /Si substrate heated to  $300^\circ\text{C}$ . Surface of the Pt layer was homogeneous and stable after further temperature treatment when the thickness of the underlying  $\text{TiO}_2$  layer was varied in the range 20-100 nm. Pt(100nm)/ $\text{TiO}_2$ (30nm)/ $\text{SiO}_2$ /Si substrates were prepared under above-mentioned conditions and were used as a base for NBT films deposition.

The ceramics of bismuth sodium titanate was prepared by traditional technique and was used as the target. The phase composition of the target was checked by X-Ray diffraction (XRD). We used the targets with a diameter of 40 mm. The films were deposited in Ar and  $\text{O}_2$  mixture atmosphere (chamber pressure 10mTorr) on Pt/ $\text{TiO}_2$ / $\text{SiO}_2$ /Si substrates heated to  $200^\circ\text{C}$ . Then the deposited thin films (250nm thickness) were synthesized by annealing in Bi-rich air atmosphere for 1 h at temperatures 500-750°C.

XRD patterns showed that the NBT films deposited in pure argon working gas were amorphous. It was observed that NBT phase was not formed after annealing at temperatures below  $650^\circ\text{C}$ . After annealing at 650 -  $750^\circ\text{C}$  the films were crystallized and exhibited two- phase composition. NBT phase was accompanied by some another phase, presumably  $\text{Bi}_4\text{Ti}_3\text{O}_{12}$  [3]. Besides that, NBT XRD peak (111) was very weak or was not visible at all. Absence of the reflex at  $40.1^\circ$  (NBT (111) plane) could be attributed to certain orientation of crystallites and formation of textured films. Presence of the non-NBT phase demonstrates difficulties of the films synthesis, so some components, sputtered from the targets, do not react to form a bismuth sodium titanate structure. It shows that synthesis of thin films differs enough from the case of bulk compounds synthesis, when titanium oxide reacts with bismuth oxide and sodium carbonate.

Addition of oxygen to working gas (up to 50%) during the NBT films deposition led to presence of some weak NBT peaks in XRD pattern of as-deposited films. Rise of oxygen concentrations above 50% in working gas mixture and further annealing at  $700^\circ\text{C}$  in air allowed to obtain films with XRD reflexes at  $2\theta = 22.8^\circ$ ,  $32.5^\circ$  and  $40.1^\circ$ , which correspond to (100), (110) and (111) planes of NBT structure. It is assumed that presence of oxygen in the chamber makes for gas-transport reactions during the deposition and thus may contribute to the NBT structure formation. The details are discussed.

[1] Z.H. Zhou, J.M. Xue, W.Z. Li and J. Wang, Ferroelectric and electrical behavior of  $(\text{Na}_{0.5}\text{Bi}_{0.5})\text{TiO}_3$  thin film, Applied Physics Letters, 85, 804-806, (2004).

[2] K.Vorotilov, O. Zhigalina, V.Vasil'ev, A.Sigov, Specific features of the formation of the crystal structure of lead zirconate titanate in the  $\text{Si-SiO}_2\text{-Ti}(\text{TiO}_2)\text{-Pt-Pb}(\text{Zr x Ti}1 - \text{x})\text{O}_3$  systems, Physics of the Solid State, 51, 1337-1340, (2009).

[3] A. Daryapurkar, J. Kolte, P. Gopalan, Influence of oxygen gas pressure on phase, microstructure and electrical properties of sodium bismuth titanate thin films grown using pulsed laser deposition, Thin Solid Films, 579, 44-49, (2015).

# Dielectric properties of the multicomponent PZT-type ceramic for actuator applications

Dariusz Bochenek<sup>a\*</sup>, Przemysław Niemiec<sup>a</sup>, Ryszard Skulski<sup>a</sup>, Beata Wodecka –Duś<sup>a</sup>,  
Zbigniew Machnik<sup>a</sup>

<sup>a</sup> *University of Silesia, Faculty of Computer Science and Material Science, Institute of Technology and Mechatronics, 12, Żytnia St., 41-200, Sosnowiec, Poland*

\*Corresponding author: niemiec.przemek@gmail.com

In the paper two compositions of the multi-component PZT-type ceramics with perovskite structure were obtained. The compositions designed considering the valence of entering admixtures ( $\text{Mn}^{4+}$ ,  $\text{Sb}^{3+}$ ,  $\text{W}^{6+}$ ,  $\text{Ni}^{2+}$ ): (i)  $\text{Pb}(\text{Zr}_{0.49}\text{Ti}_{0.51})_{0.94}\text{Mn}_{0.014}\text{Sb}_{0.02}\text{W}_{0.014}\text{Ni}_{0.02}\text{O}_3$  (PZT1) and (ii)  $\text{Pb}(\text{Zr}_{0.49}\text{Ti}_{0.51})_{0.94}\text{Mn}_{0.016}\text{Sb}_{0.02}\text{W}_{0.016}\text{Ni}_{0.01}\text{O}_3$  (PZT2). The ceramic specimens were obtained using a conventional ceramic technology from simple oxides, that is,  $\text{PbO}$ ,  $\text{ZrO}_2$ ,  $\text{TiO}_2$ ,  $\text{WO}_3$ ,  $\text{Sb}_2\text{O}_3$ ,  $\text{MnO}_2$  and  $\text{NiO}$ .

The ceramic powders were synthesized by the calcination method and their densification was carried out by free sintering method. The article presents the results of dielectric, ferroelectric, piezoelectric researches and DC electrical conductivity of the PZT-type specimens. To determine the piezoelectric properties the ceramic specimens were poling in silicon oil by the high voltage method using a Matsusada Precision Inc. HEOPS-5B6 high voltage supply in the following conditions: poling field  $E_{pol} = 30$  kV/cm, poling time  $t_{pol} = 0.5$  h, at poling temperature  $T_{pol} = 120^\circ\text{C}$ . Examinations of the piezoelectric parameters were carried out using the resonance–antiresonance method.

The results of the multi-component ceramics predispose it in micromechatronic applications, as part of the actuators.

## New forms of TGS crystals

Krzysztof Cwikiel<sup>1</sup>, Krzysztof Nowak<sup>2</sup>

*1- A. Chelkowski Institute of Physics, Silesian University, Polska*

*2- Department of Environmental Chemistry and Technology, Silesian University, Polska*

*krzysztof.cwikiel@us.edu.pl*

Triglycine sulfate (TGS) is one of the most important ferroelectric material. Growth of TGS crystals from solution at low temperature is one of the important techniques in the field of science. Single crystals of TGS have been usually grown from aqueous solution by temperature lowering or solvent evaporation method. Triglycine sulfate normally grows as a bulk size single crystal.

The authors for the first time obtained new forms of TGS crystals:

- fibers crystals,
- thin plates.

Both forms of TGS crystals have been grown by natural evaporation method using polystyrene sulfonated resin as a matrix of growth. The matrix of crystal growth is the product of virgin polystyrene sulfonation using solid silica sulfuric acid. Obtained resin contains sulfonic groups and is cross-linked hence have cation exchange properties. Additionally this resin absorbs water. The amount of sulfonic groups, cross-linking degree and water absorption depends on sulfonation conditions.

Obtained crystals fibers and plates have ferroelectric properties, are colorless and transparent. Both forms were analyzed by the scanning electron microscope and optical microscope. The fibers have a thickness of 0.01 to 1.5 mm and a length to 15 cm, and the thin plates have a surface area to 10 cm<sup>2</sup> and thickness in the range 10 – 20 μm. It was found that obtained crystals were not hollow inside.

For the investigations of surfaces and domain structures, atomic force microscope (Solver Nano - NT-MDT) was used .



# Electrical, thermoelectric and thermal properties of $\text{Li}_x\text{Na}_{1-x}\text{NbO}_3$ solid solution for $x=0$ to 0.1.

K.Konieczny

*Institute of Technology, Pedagogical University, 30-084 Kraków, Poland*

*Main author email address: [kkoniec@up.krakow.pl](mailto:kkoniec@up.krakow.pl)*

A thermoelectric generator is a solid state device that converts heat directly into electrical energy through a phenomenon of thermoelectric effect. Thermoelectric generators could be used in power station in order to convert waste heat into additional electrical power. This waste heat is estimated at 15 terawatts of power in the whole world. Therefore thermoelectric phenomenon and thermoelectric materials are so intensively investigated. In this work we present investigations of electrical, thermoelectric and thermal properties of  $\text{Li}_x\text{Na}_{1-x}\text{NbO}_3$  solid solution for  $x=0$  to 0.1.  $\text{Li}_x\text{Na}_{1-x}\text{NbO}_3$  ceramics have been prepared by a solid-state chemical reaction of stoichiometric mixtures of the component oxides and carbonates. Measurement results show, that the Seebeck coefficient and charge carriers concentration depend on content of Li. Electrical conductivity study exhibit, that charge carriers in this materials are polarons [1]. The ability of investigated solid solutions to efficiently produce thermoelectric power is related to its dimensionless figure of merit.  $\text{Li}_x\text{Na}_{1-x}\text{NbO}_3$  ceramics show interesting thermoelectric properties.

[1] I.G. Austin, N.F. Mott, Adv. Physics, 18, 41 (1969)

# Dielectric properties of $\text{Ba}_6\text{MNb}_9\text{O}_{30}$ ( $\text{M} = \text{Ga}, \text{Sc}$ ) tungsten bronze ceramics

E. Palaimiene<sup>1</sup>, J. Banys<sup>1</sup>, A. Rotaru<sup>2</sup>, F. D. Morrison<sup>2</sup>

1- Vilnius University, Faculty of physics, Saulėtekio av. 9, III b., LT-10222 Vilnius, Lithuania

2- EaStCHEM School of Chemistry, University of St. Andrews, North Haugh, St. Andrews, Fife KY16 9ST, United Kingdom

Main author email address: edita.palaimiene@ff.vu.lt

A large majority of the “multiferroic” publications of the recent years deal with perovskite-related materials. We decided to investigate completely different materials, namely ceramics of the tetragonal tungsten bronze (TTB) structural family [1]. At the crystal-chemistry level, this framework has two main advantages: (a) the number of cationic sites is much higher than in perovskites (5 instead of 2) thus enabling extended substitutions opportunities to foster magnetic interactions and (b) TTB compounds are known to display incommensurate polar state [2,3], that may favour a coupling between magnetic and ferroelectric order [1].

In this work we present broadband dielectric spectroscopy results of a  $\text{Ba}_6\text{MNb}_9\text{O}_{30}$  ( $\text{M} = \text{Ga}, \text{Sc}$ ) (TTB) relaxor system. Dielectric measurements were performed in 30 K – 425 K temperature region and 10 mHz – 46 GHz frequency range. The dielectric relaxation behaviour in the investigated ceramics revealed that both samples can be attributed to the ferroelectric relaxor family of materials. Frequency dependences of the real and imaginary parts of dielectric permittivity of these TTB ceramics were analyzed by Cole-Cole equation (Fig. 1 (a)). Also, the distribution of the relaxation times has been calculated from the dielectric spectra. Fig. 1 (b) shows the temperature dependence of the mean relaxation time for both TTB ceramics obtained from Cole-Cole formula. Solid lines represent a fit of Vogel-Fulcher law.

The dielectric relaxation in the investigated TTB ceramics will be discussed.

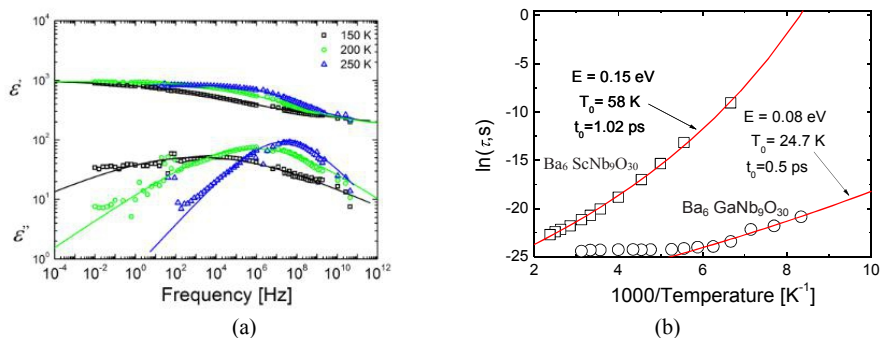


Figure 1. (a) Frequency dependence of the real  $\epsilon'$  and imaginary  $\epsilon''$  parts of complex dielectric permittivity for  $\text{Ba}_6\text{ScNb}_9\text{O}_{30}$  ceramic at different temperatures. (b) Temperature dependencies of the mean relaxation times. Solid lines represent a fit of Vogel-Fulcher law.

[1] M. Josse, O. Bidault, F. Roulland, E. Castel, A. Simon, D. Michau, R. Von der Mühl, O. Nguyen, M. Maglione, Solid State Sciences 11, 1118–1123 (2009).

[2] J. Schneek, J.C. Toledano, C. Joffrin, J. Aubree, B. Joukoff, A. Gabelotaud, Phys. Rev. B 25 (3), 1766–1785 (1982).

[3] C. Filipic, Z. Kutnjak, R. Lortz, A. Torres-Pardo, M. Dawber, J.F. Scott, J. Phys. Condens. Matter 19, 236206 (2007).

## Dielectric and ferroelectric properties of lead-free ( $\text{Na}_{0.5}\text{Bi}_{0.5}$ ) $_{1-x}\text{Sr}_x\text{TiO}_3$ ceramics ( $x=0-0.04$ )

**J. Suchanicz<sup>1</sup>, E.M. Dutkiewicz<sup>2,3</sup>, P. Czaja<sup>1</sup>, M. Antonova<sup>4</sup>, A. Sternberg<sup>4</sup>**

<sup>1</sup>*Institute of Technics, Pedagogical University, ul. Podchorążych 2, 30-084 Krakow, Poland*

<sup>2</sup>*Institute of Physics, Pedagogical University, ul. Podchorążych 2, 30-084 Krakow, Poland*

<sup>3</sup>*Institute of Nuclear Physics PAN, ul. Radzikowskiego 152, 31-342 Krakow, Poland*

<sup>4</sup>*Institute of Solid State Physics, University of Latvia, LV-1063 Riga, Latvia*

The volatilization of toxic lead oxide (PbO) during sintering of widely used lead-based ceramics causes environmental pollution and generates instability of their electrical properties. These facts have stimulated research on variants of lead-free materials, which can replace Pb-based materials.

Lead-free ( $\text{Na}_{0.5}\text{Bi}_{0.5}$ ) $_{1-x}\text{Sr}_x\text{TiO}_3$  ceramics ( $x=0-0.04$ ) were synthesized by a conventional mixed-oxide technique. The microstructure study showed a dense structure, in good agreement with that of above 96% relative density determined by Archimedes method. X-ray diffraction measurements showed that the obtained specimens possess a pure perovskite structure with rhombohedral symmetry. The dielectric and ferroelectric behavior of these ceramics were examined. The temperature dependence of the dielectric spectra revealed a frequency dependence near the depolarization temperature  $T_d$ , which is characteristic of a relaxor mechanism. This suggests that the ceramics lacked long-range ferroelectric order about  $T_d$ . This was evidenced by observation of deformed and pinched hysteresis loops, and significant decrease of remnant polarization  $P_r$  and coercive field  $E_c$  near  $T_d$ . The transition between long-range ferroelectric and nonpolar phase is smeared causing both phases to coexist over a wide temperature range. The thermal evolution of this mixture of phases results in a broad electric permittivity maximum upon heating as for pure  $\text{Na}_{0.5}\text{Bi}_{0.5}\text{TiO}_3$  [1,2, 3].

[1] Vakhrushev SB, Isupov VA, Kvyatkowsky BE, Okuneva NM, Pronin IP, Smolensky GA, Symikov PP. Phase transitions and soft modes in sodium bismuth titanate. *Ferroelectrics* 1985;63:153-160.

[2] Suchanicz J, Roleder K, Kania T, Handerek J. Electrostrictive strain and pyroelectric effect in the region of phase coexistence in  $\text{Na}_{0.5}\text{Bi}_{0.5}\text{TiO}_3$ . *Ferroelectrics*. 1988;77:107-110.

[3] Suchanicz J. Investigations of the phase transitions in  $\text{Na}_{0.5}\text{Bi}_{0.5}\text{TiO}_3$ . *Ferroelectrics* 1995;172:455-458.

# Photoluminescence and Optical Absorption of $\text{Na}_{0.5}\text{Bi}_{0.5}\text{TiO}_3$ Crystals

T.V. Kruzina<sup>1</sup>, T.V. Panchenko, V.M. Sidak<sup>1</sup>, M.P. Trubitsyn<sup>1</sup>, S.A. Popov<sup>1</sup>, J. Suchanicz<sup>2</sup>

1 - Oles Honchar Dnipropetrovsk National University, prosp. Gagarina 72, Dnipropetrovsk, Ukraine

2 - Institute of Physics, Pedagogical University, ul.Podchorazych 2, Krakow, Poland

vsidak@3g.ua

$\text{Na}_{0.5}\text{Bi}_{0.5}\text{TiO}_3$  (NBT) is one of the important lead-free ferroelectric materials with attractive dielectric parameters and high piezoelectric coefficients [1]. According to [2], electrical properties of NBT crystals strongly depend on temperature and atmosphere of annealing that is explained by changing the concentrations of mobile charged and dipolar defects formed by oxygen vacancies  $V_O$ .

In the abstract we report the effect of heat treatment on the optical properties of NBT crystals. NBT single crystals were grown by Czochralski method. As-grown samples were annealed in air at  $T_{\text{ann}}=1100$  K for 1 hour, then in vacuum at the same temperature  $T_{\text{ann}}$  for 2 hours. The optical transmission spectra were measured by using spectrophotometer Specord M-40 in the photon energies range  $h\nu = 3.0 - 1.6$  eV. The absorption spectra  $\alpha(h\nu)$  were calculated with the help of relation given in [3]. Photoluminescence was excited by light emitting diode with  $h\nu = 3.3$  eV. Photoluminescence  $I(h\nu)$  measurements were performed by using the monochromator MDR-12 and the photomultiplier as detector of the emission. All experiments were performed at room temperature.

Fig. 1a shows the heat treatment effect on the optical absorption spectra  $\alpha(h\nu)$ . One can see that annealing in air slightly decreases absorption, whereas heat treating in vacuum sufficiently increases  $\alpha$ . Such result demonstrates optical activity of the defects, formed by  $V_O$ . Extended absorption edge indicates presence of "tail" impurity energy states localized near the valence band top and the conduction band bottom.

Photoluminescence was excited by light with photon energy greater than width of NBT band gap (3.03 eV). This leads to realization the recombination as well as intracenter mechanisms. The presence of two peaks in photoluminescence spectra (Fig. 2b) indicates to the contributions of two types of defects in the "tail" of absorption. The decreasing of both peaks intensity, regardless of the temperature and atmosphere of heat treatment, may be explained by thermal filling of recombination centers with electrons. The nature of the defects responsible for the electrical and optical properties of NBT crystals and the possible mechanisms of the photoluminescence are discussed.

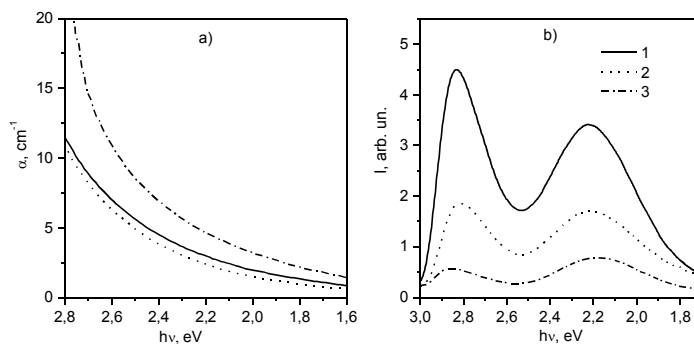


Figure 1. Absorption spectra (a) and photoluminescence spectra (b) (1 - as-grown crystal; 2 - sample after annealing in air; 3 - the sample after subsequent annealing in vacuum.)

[1] S. Nahm, S. Priya eds. Lead-Free Piezoelectrics (New York: Springer), Sodium Bismuth Titanate-Based Ceramics, (2012)

[2] T.V. Kruzina, V.M. Sidak, M.P. Trubitsyn, S.A. Popov and J. Suchanicz, Thermal treatment and dielectric properties of  $\text{Na}_{0.5}\text{Bi}_{0.5}\text{TiO}_3$  single crystal, *Ferroelectrics*, vol. 462, pp. 140-144, (2014).

[3] Ukhonov, Yu.I. Optical properties of semiconductors [in Russian] (Moscow: Nauka), (1977).

# Ferroelectricity and Semiconductor – Metal Transition in $\text{Sn}(\text{Pb})_2\text{P}_2\text{S}_6$ Compounds with Valence Fluctuations

A. Kohutych<sup>1</sup>, A. Molnar<sup>1</sup>, R. Yevych<sup>1</sup>, V. Haborets<sup>1</sup>, M. Medulych<sup>1</sup>,  
A. Dziaugys<sup>2</sup>, Ju. Banys<sup>2</sup>, Yu. Vysochanskii<sup>1</sup>

1- Uzhhorod National University, Uzhhorod, Ukraine, 88000,

2- Vilnius University, Vilnius, Lithuania, LT-10222

vysochanskii@gmail.com

The temperature dependence of dielectric susceptibility and Raman scattering spectra for  $\text{Pb}_2\text{P}_2\text{S}_6$  crystals were investigated. Some growth of dielectric susceptibility and softening of lowest energy phonon optic mode are observed at cooling from room temperature till 20 K in paraelectric phase of  $\text{Pb}_2\text{P}_2\text{S}_6$ . Experimental data on temperature - pressure ( $T - P$ ) diagram of  $\text{Sn}_2\text{P}_2\text{S}_6$  and on  $T - y$  diagram of  $(\text{Pb}_y\text{Sn}_{1-y})_2\text{P}_2\text{S}_6$  are compared and involved for explanation of unusual behavior of paraelectric phase of  $\text{Pb}_2\text{P}_2\text{S}_6$  crystal. The electron and phonon spectra of  $\text{Pb}_2\text{P}_2\text{S}_6$  crystal are calculated in GGA approximation of Density Functional Theory and compared with experimental data. For this crystal the transition from paraelectric state into ferroelectric one under negative pressure is modeled by first – principles calculations.

With taking into account the ideas about valence skipping and charge disproportionation the electronic origin of possible spontaneous polarization of  $\text{Pb}_2\text{P}_2\text{S}_6$  crystal lattice is analyzed in frame of extended Falicov - Kimball (EFK) model [1]. Also the Hubbard model and related Blume – Emery - Griffiths (BEG) model [2] approximations are used for consideration of simplified picture of half-filled lattice with sites that incorporate the  $\text{PbPS}_3$  atomic groups. The minimal energetic model was proposed that considers as core the 26 valence electrons on hybridized bonding orbitals of  $\text{PbPS}_3$  or  $\text{SnPS}_3$  structure units and only one electron is considered at every site. The charge disproportionation process  $\text{P}^{4+} + \text{P}^{4+} \rightarrow \text{P}^{3+} + \text{P}^{5+}$  is energetically favorable for phosphorus ions  $\text{P}^{4+}$  valence skipping and recharging  $3s^1 + 3s^1 \rightarrow 3s^2 + 3s^0$ . The on-site Coulomb repulsion  $U_c$  acts in opposite way to this disproportionation process with energetic gain  $U_{\text{disp}}$ . The orbitals hybridization complicates this picture, but also induce acentric state. We estimate the energy of disproportionation which is main origin of acentric ground state at condition of suppressed second-order Jahn-Teller effect. The calculated electron spectra are compared with parameters of minimal BEG like energetic model that is derived from Hubbard Hamiltonian [2] and agrees with observed  $T - P$  and  $T - y$  diagrams of  $(\text{Pb}_y\text{Sn}_{1-y})_2\text{P}_2\text{S}_6$  ferroelectrics. The quantum anharmonic oscillators models, that is based on statistics of phonon-like excitations in the lattice with three-well local potential, is proposed for description of  $T - P$  and  $T - y$  state diagrams of  $(\text{Pb}_y\text{Sn}_{1-y})_2\text{P}_2\text{S}_6$  ferroelectrics and explanation of their dielectric susceptibility growth at cooling in quantum paraelectric state. Recently, by optic and electrical investigations [3], the metallization of  $\text{Sn}_2\text{P}_2\text{S}_6$  crystals was found at compression up to 40 GPa. We have investigated the temperature dependence of electric conductivity and dielectric susceptibility of  $\text{Sn}_2\text{P}_2\text{S}_6$  crystals in frequency range  $10^{-2} - 10^5$  Hz at heating till 940 K. The metallization appears above 850 K and transition from semiconductor state into metallic phase obviously has percolation nature. These experimental data demonstrate interest for further development of the electronic correlation models which will be appropriate for description of ferroelectricity origin together with semiconductor – metal transition in phosphorous chalcogenides.

[1] T. Portengen, Th. Ostreich, L. J. Sham, Theory of electronic ferroelectricity, Phys. Rev. B, vol. 54, pp. 17452-17463 (1996).

[2] T. M. Rice and L. Sneddon, Real-space and k-space electron pairing in  $\text{BaPb}_{1-x}\text{Bi}_x\text{O}_3$ , Phys. Rev. Lett., vol. 47, pp. 689-692 (1981).

[3] Sergey V. Ovsyannikov, Huiyang Gou, Natalia V. Morozova e.a., Raman spectroscopy of ferroelectric  $\text{Sn}_2\text{P}_2\text{S}_6$  under high pressure up to 40 GPa: Phase transitions and metallization, Journal of Applied Physics, vol. 113, pp. 013511-1-013511-9 (2013).

# Hybrid inorganic-organic compounds as promising ferroelectric materials

**A. Laurikenas<sup>1</sup>, J. Reklaitis<sup>2</sup>, D. Niznansky<sup>3</sup>, D. Baltrunas<sup>2</sup>, A. Kareiva<sup>1</sup>**

*1- Department of Inorganic Chemistry, Vilnius University, Naugarduko 24, LT-03225 Vilnius, Lithuania*

*2- Center for Physical Sciences and Technology, Institute of Physics, Savanoriu 231, LT-02300 Vilnius, Lithuania*

*3- Department of Inorganic Chemistry, Charles University, Albertov 6, 12843 Praha 2, Czech Republic*

*Main author email address: andrius.laurikenas@chf.vu.lt*

Metal-organic frameworks (MOFs) are hybrid organic-inorganic compounds comprised of an extended ordered network made up of organic molecules, organic linkers and metal cations, and have received great attention in different applications. MOFs have great potential for application in gas storage, separation, sensing, catalysis, ferroelectric materials and nonlinear optics. Moreover, they show incomparable potential in enantioseparation and asymmetric catalysis, which are emergent technologies in modern chemical engineering [1]. The ferroelectric behaviour of a lanthanide based metal-organic framework has been recently investigated [2]. Dielectric studies revealed two anomalies at 295 K and 185 K. The former is a paraelectric- ferroelectric transition, and the later is attributed to the freezing down of the motion of the hydroxyl groups. The phase transition is of second order, and the spontaneous polarization in low temperature phase is attributed to the ordering of protons of hydroxyl groups. The Cu containing polar MOFs displayed a promising ferroelectricity [3]. The MOFs constructed from manganese (II) and organic ammonium cation can be considered as potential multiferroics. Recently it was shown, that compressive strain in the Cr(III) containing MOFs can substantially increase the ferroelectric polarization by more than 300% [4]. The paraelectric-ferroelectric phase transition in two isostructural metal-organic frameworks was investigated by in situ variable-temperature Mg-25, Zn-67, N-14, and C-13 solid-state NMR (SSNMR) spectroscopy [5]. With decreasing temperature, a disorder-order transition of  $\text{NH}_4^+$  cations caused a change in dielectric properties. It was determined that  $[\text{NH}_4][\text{Mg}(\text{HCOO})_3]$  exhibits a higher transition temperature than  $[\text{NH}_4][\text{Zn}(\text{HCOO})_3]$  due to stronger hydrogen-bonding interactions between  $\text{NH}_4^+$  ions and framework oxygen atoms.

Using second harmonic generation microscopy the authors [6] found that fluoride doping of the microporous iron(III) terephthalate MOF MIL-53(Fe) induces a polar organization in its structure. The polar order is only observed when both fluoride and guest molecules are present, and may be related to a complex interplay between the adsorbates and the framework, leading to a modification of the positioning of fluoride in the inorganic Fe-chains. This finding showed how MOF materials can be endowed with useful properties by doping MOFs with fluoride. It was also demonstrated, that physical properties of iron (III) carboxylate MOFs depend significantly on the synthesis method [7]. Moreover, magnetic properties of iron associated magnetic metal-organic framework nanoparticles depend on the morphological features of precursors and MOFs [8]. Recently, we presented a facile and large-scale synthesis of iron (III) acetate as a precursor for porous mixed-valence, iron metal-organic frameworks (MOFs) in “solvent-free” type synthesis [9]. The recrystallized iron (III) acetate was successfully used as precursor for the fabrication of mixed-metal-organic frameworks (MOFs). The results of characterization of obtained iron-containing MOFs are presented herein. In this highlight, we summarize the classical ways to construct MOFs based on the selection of ligands.

[1] C. Zhuo, Y.H. Wen and X.T. Wu, Strategies to construct homochiral metal-organic frameworks: ligands selection and practical techniques, *Cryst. Eng. Commun.*, 18, 2792-2802, (2016).

[2] B.Z. Ahmad and B. Want, Structure, ferroelectric ordering, and semiempirical quantum calculations of lanthanide based metal-organic frameworks:  $[\text{Nd}(\text{C}_4\text{H}_5\text{O}_6)(\text{C}_4\text{H}_4\text{O}_6)]\cdot 3\text{H}_2\text{O}$ , *J. Appl. Phys.*, 119, Article Number: 144104, (2016).

[3] J.L. Qi, Y.Q. Zheng and W. Xu, Three Acentric Cu(II) D-( $\bar{1}$ )-quinate complexes: Solvent-dependent assemblies, magnetic and ferroelectric properties, *Synth. React. Inorg. Metal-Org. Nano-Metal Chem.*, 46, 257-267, (2016).

[4] S. Ghosh, D. Di Sante and A. Stroppa, Strain tuning of ferroelectric polarization in hybrid organic inorganic perovskite compounds, *J. Phys. Chem. Lett.*, 6, 4553-4559, (2015).

[5] J. Xu, B.E.G. Lucier, R. Sinelnikov, V.V. Tersikh, V.N. Staroverov and Y.N. Huang, Monitoring and understanding the paraelectric-ferroelectric phase transition in the metal-organic framework  $[\text{NH}_4][\text{M}(\text{HCOO})_3]$  by solid-state NMR spectroscopy, *Chem. – A Europ. J.*, 21, 14348-14361, (2015).

[6] K. Markey, T. Putzeys, P. Horcajada, T. Devic, N. Guillou, M. Wubbenhorst, S. Van Cleuvenbergen, T. Verbiest, D.E. De Vos and M.A. van der Veen, Second harmonic generation microscopy reveals hidden polar organization in fluoride doped MIL-53(Fe), *Dalton Trans.*, 45, 4401-4406, (2016).

[7] M. Pilloni, F. Padella, G. Ennas, S.R. Lai, M. Bellusci, E. Rombi, F. Sini, M. Pentimalli, C. Delitala and A. Scano, Liquid-assisted mechanochemical synthesis of an iron carboxylate metal organic framework and its evaluation in diesel fuel desulfurization, *Micropor. Mesopor. Mater.*, 213, 14-21, (2015).

[8] X.M. Quan, Y.D. Liu and H.J. Choi, Magnetorheology of iron associated magnetic metal-organic framework nanoparticle, *J. Appl. Phys.*, 117, Art. No. 17C732, (2015).

[9] A. Laurikenas, J. Barkauskas, J. Reklaitis, G. Niaura, D. Baltrunas and A. Kareiva, Formation peculiarities of iron (III) acetate: Potential precursor for iron and mixed-metal-organic frameworks (MOFs). *Lithuanian J. Phys.*, 56, 35-41, (2016).

## Basic characterization of ferroelectric lead lanthanum zirconate titanate based on correlation coefficients

**K. Pytel<sup>1</sup>, J. Suchanicz<sup>1</sup>, W. Hudy<sup>1</sup>, M. Livinsh<sup>2</sup> and A. Sternberg<sup>2</sup>**

<sup>1</sup> *Institute of Technology, Pedagogical University, ul. Podchorążych 2, 30-084 Krakow, Poland*

<sup>2</sup> *Institute of Solid State Physics, University of Latvia, Kengaraga 8, LV-1063 Riga, Latvia*

**kpytel@up.krakow.pl**

An effect of La (2-13 at.%) substitution for Pb on PLZT with the Zr/Ti ratio of 65/35 under uniaxial pressure applied parallel to an ac-electric field was investigated. PLZT x/65/35 with different contents of lanthanum powders were obtained by two-stage co-precipitation process described in paper [1]. Applying pressure leads to a change in the peak intensity of the electric permittivity of its frequency dispersion as well as in the dielectric hysteresis [2-4]. Results based on nanoregion switching processes under combined electromechanical loading were interpreted. Along with the growth in pressure, the phase transition temperature, the frequency dispersion and the thermal hysteresis alters, and the dielectric behaviour features expands [5-7].

The purposes of analysis was to determine the correlation between the experimental data. A computed correlation coefficients showing the quantitative measure of some type of correlations and dependencies. Kinds of analysis by correlation coefficients included Pearson product-moment correlation coefficient and Spearman's rank correlation coefficient. A Kolmogorov Smirnov test was used to analyze results and to determine whether the sample comes from a population of a given distribution [8].

Surveys demonstrated that applied stress has a significant influence on the dielectric properties of PLZT ceramics.

[1] M. Dambekalne, M. Antonova, M. Livinsh, B. Garbarz-Glos, W. Smiga, A. Sternberg, PLZT-synthesis, sintering and ceramics microstructure. *Journal of the European Ceramic Society*, vol. 26, pp. 2963–2966, (2006).

[2] GH. Haertling, *Ferroelectric Ceramics: History and Technology*, *Journal of the American Ceramic Society*, vol. 82, pp. 797–818, (1999).

[3] C. Carter and MG. Norton, *Ceramic Materials Science and Engineering*, Springer, (2013).

[4] K. Uchino and S. Nomura, Critical exponents of the dielectric constants in diffused-phase-transition crystals, *Ferroelectrics*, vol. 44, pp. 55–61, (1982).

[5] N. Izyumskaya, Y. Alivov, H. Morkoc, *Oxides, Oxides, and More Oxides: High-κ Oxides, Ferroelectrics, Ferromagnetics, and Multiferroics. Critical Reviews in Solid State and Materials Sciences*, vol. 34, pp. 89–179, (2009).

[6] X. Dai, and D. Viehland, Impurity-induced incommensuration in antiferroelectric La-modified lead zirconate titanate. *Physical Review B*, vol. 51, pp. 6261–6271, (1995).

[7] S. Kamba, V. Bovtun, J. Petzelt, I. Rychetsky, R. Mizaras, A. Brilingas, J. Banys, J. Grigas, M. Kosec, Dielectric dispersion of the relaxor PLZT ceramics in the frequency range 20 Hz-100 THz. *Journal of Physics: Condensed Matter*, vol. 12, pp. 497–517, (2000).

[8] K. Pytel, W. Hudy, H. Noga, W. Kulinowski, An influence of selected conditions on the production of energy in photovoltaic panels based on correlation coefficients, 17th International Carpathian Control Conference, (2016)

# PHASE TRANSITIONS IN $[\text{Net}_4][\text{NMe}_4][\text{ZnBr}_4]$ CRYSTAL

M. K. Krawczyk<sup>1</sup>, A. Ingram<sup>2</sup>, R. Cach<sup>1</sup>, Z. Czapl<sup>2</sup>, O. Czupiński<sup>3</sup>, S. Dacko<sup>1</sup>,

<sup>1</sup>Institute of Experimental Physics, University of Wrocław, M. Born Sq. 9, 50-204 Wrocław, Poland

<sup>2</sup>Department of Physics, Opole University of Technology, Ozimska 75, 45-271 Opole, Poland

<sup>3</sup>Faculty of Chemistry, University of Wrocław, F. Joliot-Curie 14, 50-383 Wrocław, Poland

*e-mail: monika.krawczyk@ifd.uni.wroc.pl*

Crystal of the formula  $[\text{Net}_4][\text{NMe}_4][\text{ZnBr}_4]$  was obtained and characterized with thermal, structural and dielectric studies that revealed the reversible first order phase transition at 486/484 K on heating and cooling run. An optical visualization of the high temperature ferroelastic domain structure proved an untypical lowering of crystal symmetry during the phase transition. The satisfying crystal structure solution at room temperature was found in the tetragonal system, in the  $P\bar{4}2_1m$  space group. However, the solution could also be found in the orthorhombic  $P2_12_12$  space group. The phase transition was seen very well in dilatometric studies as presented in Fig.1

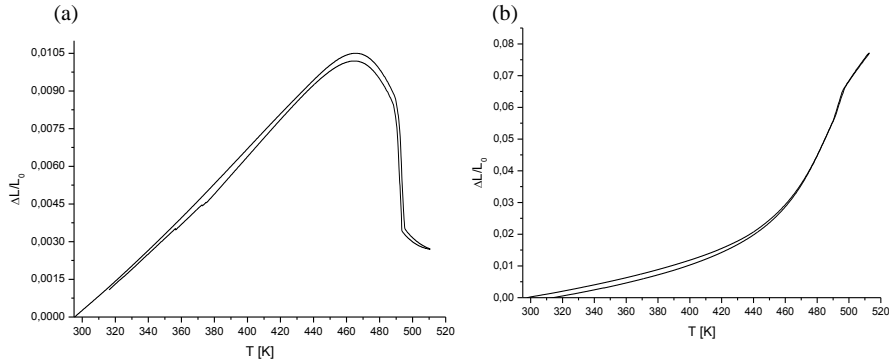


Figure 1. Temperature dependence  $\Delta L/L_0 = f(T)$  (a) along the  $a$  axis; (b) along the  $c$  axis, upon heating and cooling runs

The dielectric studies around the phase transition temperature are presented as complex impedance. The dependences of  $\log \sigma_c$  versus  $1000/T$  and corresponding activation energies are depicted in Fig. 2.

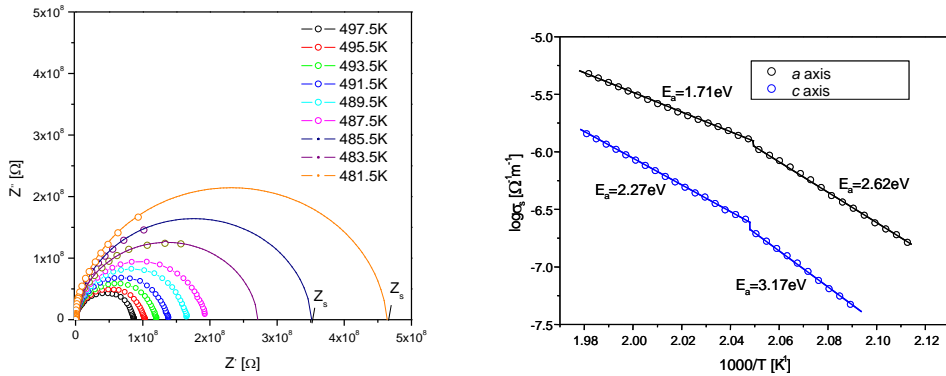


Figure 2. (a) Dependence of the imaginary part of the electrical impedance on its real part, (b) dependences of  $\log \sigma_s = f(1000/T^{-1})$  along the  $a$  and  $c$  axes



# PROPERTIES OF $(C_3H_4N_2)HClO_4$ CRYSTAL: STRUCTURAL, INFRARED AND THERMAL STUDIES

**D. Podsiadła<sup>1</sup>, J. Baran<sup>2</sup>, Z. Czapla<sup>3</sup>, M.K. Krawczyk<sup>1</sup>**

1-Institute of Experimental Physics, University of Wrocław, M.Born Sq. 9, 50-204 Wrocław, Poland

2-Institute of Low Temperature and Structure Research of the Polish Academy of Sciences, Wrocław, Okólna 2, 50-422 Wrocław, Poland

3-Department of Physics, Opole University of Technology, Ozimska 75, 45-271 Opole, Poland

*Main author email address: dorota@ifd.uni.wroc.pl*

Pyrazole perchlorate crystal,  $(C_3H_4N_2)HClO_4$ , abbreviated as PyrClO was investigated. It is a new crystal gained from aqueous solution. The crystal consists of pyrazole cations,  $[C_3H_5N_2]^+$  and perchlorate anions,  $[ClO_4]^-$ . Various thermal methods of experiment, as differential scanning calorimetry (DSC), differential thermal analysis (DTA) and thermogravimetric analysis (TGA) (Fig. 1.) were used to investigate the phase transitions in the crystal. DSC showed the existence of phase transition at  $T = 339$  K. Single crystal X-ray diffraction measurement was undertaken on PyrClO crystal at the temperature above the phase transition temperature. According to them the PyrClO crystal belongs to the orthorhombic crystal system and the space group is  $Cmc2_1$ . The vibrational IR spectra in Nujol and Perfluorolube mulls were studied in the wide temperature range, from room temperature to 350 K in the frequency range  $4000 - 450$   $cm^{-1}$ . The special attention was put to the temperature range around the phase transition temperature. The assignment of the observed bands was discussed. The temperature changes of wavenumbers, gravity centre and band intensities were analyzed to clarify the phase transition molecular mechanism. The exemplary spectral parameter changes versus temperature are presented in Fig. 2. Information about hydrogen bonds was obtained.

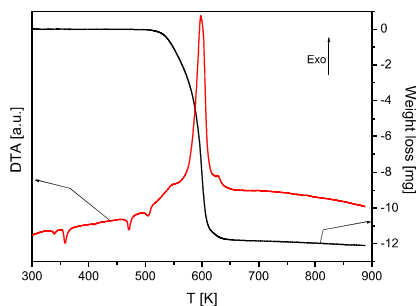


Fig. 1.

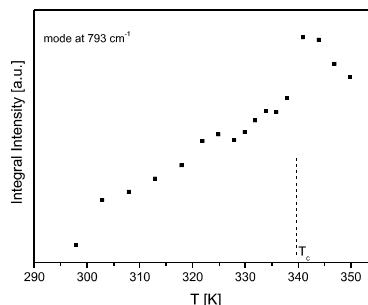


Fig. 2.

Figure 1: The DTA and TGA signals as a function of temperature for the PyrClO crystal for the heating run.

Figure 2: The integral intensity changes near the phase transition temperature ( $T_c$ ) for the bending C–H vibrations.

# Reduced Bimolecular Recombination in a Ternary Silole-Based Polymer:P3HT:PCBM Solar Cell

**Julius Vazgėla, Meera Stephen, Gytis Juška, Kristijonas Genevičius, Kęstutis Arlauskas**

*Department of Solid State Electronics, Vilnius University, Saulėtekio 9, 10222 Vilnius, Lithuania*

[julius.vazgela@ff.vu.lt](mailto:julius.vazgela@ff.vu.lt)

Due to the simple solution processing organic semiconductors are promising materials for solar cells application. During the last five years the performance of organic bulk heterojunction (BHJ) solar cells has improved considerably [1, 2]. Light absorbance in BHJ, effective charge carriers' separation and collection at the electrodes describes solar cell's efficiency. Due to limitation of bimolecular recombination the thickness of most high efficiency organic solar cells is limited to 60–110 nm [3, 4]. It is highly desirable to use thicker layers for BHJ in terms of processing, for which it is a prerequisite for the active layer to exhibit reduced Langevin recombination.

The Langevin bimolecular recombination is given by the equation:

$$\beta = \xi \beta_L = \frac{e(\mu_n + \mu_p)}{\varepsilon \varepsilon_0} \quad (1)$$

where  $\beta(\beta_L)$  is the rate of bimolecular (Langevin) recombination,  $\xi$  – Langevin prefactor,  $\xi=1$  in a pure Langevin recombination case and  $\xi<1$  if the recombination is reduced,  $e$  – elementary charge,  $\mu_n(\mu_p)$  – electron (hole) mobility,  $\varepsilon(\varepsilon_0)$  – relative (absolute) dielectric permittivity.

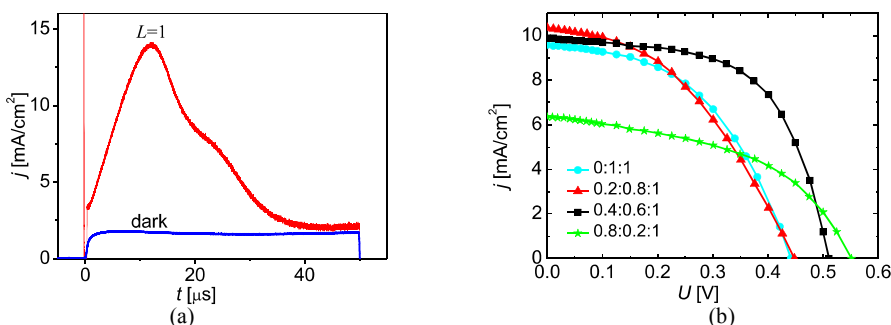


Figure 1. (a) P3HT:PCBM bkend's photo-CELIV curves for mobility evaluation with no laser intensity (dark) and at maximum obtained laser intensity ( $L=1$ ). Using the position of peak and cusp at around 25  $\mu\text{s}$  mobility of electron and holes respectively were evaluated. (b) J-V curves of different composition Si-PCPDTBT:P3HT:PCBM solar cells under AM1.5 illumination.

Most widely investigated BHJ organic solar cell consist of poly(3-hexylthiophene-2,5-diyl) (P3HT) and fullerene derivative [6,6]-phenyl- $\text{C}_{61}$ -butyric acid methyl ester (PCBM). Annealed P3HT:PCBM solar cells possess strongly reduced Langevin recombination. However, these cells have got low open circuit voltage and poor absorption in longer wavelength regions of the visible light spectrum. In order to overcome these limitations different ratios of silole-based polymer Si-PCPDTBT were added to conventional P3HT:PCBM solar cells to give ternary Si-PCPDTBT:P3HT:PCBM active layers.

Photoelectric properties of devices consisting of these ternary blends as active layers were investigated employing different techniques: Current–voltage characteristic, the extraction of the photogenerated charge carriers by linearly increasing voltage (photo-CELIV) (Fig. (a)), double injection (DoI) and integral Time-of-Flight (TOF). It was found that the open circuit voltage as well as the mobility of faster charge carriers increases with increasing ratio of Si-PCPDTBT. However, the Langevin prefactor was also found to be increasing with increasing Si-PCPDTBT content. Blends with optimized ratios of 0.4:0.6:1 Si-PCPDTBT:P3HT:PCBM composition were found to yield maximum power conversion efficiencies (Fig. 1 (b)).

[1] M. A. Green, K. Emery, Y. Hishikawa, W. Warta, E. D. Dunlop, Solar Cell Efficiency Tables (Version 47), Prog. Photovoltaics, **24**(7), 905–913 (2016), <https://dx.doi.org/10.1002/pip.2788>.

[2] M.C. Scharber, N.S. Sariciftci, Prog. Polym. Sci., **38**, 1929–1940 (2013), <https://dx.doi.org/10.1016/j.progpolymsci.2013.05.001>.

[3] Steve Albrecht, Sebastian Schäfer, Ilja Lange, Seyfullah Yilmaz, Ines Dumsch, Sybille Allard, Ullrich Scherf, Andreas Hertwig, Dieter Neher, Org. Electron. **13**, 615–622 (2012), <https://dx.doi.org/10.1016/j.orgel.2011.12.019>.

[4] J. Peet, L. Wen, P. Byrne, S. Rodman, K. Forberich, Y. Shao, N. Drolet, R. Gaudiana, G. Dennler in D. Waller, Appl. Phys. Lett. **98**, 043301 (2011), <https://dx.doi.org/10.1063/1.3544940>.

# Carbon fiber material defectoscopy using mm wave near field microscopy methods

**S. Rudys<sup>1,3</sup>**, **P. Anbinderis<sup>1</sup>**, **T. Anbinderis<sup>1</sup>**, **A. Laurinavičius<sup>2</sup>**, **J. Banys<sup>3</sup>**

*1-UAB Elmika, Naugarduko st. 4, Vilnius, Lithuania*

*2- Semiconductor Physics Institute, Gostauto st. 11, Vilnius, Lithuania*

*3- Vilnius University Faculty of Physics Sauletekio str. 9 III, 817, Vilnius, Lithuania*

Carbon fiber reinforced plastic (CFRP) is gaining importance as a light-weight material. Most popular method of non destructive testing is eddy current scanning method. Sensors operate at low (MHz order) frequency. Consequently sensor dimensions are big and resolution is low (cm order). High frequency probes are not useful because due to carbon high conductivity penetration depth of high frequency (GHz order) electromagnetic fields is very low.

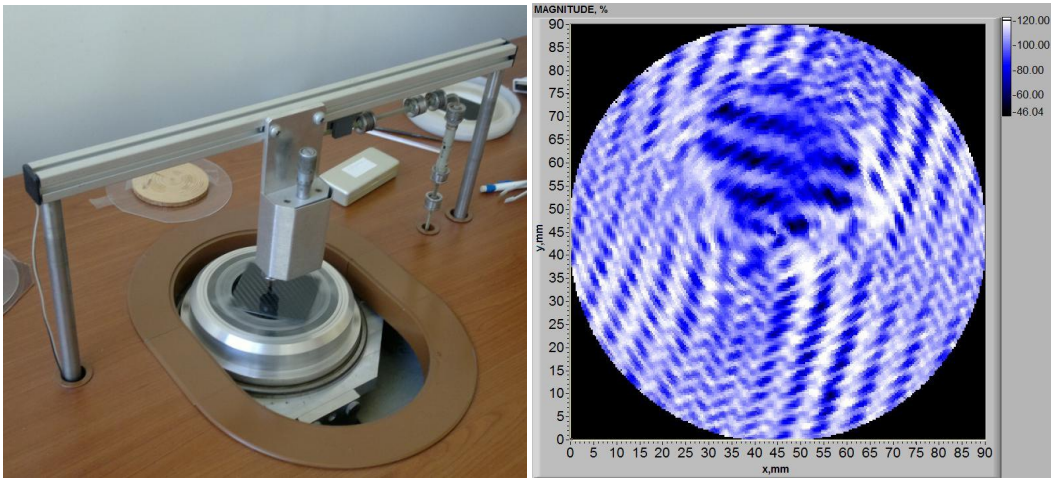


Fig. 1

Fig.2

We have scanned various defected samples of CFRP using near field millimeter wave scanner (fig.1). Operation frequency was 100 GHz. Wave length was comparable to dimensions of a flat bundle of carbon fabric. In this case electromagnetic field penetration was at least two carbon fiber layers. Due to short wavelength and small near field probe dimensions an image of bundle structure was obtained as well as defects behind outer layers of carbon fiber fabric (fig.2).

# Dynamic interferometer based on photorefractive effect in Sb-doped $\text{Sn}_2\text{P}_2\text{S}_6$ ferroelectric

**A. A. Grabar, M. V. Tsyhyka, I. M. Stoika**

*Institute for Solid State Physics and Chemistry of Uzhhorod National University,  
54 Voloshin st., 88000, Uzhhorod, Ukraine*

*alexander.grabar@uzhnu.edu.ua*

$\text{Sn}_2\text{P}_2\text{S}_6$  is known as one of the most efficient photorefractive materials for red and near IR spectral range [1]. Among the most prospective applications of the photorefractive crystals is dynamic interferometry based on two-wave mixing with laser beams. These interferometers are useful for detection of small phase variations, which partially are produced by vibrations of the tested objects that reflect the probe laser beam. The main advantage of such schemes is their adaptation to slow variations of the phase, i.e. occurring in time larger than the time response of the photorefractive grating. The basic element of the interferometer is a photorefractive crystal. In this work we used a  $\text{Sn}_2\text{P}_2\text{S}_6$  crystal doped with Sb, which is characterized by the diffusion mechanism of the photorefractive effect and demonstrates the values of the two-wave mixing gain up to  $18 \text{ cm}^{-1}$  at 633 nm and a relatively short response time (10-100 ms) [1, 2]. These parameters allow to construct a holographic scheme applicable for optical detection of micro-vibrations, and which also can be used for remote detection of the vibrations whose frequency is much higher than the reversal response time of the photorefractive material by using a heterodyne principle (Figure 1). In this case the “pump” beam  $I_p$  is phase modulated by reflection of this beam from a piezo-mirror (PM) driven by sound generator (SG), and the interference pattern inside the photorefractive crystal, that forms the dynamic hologram, is moving with the frequency equal to the difference between frequencies of the “signal” ( $\nu_s$ ) and “pump” ( $\nu_p$ ) phase modulations. Using this scheme, the frequency  $\nu_s$ , amplitude and relative phase of the testing point on the vibrating object can be measured.

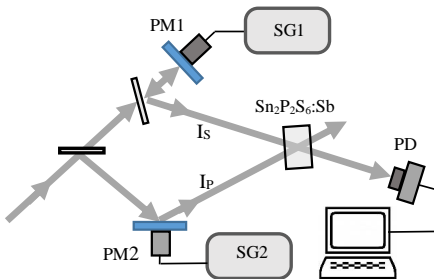


Figure 1. The optical scheme of the heterodyne dynamic interferometer. Here PM – piezomirror, SG – sound generator, PD – photodiode,  $I_p$  and  $I_s$  – interacting beams of He-Ne laser (633 nm).

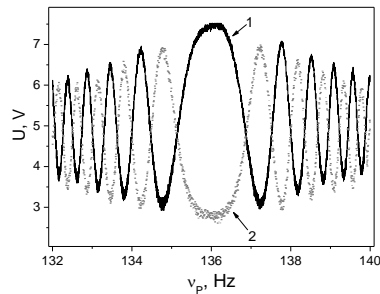


Figure 2. Variation of the signal beam intensity, measured by PD, at linear in time variation of  $\nu_p$  when object PM1 is vibrating with frequency  $\nu_s = 136 \text{ Hz}$ . Curves 1 and 2 correspond to “in-phase” and “anti-phase” vibrations when  $\nu_s = \nu_p$ .

By sweeping the “pump” beam phase modulation, one can detect the “object” vibration frequency  $\nu_s$  with a high precision. As shown in Figure 2, the intensity of the amplified signal beam, detected at linear with time variation of  $\nu_p$ , is symmetrical relative to the value of the frequency of phase modulation equal for the both interfering beams. The shape of the signal beam intensity depends on the amplitude of the vibrating object, and the higher harmonics appear in the signal at higher amplitudes of the “signal” (or “pump”) phase modulation. This allows to estimate the amplitude of the vibration of the objects by an analysis the waveform of the signal at various amplitudes of the “pump” modulation with PM2. In addition, the relative phases of the modulations of the “signal” and “pump” also can be estimated basing on the signal level at equalized modulation frequencies. As an example, two curves shown in Figure 2 correspond to the cases when the phases of the modulation of the interfering beams are equal (1) and opposite (2). When the relative phase of  $I_s$  and  $I_p$  modulation is between 0 and  $\pi$ , the measured value of the signal beam intensity at  $\nu_p = \nu_s$  is intermediate between these extremal values, and can be estimated after some calibration.

- [1] A.A. Grabar, M. Jazbinšek, A. N. Shumelyuk, Yu. M. Vysochanskii, G. Montemezzani, P. Günter. Photorefractive Materials and Their Applications, v.2 (Springer Springer Series in Optical Sciences, 114), “Photorefractive effects in  $\text{Sn}_2\text{P}_2\text{S}_6$ ”, p. 327-362 (2007).  
[2]. I. V. Kedyk, P. Mathey, G. Gadret, A. A. Grabar, K. V. Fedyo, I. M. Stoika, I. P. Prits, Yu. M. Vysochanskii. “Investigation of the dielectric, optical and photorefractive properties of Sb-doped  $\text{Sn}_2\text{P}_2\text{S}_6$  crystals”, Appl. Phys. B, vol. 92, p. 549-554 (2008).

## **INDEX OF AUTHORS**

**A**

Abd-Lefdil, M. 12  
 Aftabuzzaman, M. 10  
 Aidas, K. 67  
 Albassam, A. A. 12  
 Anbinderis, P. 93  
 Anbinderis, T. 93  
 Andriyevsky, B. 31  
 Andrzejewski, B. 58  
 Aniskevich, A. 52  
 Antonova, M. 71, 85  
 Arlauskas, K. 92

**B**

Bagdzevicius, S. 32  
 Bahraoui, T. El 12  
 Balciunas, S. 18, 77  
 Baltrunas, D. 88  
 Banys, J. 16, 18, 20, 32, 44, 46, 52, 63, 64, 67, 68, 77, 79, 84, 87, 93  
 Baran, J. 91  
 Bednarchuk, T. J. 42, 54  
 Belayachi, A. 12  
 Bellaiche, L. 39  
 Bellucci, S. 47  
 Birks, E. 20  
 Bistarelli, S. 47  
 Bochenek, D. 29, 62  
 Bocheneka, D. 81  
 Borisova, A. 52  
 Bragiel, P. 12  
 Brzezinska, D. 29, 62  
 Bujakiewicz-Koronska, R. 25

**C**

Cach, R. 90  
 Cataldo, A. 47  
 Chapagain, K. 28  
 Chlan, V. 21  
 Chmaissem, O. 28  
 Chrobak, A. 62  
 Chyasnavichyus, M. 44  
 Ciomaga, C. 64  
 Ciupa, A. 41, 67  
 Cwikiel, E. 53  
 Cwikiel, K. 82  
 Czaja, P. 17, 61, 85  
 Czapla, Z. 31, 38, 66, 69, 75, 90, 91  
 Czupinski, O. 66, 75, 90

**D**

Dabrowski, B. 28  
 Dacko, S. 90  
 Dec, J. 10, 15, 19  
 Dementjev, A. 47  
 Desnenko, V. A. 27  
 Dovbeshko, G. 47  
 Dunce, M. 20  
 Dutkiewicz, E. M. 71, 85  
 Dyachenko, A. A. 59  
 Dziaugys, A. 44, 87

**E**

El-Bey, A. 12  
 Eliseev, A. 14, 39, 44  
 El-Naggar, A. M. 12

**F**

Fedorchenko, A. V. 27

Feher, A. 27

Fertman, E. L. 27

**G**

Galassi, C. 35  
 Genenko, Y. A. 35  
 Genevicius, K. 92  
 Gheorghiu, F. 64  
 Giffin, G. A. 68  
 Giordano, M. 52  
 Glaum, J. 35  
 Glinchuk, M. 24  
 Glukhov, K. E. 30  
 Goian, V. 28

Grabar, A. A. 30, 94

Grigalaitis, R. 32

Gruszka, I. 63

**H**

Haborets, V. 87  
 Hafid, M. 15  
 Hilczar, A. 58  
 Horchidan, N. 64  
 Hudy, W. 89

**I**

Ignatans, R. 20  
 Ilkovic, S. 78  
 Ingram, A. 66, 69, 75, 90

Ivanov, M. 32, 68, 77

Izai, V. 78, 79

**J**

Jablonskas, D. 68  
 Janczak, J. 66, 75  
 Juska, G. 92

**K**

Kalendra, V. 64  
 Kalvane, A. 61  
 Kamba, S. 28  
 Kania, A. 15, 63  
 Kaplas, T. 47  
 Kareiva, A. 70, 88  
 Karpierz, M. 72  
 Karpinsky, D. V. 26  
 Khachaturyan, R. 35  
 Khalyavin, D. D. 27, 70

Kharchenko, M. 57

Khrustalyov, V. 57

Kinzhybalo, V. 42, 54, 58

Kityk, I. V. 12

Kizhibalo, V. 69

Kleemann, W. 10, 19

Kohutych, A. 87

Kohutych, A. A. 30

Kojima, S. 10

Kokhan, O. 55

Kolesnik, S. 28

Komornicka, D. 42

Kondakova, I. V. 21

Konieczny, K. 17, 61, 71, 72, 76, 83

Koptev, M. M. 80

Koruza, J. 35

Kostrzewa, M. 66

Kotlyar, O. V. 27

Kozdras, A. 69

Kranauskaite, I. 52

Krawczyk, M. K. 90, 91

Krupych, O. 11

Kruzina, T. V. 80, 86

Kryvyy, T. 56

Kugel, G. E. 15

Kungl, H. 35

Kuzhir, P. 48

Kuzian, R. O. 21

**L**

Laguta, V. V. 21, 39  
 Laurikenas, A. 88  
 Laurinavicius, A. 93  
 Lewczuk-Jodlowiec, U. 76  
 Livinsh, M. 89  
 Lupascu, D. 20

**M**

Machnik, Z. 81  
 Mackeviciute, R. 32  
 Macutkevici, J. 46, 48, 52, 63  
 Maczka, M. 18, 41, 67

Maksymovych, P. 44  
 Malyshkina, O. 14  
 Markiewicz, E. 58  
 Martone, A. 52  
 Martunyuk-Lototska, I. 55  
 Matyjasek, K. 60  
 Medulych, M. 87  
 Micciulla, F. 47  
 Miga, S. 15  
 Mitoseriu, L. 64  
 Molak, A. 46  
 Molnar, A. 30, 87  
 Monasterski, P. 42  
 Morozovska, A. 24, 39, 44  
 Morrison, F. D. 84  
 Mys, O. 11, 55, 56

**N**

Nalecz, D. M. 74  
 Nesterov, O. 45  
 Niemiec, P. 29, 62, 81  
 Niewiadomski, A. 15  
 Niznansky, D. 88  
 Nowak, K. 82

**O**

Olekhnovich, N. M. 27, 70  
 Orliukas, A. 78  
 Osak, A. 65

**P**

Palaimiene, E. 84  
 Panchenko, T. V. 59, 86  
 Parasyuk, O. 55  
 Pasinska, K. 58

Passerini, S. 68  
 Piasecki, M. 12  
 Pidgirniy, D. 47  
 Piekarczyk, W. 61  
 Pietraszko, A. 42, 54, 58  
 Plyaka, S. 45  
 Plyushch, A. 48  
 Podsiadla, D. 91  
 Popov, S. A. 80, 86  
 Poppl, A. 67  
 Poprawski, R. 40  
 Poprawski, W. 40  
 Posudievsky, O. 47

Potapovich, Yu. N. 80  
 Prosandeev, S. A. 39  
 Przeslawski, J. 66  
 Ptak, M. 41  
 Pushkarev, A. V. 27, 70  
 Pytel, K. 89

**R**

Radojewska, E. B. 40  
 Radwanski, R. J. 74  
 Radyush, Yu. V. 27, 70  
 Raevskaya, S. I. 39  
 Raevski, I. P. 39  
 Reiffers, M. 78  
 Reklaitis, J. 88  
 Ropka, Z. 74  
 Rotaru, A. 84  
 Rubanik, V. V. 70  
 Rudys, S. 93  
 Rutskiy, A. S. 80

**S**

Salak, A. N. 27, 70  
 Salkus, T. 78, 79  
 Samulionis, V. 16  
 Savitsky, V. 57  
 Schultheiss, J. 35  
 Seggern, H. von 35  
 Shenderova, O. 48  
 Shvartsman, V. V. 20  
 Shylin, A. D. 70  
 Sidak, V. M. 86  
 Sieradzki, A. 42  
 Silibin, M. V. 26  
 Simenas, M. 18, 64, 67

Sitalo, E. I. 39  
 Sitko, D. 17, 61, 76  
 Skab, I. 56  
 Skulski, R. 29, 62, 81  
 Stachowski, G. 17  
 Stanulis, A. 70  
 Stepankova, H. 21  
 Stephen, M. 92  
 Sternberg, A. 71, 85, 89  
 Stoika, I. M. 30, 94  
 Studenyak, I. 78, 79  
 Suchanec, G. 33  
 Suchanicz, J. 17, 61, 71, 72, 76, 85, 86, 89  
 Svirskas, S. 20

**T**

Taibi, M. 12  
 Timko, M. 78  
 Tornau, E. E. 18  
 Troyanchuk, I. O. 26  
 Trubitsyn, M. 45, 80, 86

**V**

Vasyukiv, Yu. 56  
 Vazgela, J. 92  
 Vlokh, R. 11, 55, 56  
 Volnianskii, M. 45  
 Vysochanskii, Y. 16, 30, 44, 87

**W**

Wacke, S. 75  
 Wada, S. 77  
 Wang, J. 34  
 Wang, X. 13  
 Wodecka-Dusa, B. 81  
 Wolcyrz, M. 42

**Y**

Yang, T. 34  
 Yevych, R. 87

**Z**

Zagorodny, Yu. 21  
 Zapeka, B. 11, 55  
 Zarrelli, M. 52  
 Zhukov, S. 35

ISBN 978-609-459-735-0

## **IV**

### **Lithuanian-Ukrainian-Polish meeting on physics of ferroelectricity**

**Programme & abstracts**

**5<sup>th</sup> – 9<sup>th</sup> of September 2016**

**Palanga, Lithuania**

Tiražas 65 egz.

Išleido Vilniaus universiteto leidykla

Universiteto g. 1, Vilnius

Spausdino UAB „BMK leidykla“

J. Jasinskio g. 16, Vilnius